

# A Study on the Design and Economic Evaluation of HTS Power Platform with 23 kV Tri/axial HTS Power Cables for Urban Power Supply

李, 哲休

<https://doi.org/10.15017/4060194>

---

出版情報 : 九州大学, 2019, 博士 (工学), 課程博士  
バージョン :  
権利関係 :



**Dissertation for the *Doctor of Engineering***

**A Study on the Design and Economic  
Evaluation of HTS Power Platform with  
23 kV Tri-axial HTS Power Cables for  
Urban Power Supply**

***March 2020***

**Department of Electrical and Electronic Engineering,  
Graduate School and Faculty of Information Science and  
Electrical Engineering, Kyushu University**

***Lee, Chulhyu***

## 論文概要

現在、世界中で超伝導ケーブルの実用化に向けた研究開発が活発に進められている。既存のさまざまな電圧階級の送配電系統と連系するために、仕様が異なる超伝導ケーブルの試験も行われた。韓国電力では、このような開発状況を鑑み、高温超伝導ケーブルの実用化を目指して、1 km以上離れた二ヶ所の154 kV変電所を23 kV HTSケーブルで連系するShingalプロジェクトを実施し、この高評価を受け、世界初の商業運転に展開した。

超伝導ケーブルの長所は高電流密度送電であり、同サイズの配電用フィーダーより約5～10倍以上の電力を送電することができる。これにより、都心の変電所建設を省略したり、変電所の都市外郭への移転のみならず、技術的制約で解決が困難だった様々な状況を克服できるようになる。しかし、既存の三相一括型超伝導ケーブルはその高い価格により、広範囲の導入と新規投資が難しいという欠点があった。三相同軸型ケーブルはこの課題を解決し、さらに超伝導シールドを必要とせず、さらなる価格低減を可能とし、ドイツのAmpacityプロジェクトなどでその性能が立証された。しかしながら、冷却システムの制約により、1km以上の系統に導入できないという限界を露呈した。

本研究では、この課題を解決するために、三相同軸ケーブル内に冷却バスを二つ設け、ケーブル外部循環経路を別途に確保する方式を提唱、採用した。また、都心の電力供給のための新しい電力系統構成として、23kVの超伝導同軸ケーブルを活用したHTSパワープラットフォームを提案し、伝統的な方式との経済効果を検討した。ここでHTSパワープラットフォームとは、負荷密度が高く、かつ、地価が高い都心に154kV変電所を建設する代わりに、敷地面積が非常に小さい23kV開閉所を2～3ヶ所建設し、23kV HTSケーブルで都市外郭に配置した変電所と環状網で連携して安定的に電力を供給する方式を指す。ここでは、N-1信頼度基準を考慮しながらも、23kV開閉所の電力供給能力と、これを連系する23kV超伝導ケーブルの回線数および送電容量の間に経済的観点で適切な調和が求められる。特に、投資代案間の比較検討におい

て、超電導ケーブルの経済性だけでなく、現場の建設環境も反映されなければならない。建設環境には、地中建設方式、ステーション用敷地価格、送電線の経過地の制約など、経済性評価に影響を及ぼしうるさまざまな要因が含まれる。これらを鑑みて、HTSパワープラットフォームの経済効果について、従来の伝統的方式と比較検討した。

本論文は、23kV超電導ケーブルを活用したHTSパワープラットフォームのデザインおよび経済性評価に関する一連の研究をまとめたもので六章で構成される。第一章は序論で、研究背景、国内外の超電導ケーブルの開発状況および研究目的について記述している。第二章では、各種超電導ケーブルの比較とともに、液体窒素の外部循環経路を備えた三相同軸型超電導ケーブルの構成について説明している。第三章では、都心の電力供給のための新しい概念のHTSパワープラットフォームを提案し、経済性評価のために超電導ケーブルと冷却システムの価格算出手順を記述した。第四章では、最大360MVA負荷供給容量を持つHTSパワープラットフォームの経済性について、多様な設備計画シナリオ別に比較評価した。特に、超電導ケーブルの容量別の総投資費の比較を通じて、HTSパワープラットフォームと最も適切に符合する超電導ケーブルの容量を定量的に検討した。第五章では、実際に電力系統に適用するための60MVA容量のHTSパワープラットフォームモデル事業の候補地の選定およびシステムの構成について記述した。第六章は総括で、今後の課題に対する意見も記した。

## ABSTRACT

Research on the development of superconducting power cables for commercialization is underway worldwide. Many demonstrations of superconducting power cables connected to real power grids have been conducted with various designs depending on the voltage levels of the distribution and transmission lines. In Korea, the Korea Electric Power Corporation (KEPCO) has fully funded the Shingal Project, the first commercial project of high temperature superconducting (HTS) power cables to connect two substations with a 23 kV HTS cable over a distance of 1 km, and it has started operations successfully.

The advantage of superconducting cables, which have been rapidly developed in recent years, is their capability to transmit 5–10 times more capacity than those of feeders of the same size, making them an excellent means of avoiding building new substations and replacing transmission cables. Given these advantages, studies on how to utilize superconducting cables are required in high load density urban areas where installing new substations and transmission cables is hindered by mounting public opposition.

The author conducted a study to supply power to urban areas using 23 kV HTS cables and proposed a new power system model called the HTS power platform to prove the method's feasibility. This platform refers to the new configuration of an electric power grid composed of two to three 23 kV switching stations connected with each other by the 23 kV HTS cables in urban areas with high load densities and land costs. The size of the 23 kV switching stations is only 20%–30% of that of the conventional 154 kV substations.

However, the disadvantage of the conventional HTS cable (three phases in one cryostat; triad type) is that it is not easy to utilize further owing to its high investment cost. As an alternative, the development of tri-axial HTS cables without using HTS shield wires, such as those used in the AMPACITY project in Germany, enables cost reductions, but a limitation of the cooling system keeps the HTS cables from exceeding a length of 1 km. Thus,

technical improvements in tri-axial HTS cables are needed to configure the HTS power platform.

This study verifies that the cable distance can be increased to 3 km by improving the cooling configuration of tri-axial HTS cables from the conventional internal circulation to an external circulation channel for liquid nitrogen(LN<sub>2</sub>). Consequently, the urban power supply area of the HTS power platform can be expanded with considerable flexibility. In addition, the economic impacts of construction environments, such as land costs, underground structures, and HTS cables were verified by modeling them as mathematical factors. Furthermore, the optimal circuit number and capacity ratings of HTS cables are presented through the design algorithm development of the 23 kV HTS cable system, which is a key facility for the HTS power platform. This enabled a detailed verification for the installation of an HTS power platform in a real grid in consideration of the N-1 reliability criteria and resulted in an increased feasibility of the 23 kV tri-axial HTS cables.

This doctoral dissertation is among a series of studies developing new configurations for an HTS power platform using 23 kV HTS power cables, and it consists of six chapters. Chapter 1 presents the background, purpose, and outline of this paper. Chapter 2 describes the configuration of the 23 kV tri-axial HTS cable system with an external return path for LN<sub>2</sub>. Chapter 3 introduces the new design of the HTS power platform for urban power supply. Furthermore, it explains the estimation process for the prices of tri-axial HTS cables and a cooling system. Chapter 4 describes the economic evaluation of the HTS power platform with a load supply capacity of up to 300 MVA in consideration of its construction environments, life cycle cost and benefit, and closed-loop or radial type configuration. In particular, a comparison of the total investment cost of the HTS power platforms is described to present an appropriate HTS cable rating selection that corresponds well to the HTS power platform. Chapter 5 describes the demonstration of the 23 kV 60 MVA closed-loop HTS power platform in an actual power grid. Finally, chapter 6 summarizes the results and discusses future issues.

# CONTENTS

---

## CHAPTERS

### ABSTRACT

<b>1 INTRODUCTION .....</b>	<b>1</b>
1.1 Electric power grid for an urban power supply	1
1.1.1 Rapid load growth and high load density in urban areas	1
1.1.2 Increasing public opposition to construction of electric power facilities	3
1.1.3 Strategies for improving social acceptability	5
1.2 Challenge of hub-type 154 kV substation for an urban power supply	7
1.2.1 Background of hub-type substation implementation	7
1.2.2 Specification of hub-type 154 kV substation	8
1.2.3 Lessons learned from hub-type 154 kV substation	9
1.3 Recent progress of HTS power cables applications	11
1.3.1 Progress of HTS power cables worldwide	12
1.3.2 Progress of HTS power cables in south Korea	14
1.3.3 Commercial operation of 23 kV HTS power cable	20
1.3.4 Challenges preventing massive adoption of HTS cables	23
1.4 Objectives and contributions of this study	25
<b>2 CONFIGURATION OF 23 kV TRI-AXIAL HTS POWER CABLES</b>	<b>27</b>
2.1 Comparison of various types of HTS power cables	27

2.2	LN <sub>2</sub> circulation method for tri-axial cable structure	29
2.2.1	Design consideration of core structure	29
2.2.2	Tri-axial cable structure by LN <sub>2</sub> circulation method	34
2.3	Engineering factors of 23 kV tri-axial HTS cable	37
2.4	Configuration of cooling system	41
<b>3</b>	<b>DESIGN OF 23 kV HTS POWER PLATFORM FOR URBAN POWER SUPPLY</b>	<b>43</b>
3.1	Basic data of conventional power system	43
3.1.1	Construction cost of 154 kV substation	43
3.1.2	Installation cost of 154 kV cables	45
3.1.3	Construction cost of underground structures	45
3.2	Cost calculation of 23 kV tri-axial HTS cable system	48
3.2.1	Cost calculation procedure of 23 kV HTS power cable	48
3.2.2	Cost calculation procedure of cooling system	54
3.3	Basic application of 23 kV HTS power cables	58
3.3.1	Hybrid power system with HTS power cables	58
3.3.2	Elimination of 154 kV substation	59
3.3.3	Relocation of 154 kV substation	60
3.3.4	Other applications of 23 kV HTS cables	62
3.4	New application design of 23 kV HTS power platform	64
3.4.1	Description of HTS power platform	64



3.4.2	Configuration of 23 kV switching station	66
3.4.3	Detailed configuration of HTS power platform	69
3.4.4	Fault current mitigation	74
<b>4</b>	<b>ECONOMIC EVALUATION OF 23 kV HTS POWER PLATFORM UP TO 300 MVA</b>	<b>77</b>
4.1	General requirements for economic analysis	77
4.1.1	The scope of analysis	77
4.1.2	Analysis method	79
4.1.3	Calculation of operation costs	82
4.1.4	Calculation of benefit	83
4.2	Economic evaluation of radial-type 23 kV HTS cable application to replace 154 kV conventional cables	87
4.2.1	Total investment cost of 23 kV HTS cable for substation elimination	87
4.2.2	Total investment cost of 23 kV HTS cable for substation relocation	92
4.2.3	Life-cycle cost and benefit of 23 kV HTS cable compared with the conventional method	95
4.3	Economic evaluation of 23 kV HTS power platform with two or three 23 kV switching stations	98
4.3.1	Configuration of HTS power platform up to 300 MVA capacity	98
4.3.2	Total investment cost of a 23 kV HTS power platform by load supply capacity and configuration types	101
4.3.3	Life-cycle cost and benefit analysis of HTS power platform compared with conventional methods	109
4.3.4	Economic impact of land price in urban areas	116
4.3.5	The cost effects of an external single return path of $LN_2$	117
4.4	Optimal rating selection of 23 kV HTS power cables for a 23 kV HTS power platform by load supply capacity	119

4.4.1 A 23 kV HTS power cable rating for an HTS power platform comprising two 23 kV switching stations	119
4.4.2 A 23 kV HTS power cable rating for an HTS power platform comprising three 23 kV switching stations	120
<b>5 INSTALLATION OF 23 kV 60 MVA HTS POWER PLATFORM IN A REAL GRID</b>	122
5.1 Site selection for 23 kV 60 MVA HTS power platform	123
5.2 Configuration of 23 kV 60 MVA HTS power platform	126
5.3 Fault current mitigation of 23 kV loop-type HTS power platform	129
<b>6 CONCLUSIONS</b>	132
<b>REFERENCES</b>	135
<b>PAPERS LIST</b>	140

## LIST OF FIGURES

---

- Figure 1.1      Trend of national power demand growth and urbanization
- Figure 1.2      KEPCO's plan for construction of high-voltage transmission lines is being met with mounting public opposition
- Figure 1.3      Various underground structures for the installation of electric power cables
- Figure 1.4      Financial compensation area for the surrounding communities around the transmission lines or substations
- Figure 1.5      Floor design of 154 kV hub-type substation
- Figure 1.6      The HTS technology readiness levels for the various electric power application
- Figure 1.7      Demonstration of 275 kV/3 kA 30 m-HTS cables in China
- Figure 1.8      Worldwide HTS power cable projects
- Figure 1.9      Demonstration projects of 23 kV and 154kV HTS AC power cables and 80 kV HTS DC cables in actual power systems, including the 154 kV Icheon and Jeju substations, were conducted and completed successfully
- Figure 1.10     23 kV HTS cable system configuration of the Shingal Project in south Korea
- Figure 1.11     A block diagram and 3D design of the cooling system configuration for the 23 kV HTS power cable in Shingal Project
- Figure 1.12     The cooling performance test results of the product refrigerator
- Figure 1.13     A 23 kV HTS cable installation and joint works at Shingal substation (M/H #1 – M/H #3 section)

- Figure 1.14 Normal joint box and termination were installed
- Figure 1.15 Power system operation and protection schemes were reviewed when the substation was linked with the 23 kV HTS cable
- Figure 1.16 The current curve of the 23 kV HTS power cable in real operation from July 16 to Sep. 14, 2019
- Figure 1.17 The temperature curves on the inlet and outlet of the 23 kV HTS power cable in real operation from July 16 to Sep. 14, 2019
- Figure 1.18 Projects of HTS power cable (Length vs. Voltage)
- Figure 2.1 The structure of three phase in one cryostat type and tri-axial type of distribution voltage level HTS cable
- Figure 2.2 Cooling system configuration of AC 154 kV HTS cables (single phase in one cryostat) demonstrated in Jeju, Korea
- Figure 2.3 View of the tri-axial HTS cable where the cooling is done within the innermost cryostat and an outer cryostat
- Figure 2.4 Maximum temperature of LN<sub>2</sub> along the cable length
- Figure 2.5 Distance where the maximum temperature of LN<sub>2</sub> occurred by the cable length
- Figure 2.6 Maximum temperature distribution by the heat resistivity and mass flow rate of LN<sub>2</sub> at (a) 1 km , (b) 2 km, and (c) 3km
- Figure 2.7 Function of layers of tri-axial HTS cable
- Figure 2.8 The Design process of the cooling system
- Figure 3.1 Various types of underground structure including duct pipe, cable box and cable tunnel
- Figure 3.2 The structural difference between transmission or distribution cable allocation in the pipe duct
- Figure 3.3 The procedure for designing the HTS cable to calculate the number of HTS tapes
- Figure 3.4 The structure of HTS cable core

- Figure 3.5 The number of HTS tapes corresponding to cable capacity by considering the size of former, HTS tape, and vacuum insulation layers with outer cryostat and jacket
- Figure 3.6 The price of the HTS cables by capacity and by distance
- Figure 3.7 The results of calculating the investment cost of a tri-axial HTS cable and the cooling system by distance.
- Figure 3.8 Path for superconducting wire cost reduction by volume
- Figure 3.9 The structure of EBA terminations (a) for three phase in one cryostat HTS cable (b) for tri-axial HTS cable
- Figure 3.10 The investment cost of cooling system by cooling capacity based on a combination of 5 kW and 10 kW cooling systems
- Figure 3.11 The results of the cost estimates of the cooling system by the 23 kV tri-axial HTS cable capacity
- Figure 3.12 The conventional method used to install substations in urban areas
- Figure 3.13 The concept of a hybrid power system combined with 23 kV HTS power cables.
- Figure 3.14 (a) the conventional method requires the construction of a new 154 kV substation at the center of loads (b) the HTS method requires only 23 kV switching stations
- Figure 3.15 The substation can be relocated to the outskirts of towns by replacing 154 kV cables with 23 kV HTS cables
- Figure 3.16 (a) conventional method of substation relocation  
(b) hybrid power system configuration with 23 kV HTS cables in conduits
- Figure 3.17 The application of the HTS cables to connect the distributed energy resources(DER) including solar PV farm, wind farm, etc.
- Figure 3.18 Conceptual diagram of conventional power system and proposed HTS power platform
- Figure 3.19 The circuit number of 154 kV underground cables by length in KEPCO's power system
- Figure 3.20 The load density distribution of substations by supply area

- Figure 3.21 Layout of a small substation with two story building on the cross sectional area of  $1,200 \text{ m}^2$
- Figure 3.22 Simplified layout of a 23 kV switching station with single story building on the cross sectional area of  $180 \text{ m}^2$
- Figure 3.23 HTS power platform with three switching stations linked with 23 kV HTS cables, which is a new power system configuration for power supply in urban areas
- Figure 3.24 The HTS power platform with two 23 kV switching stations linked with 23 kV HTS cables
- Figure 3.25 The shape of an HTS power platform can be either ring type or line type. The ring type consists of HTS cable network fed from a single substation and 2–3 switching stations in the middle
- Figure 3.26 A platform consisting of two stations with 120 MVA load supply capacity and every HTS cable connecting between stations has a capacity of 90 MVA
- Figure 3.27 On a platform of two stations with 120 MVA capacity, the optimal number of lines can be five, not six
- Figure 3.28 A platform consisting of two stations with 120 MVA load supply capacity and every HTS cable connecting between stations has a capacity of 120 MVA
- Figure 3.29 A platform consisting of three switching stations with the same 120 MVA supply capacity and (a) with the 90 MVA HTS cables (b) with the 120 MVA HTS cables
- Figure 3.30 First peak limiting resistor type superconducting fault current limiter (SFCL)
- Figure 3.31 The SFCL can be divided into the first peak limiting type, and the first peak non-limiting type
- Figure 4.1 Life cycle cost analysis (LCCA) includes investment cost, operation cost, and replacement cost
- Figure 4.2 Application of 23 kV HTS cables to replace the 154 kV transmission cables and 154 kV substations
- Figure 4.3 (a) The investment cost of conventional method and 90 MVA HTS cables by distance and the percentage of distance taken up by the cable tunnel  
(b) The investment cost of conventional method and 120 MVA HTS cables by distance

- Figure 4.4 The land price difference that makes the investment cost of the conventional method and the HTS only method the same when two 90 MVA HTS cables are applied
- Figure 4.5 The land price difference that makes the investment cost of the conventional method and the HTS alone method the same when two 120 MVA HTS cables are applied
- Figure 4.6 Total investment cost comparison between conventional and HTS cable application method considering the land cost \$4 million of substation (distance 2 km and 3 km, respectively)
- Figure 4.7 If 23 kV HTS cables are applied rather than a bundle of distribution feeders, less expensive conduits can be constructed instead of a cable tunnel
- Figure 4.8 The investment cost by distance when two circuits of 120 MVA HTS cables are installed
- Figure 4.9 The overall change in total investment cost due to land price changes
- Figure 4.10 A 30-year load increase model and the sequential installation of 23 kV switching station for the two-station platform
- Figure 4.11 The construction of the two 23 kV switching stations by phases based on the demand forecast for the two-station platform
- Figure 4.12 A 30-year load increase model and the sequential installation of 23 kV switching station for the three-station platform
- Figure 4.13 The construction of the two 23 kV switching stations by phases based on the demand forecast for the three-station platform
- Figure 4.14 The total investment cost of HTS power platform based on the load supply capacity the capacity of 23 kV HTS cables
- Figure 4.15 For the three-station platform, loop-type configuration seems to be more economical
- Figure 4.16 For the two-station platform, radial-type configuration seems to be more economical
- Figure 4.17 The comparison of the investment costs and BCRs between the two-station or three-station platform with the same load-supply capacity by the HTS cable capacity

- Figure 4.18 Total investment cost of HTS power platform by the land price
- Figure 4.19 Cost comparison between conventional method and HTS power platform
- Figure 4.20 Cost comparison of 1 Go-1 Return and 2 Go-1 return
- Figure 4.21 The total investment cost of the HTS power platform based on the load supply capacity and the capacity of 23 kV HTS cables according to the 23 kV switching station's capacity
- Figure 4.22 The total investment cost of the three-station loop-type HTS power platform by the capacity of 23 kV HTS cables
- Figure 4.23 The total investment cost of the three-station radial-type HTS power platform by the capacity of 23 kV HTS cables
- Figure 5.1 One cell of the 23 kV HTS power platform
- Figure 5.2 The demonstration project of an 23 kV 60 MVA HTS power platform between KEPCO's 154 kV Munsan and Sunyou substations
- Figure 5.3 The configuration of a cooling system installed in the Sunyou substation to cool the superconducting cables on both sides together
- Figure 5.4 The temperature and pressure profiles of a cooling system installed in the Sunyou substation
- Figure 5.5 The configuration of the cooling systems installed separately in the Munsan and Sunyou substations to achieve higher reliability of power supply
- Figure 5.6 The temperature and pressure profiles of the two cooling systems installed separately in the Munsan and Sunyou substations
- Figure 5.7 Load flow analysis on the HTS power platform based on KEPCO's 8<sup>th</sup> long-term transmission expansion plan



## LIST OF TABLES

---

Table 1.1	Number of public complaints and substation construction delay
Table 1.2	Specification of hub-type 154 kV substation
Table 1.3	Specification of 23 kV HTS power cable system of the Shingal Project in south Korea
Table 1.4	The effect of sharing the supply capability between two substations during test operation
Table 2.1	The configuration of superconducting cables according to their structure including the improved tri-axial HTS cable with external return pipe
Table 2.2	Tri-axial HTS cable structure by LN2 circulation method
Table 2.3	Temperature and pressure difference by circulation method and by cable length of tri-axial cable
Table 2.4	Verification tests of HTS cables considering engineering factors
Table 3.1	The total construction cost breakdown for a 154 kV substation with a total capacity of 240 MVA
Table 3.2	The cost sample of purchasing the substation site by categories
Table 3.3	The cost of the double circuit 154 kV XLPE cables by length
Table 3.4	The construction cost of various underground facilities by distance
Table 3.5	Cost breakdown of 23 kV tri-axial HTS cables(120 MVA, 3 CCTs)
Table 3.6	The average construction cost of the small distribution transformer stations in Myeong-dong, Seoul
Table 4.1	The values for 154 kV substation construction

Table 4.2	The amount of carbon emission per unit megawatt-hour based on 2011 data from the Korea Power Exchange
Table 4.3	The average emission trading price of the Korea Power Exchange between January and April 2019
Table 4.4	The economic indicators based on the land price when constructing a substation in the center of loads located 2 km away from existing substations
Table 4.5	The economic indicators based on the land price when constructing a 23 kV switching station connected with two 23 kV 90 MVA HTS cables
Table 4.6	The economic indicators based on the land price when constructing a 23 kV switching station connected with two 23 kV 120 MVA HTS cables
Table 4.7	The investment cost breakdown of two-station loop-type HTS power platform (120 MVA $\times$ 2 stations)
Table 4.8	The investment cost breakdown of two-station loop-type HTS power platform (150 MVA $\times$ 2 stations)
Table 4.9	The investment cost breakdown of three-station loop-type HTS power platform (120 MVA $\times$ 3 stations)
Table 4.10	The investment cost breakdown of three-station loop-type HTS power platform (150 MVA $\times$ 3 stations)
Table 4.11	The investment cost breakdown of three-station radial-type HTS power platform (150 MVA $\times$ 3 stations)
Table 4.12	The specifications of conventional method and the HTS power platform with the load supply capacity of 240 MVA
Table 4.13	The specifications of conventional method and the HTS power platform with the load supply capacity of 300 MVA
Table 4.14	The BCR and IRR of the two-station HTS power platform with the load supply capacity of 240 MVA
Table 4.15	The BCR and IRR of the three-station HTS power platform with the load supply capacity of 240 MVA
Table 4.16	The BCR and IRR of the two-station HTS power platform with the load supply capacity of 300 MVA

Table 4.17	The BCR and IRR of the three-station HTS power platform with the load supply capacity of 300 MVA`
Table 5.1	Six 154 kV substation candidate locations derived from the eighth long-term transmission expansion plan of KEPCO
Table 5.2	The result of the load flow analysis for the HTS power platform
Table 5.3	The fault currents before and after the installation of the HTS power platform

# CHAPTER 1

## INTRODUCTION

### 1.1 Electric power grid for an urban power supply

#### 1.1.1 Rapid load growth and high load density in urban areas

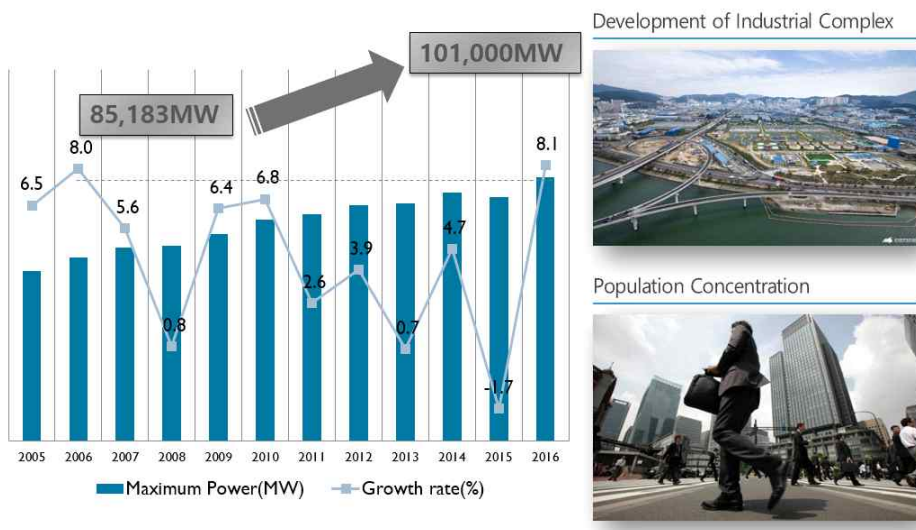


Fig. 1.1 Trend of national power demand growth and urbanization

The Korean economy has achieved very rapid economic growth of more than 8%–10% a year since the 1960s. As a result, per capita GDP increased from only 12% of that of the U.S. in the 1970s to 62% in 2010. Along with economic growth, electricity demand has also increased significantly. However,

the economic growth rate has decreased slightly since the 1990s, although it still appears to be higher than that of developed countries. As shown in Fig. 1.1, from 2005, the power demand and power demand growth rate graphs have still shown growth rates of 5%–8%. The electricity demand growth rate has decreased to below 5% since the 2010s; however, it is still growing at a very fast pace compared to that in advanced countries. Further, the peak demand has steadily increased from 85,153 MW in 2005 to 101,000 MW in 2016 [1]. In particular, power demand tends to be focused locally owing to industrial park development plans and urbanization. In addition, power demand growth is estimated to remain at 2%–3% for now owing to the increasing use of electronic devices in everyday life. The expected electricity demands must inevitably be accompanied by the construction of power plants and a grid construction plan to transmit them. Experts have predicted that the need for large power transmission networks could change thanks to the recent introduction of decentralized power sources; however, the reality is that power grids are more important than ever for connection and transmission with large renewable power complexes. In addition, the increased load density in urban areas due to urbanization necessitates the construction of power facilities to send more capacity. Technological developments in power systems inevitably focus on increasing capacity and improving efficiency. The government is also actively pushing for the expansion of traditional power facilities as well as the introduction of new technologies such as high voltage direct current (HVDC) and flexible alternating current transmission system for solving problems such as power transmission congestion that are caused by regional imbalances between supply and demand.

A long-term transmission expansion plan, including the construction of new substations and transmission lines, has been established based on various factors such as economic growth rate, population changes, urban development policies [1]–[2]. The construction of power facilities has been promoted so that loads can be supplied at the right time; however, during such a process, serious construction delays are often caused by public opposition, or the project

itself may be aborted. To overcome these challenges, attempts have been made to increase the size of the substation rather than increasing the number of substations; unfortunately, the projects were not carried out successfully because it was difficult to secure sites for large substations in the downtown area and to connect the several dozens of distribution feeders owing to the constraints on the land for power lines. These projects will be further described with lessons learned in the next subsection 1.2.



Fig. 1.2 KEPCO's plan for construction of high-voltage transmission lines is being met with mounting public opposition

### 1.1.2 Increasing public opposition to construction of electric power facilities

Local residents' strong opposition to the construction of electric power facilities has recently emerged as one of the biggest social issues. The frequent issues raised by residents are mainly noise, problems related to electromagnetic fields (EMF), and falling property values. However, ultimately, residents are very dissatisfied with the unsightly environmental degradation caused by power

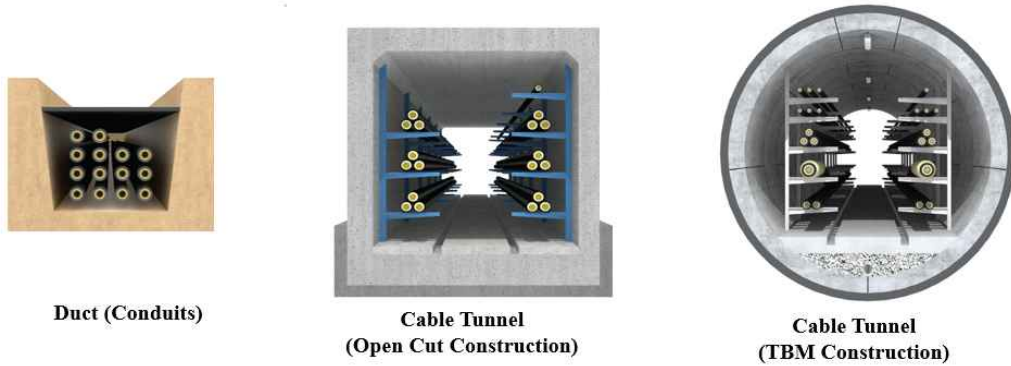


Fig. 1.3 Various underground structures for the installation of electric power cables

facilities and its impact on real estate values. The new standard of social acceptability is important in this regard. The issues of social acceptability, and economic efficiency have been greatly highlighted recently as they call for the active resolution of residents' complaints during the licensing process of local governments for all matters, such as new construction or extension of power facilities. To enhance social acceptability, KEPCO has established and applied measures to mitigate damage to residents and to compensate them financially. However, they remain a long way from satisfying residents' desires. Fig. 1.2 shows local residents' opposition and the media's coverage showing negative reporting attitudes.

Residents' opposition to the reduction of property value and environmental hazards in the areas surrounding power facilities often leads to arguments calling for an underground construction. Underground construction is largely divided into three types, as shown in Fig. 1.3. Direct burial or duct construction with the installation of conduits is the cheapest underground construction method; it costs around \$2 million per km and has the advantage of minimizing the construction space. If the number of cables increases above 9 or 10, then duct construction cannot accommodate all the cables. In such cases, cable boxes should be installed with the open cut method. In some difficult construction environments, tunnel construction is inevitable when cable

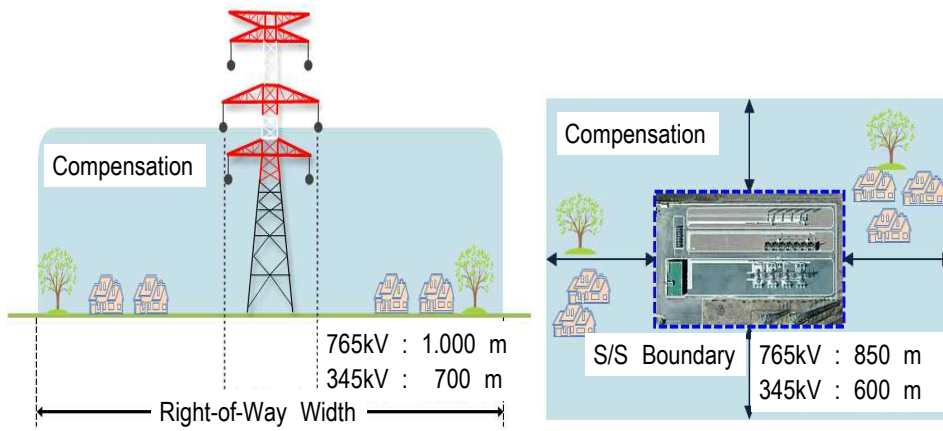


Fig. 1.4 Financial compensation area for the surrounding communities around the transmission lines or substations

boxes are difficult to install, which requires construction at a depth of 60 m below ground level; further, the construction method requires the use of shield tunnel boring method (TBM), and therefore, the unit cost of construction is five times higher at approximately US\$10 million. Around 20% of underground construction often requires cable tunnel construction owing to difficult construction environments such as river crossings, densely populated areas, or heavy traffic areas [3].

### 1.1.3 Strategies for improving social acceptability

Various measures are being considered and applied in practice to enhance social acceptability. While it would be a priority to devise such a method if a technological alternative could be found, it often poses the problem of excessive investment costs. Where necessary, financial support is available where financial compensation is sought. Fig. 1.4 shows a case in which the legal distance of compensation for support around a steel tower or substation is prescribed [4]. For the construction of the power line, support projects are carried out up to 1 km away from the transmission line, and for the substation, support is provided up to 850 m away from the substation. Houses located at a shorter distance are either purchased or land price compensation is



offered. This process could reduce opposition to the construction of power facilities such as steel towers and simultaneously increase social acceptability. Nevertheless, cases that still require an underlying construction or claim to change to a lower voltage reveal the increasingly difficult aspects of power facility construction projects. Fortunately, it is encouraging that the various new technologies that have been introduced in recent years can offer various measures on a case-by-case basis. For example, introducing new technology facilities, such as HVDC, may be effective at locations that inhibit fault currents or require long-range, high-capacity transmission. In the past, it was expected that the need for the extension of the transmission system may be reduced owing to the installation of distributed energy resources using solar or wind power; however, the demand for the grid has increased more than ever owing to the recent large-scale and distant deployment of new and renewable sources such as wind power. Fortunately, the introduction of smart grids along with the introduction of energy-saving energy storage systems suggests new possibilities to increase system efficiency, and it seems that the company has begun opening the door to a new paradigm for power systems. It is expected that the rapid development of superconducting technology will further enhance its usability in the power system while many diverse methods are being explored. In the next subsection, the superconducting cable technology that is gaining the most attention among superconducting technologies will be explained.

## 1.2 Challenge of hub-type 154 kV substation for an urban power supply

In this subsection, the progress made in the mid-2000s will be reviewed when the peak load increased very rapidly and substations were being constructed urgently. The construction of large-scale substations, called hub-type substations, was pushed forward to address power system expansion during this period. However, critical constraints during operations have left hub-type substation being abandoned. The lessons learned from the trials and errors caused by hub-type substations faced during their operations will be discussed [5].

### 1.2.1 Background of hub-type substation implementation

The need for stable power supply in areas with high load density, such as large-scale housing and industrial complexes, has increased over time. The introduction of a new concept of power supply with economies of scale was urgently needed to overcome opposition from residents and ease difficulties in securing substation sites. In 2007, the number of civil petitions per unit project and delayed completion date were increasing, as shown in Table 1.1, owing to a situation in which timely substation construction was becoming very difficult with the increasing difficulty of securing substation sites.

Table 1.1 Number of public complaints and substation construction delay

Year		2001	2003	2003	2004	2005
Construction opposition	number of petitions per substation	1.25	1.45	2.12	3.19	3.90
	number of petitions per km of transmission lines	0.27	0.3	0.37	0.34	0.35
Construction delay	substations	15	18	22	22	24
	transmission lines	10	13	15	14	16



uncertainties such as a sudden load increase. The supply capacity of a substation with three banks installed is considered to be 120 MVA when considering the N-1 reliability criteria of a single transformer. In comparison, hub-type substations were constructed in areas expected to exceed 200 MW, as shown in Fig 1.5. This is to deal with the case of one bank fault at a substation equipped with four banks of transformers with higher capacity than that of ordinary substations. Supply of 200 MW was considered enough for a population of 200,000 or an area of nearly 4,000 hectares. On the other hand, most large industrial parks have a much smaller area of  $\sim 500$  hectares. The load density of the new town is  $4.5 \text{ MW/km}^2$  and that of the industrial park is  $44 \text{ MW/km}^2$ . This corresponds to the high-density subregion on the left-hand side of the load density curve. The supply of electricity in areas with high load density remains a major. Table 1.2 shows the specifications of the 154 kV hub-type substation. In fact, nine hub-type substations had been selected for installation in the Seoul metropolitan area, four of which have been constructed and are in operation.

Table 1.2 The Specifications of hub-type 154 kV substation

Item	Specification	Item	Specification
Transformer	8 banks (60 MVA $\times$ 8)	Shunt facility	40 MVar (5 MVar $\times$ 8)
Rating of circuit breaker	50 kA	Connection type	cable box (both directions)
Number of GIS bays	(Transmission) underground 8 (Distribution) underground 4	154 kV bus	4,000 A double-bus type

### 1.2.3 Lessons learned from hub-type 154 kV substation

The site of the 154 kV substation had an area of  $3,300 \text{ m}^2$ , and the hub-type substation, which is equivalent to two substations, required an area of  $\sim 4,400 \text{ m}^2$ , thereby reducing the required area by 34%. Economy of scale was

also realized in terms of the facility investment, resulting in a  $\sim 30\%$  reduction (\$16 million) in the total investment cost. Despite achieving this economic feasibility, during actual operation, a very real challenge was faced with the 48-line connection to underground power lines. Large-scale cable box tunnel construction was carried out for connecting multiple power lines. In this process, a double cable box tunnel had to be built on both sides of the road; however, getting government approval was very difficult and residents' opposition never reduced. On the other hand, because the substation is not the optimal location for the extraction of power lines, excessive investment in underground construction could have occurred. These constraints have left the hub-type substations being abandoned, contrary to the hopeful expectations, and they have further affirmed that closer power facility planning cooperation between the distribution and the transmission sides is required. It is expected that hub-type substations will find a renewed role today if technological means are provided to address the route restrictions for the connection of power lines while achieving economies of scale to a certain level through the use of large-scale substations. In this regard, distribution superconducting cable technology, which can eliminate substations or accommodate multiple power lines in a single superconducting cable, seems very promising [7]-[10]. The next chapter discusses the current status of superconducting cable development and superconducting technology.

### 1.3 Recent progress of HTS power cable applications

Significant and rapid technical progress has been made in the area of high-temperature superconductivity (HTS) since its discovery in 1986. HTS wire and power system application developments have progressed toward technology commercialization, and large demonstration projects have been conducted for several applications. The application in which superconductivity has the potential to be effective in an electric power system can be separated into two general classes. The first class includes cables, motors, generators, and transformers where superconductors replace resistive conductors. The second class includes technologies that are enabled by superconductivity and those have little, or at most limited, capability if conventional materials are used. Examples of such technologies are superconducting magnetic energy storage (SMES), fault-current limiters (FCLs), and fault-current controllers (FCCs) [11].

Fig. 1.6 shows the technology readiness levels for various power system applications. The vertical axis units provide a relative scale of the number of

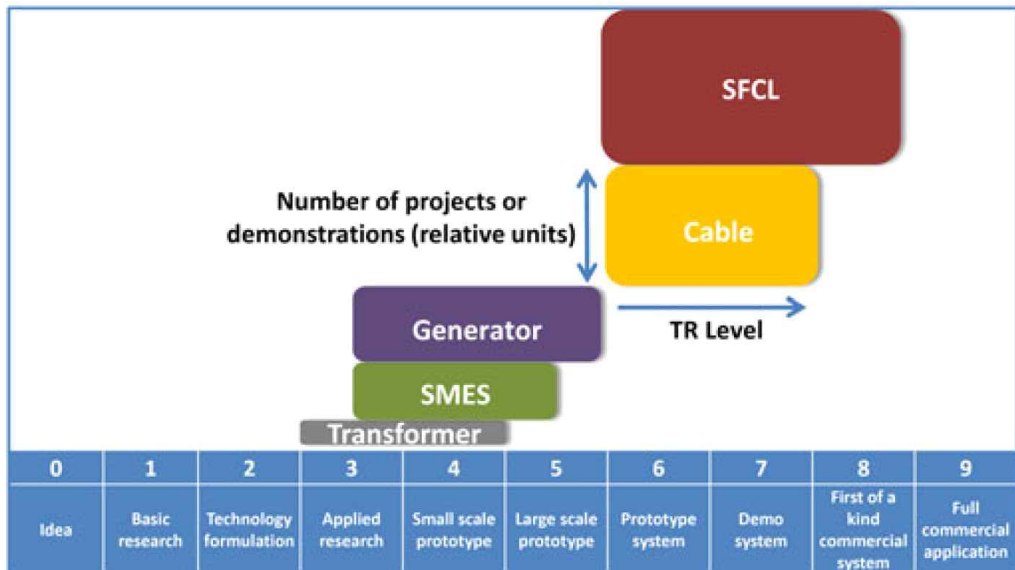


Fig. 1.6 The HTS technology readiness levels for the various electric power application

## Demonstration of 275kV-3kA Cable

### 275kV/3kA 30m-HTS Cable System



Fig. 1.7 Demonstration of 275 kV/3 kA 30 m-HTS cables in China

projects. For instance, there are more superconducting fault current limiter (SFCL) and cable projects than there are other applications [12-13]. This part outlines the current state of HTS cable applications worldwide and describes the commercialization project of 23 kV HTS cables in South Korea.

### 1.3.1 Progress of HTS power cables worldwide

Superconducting cables have been developed for application to power systems owing to their continuous technological innovation and price reduction. Several demonstration projects have been conducted worldwide to promote the availability of superconducting cables.

Generally, distribution superconducting cables are of the three-phase bundle type and three-phase superconducting cable cores are contained in one cryostat. In transmission superconducting cables, each phase superconducting cable core is contained in a separate cryostat. To realize the economic advantages of HTS power cables, as a new concept of 23 kV HTS power cables, tri-axial cable

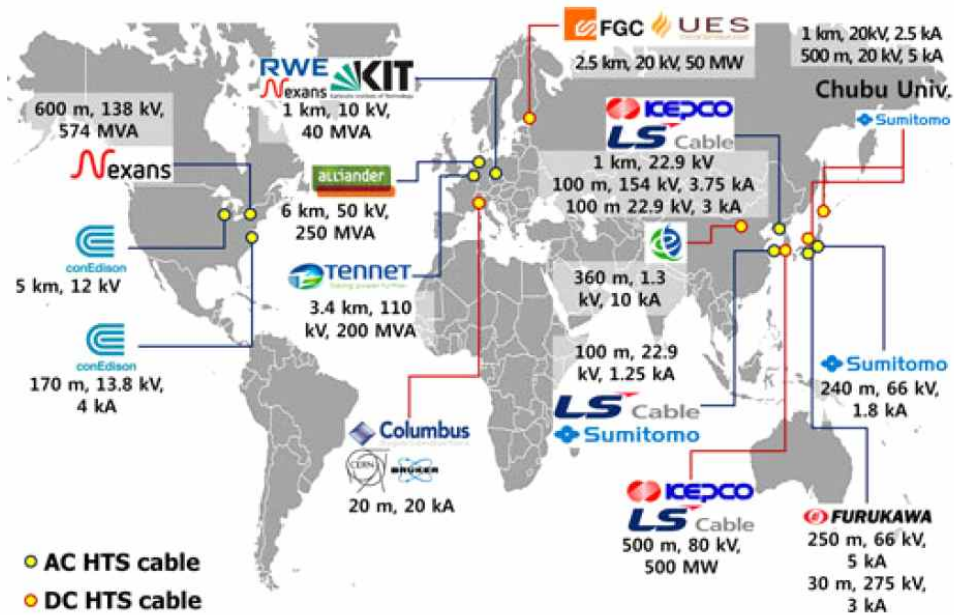


Fig. 1.8 Worldwide HTS power cable projects

was proposed. Tri-axial superconducting cables in which superconducting conductors of each phase are arranged on the same central axis to reduce superconducting shield wires, are emerging as the next generation of power distribution superconducting cables. Development of tri-axial superconducting cables has already begun in many countries, and some countries and organizations have completed development testing and are working on the installation of a real grid system connection [7]. Countries and organizations around the world have been developing and operating various types of superconducting power cables to meet future demands for electricity. Fig. 1.8 shows HTS power cable projects worldwide [11].



### 1.3.2 Progress of HTS power cables in south Korea

Over two decades, superconducting cable systems has been developed and demonstrated in Korea under government sponsorship with collaborating among joint industrial-academic research laboratories, national research institutes, corporations and KEPCO, as shown in Fig. 1.9. The related industry and academia in Korea have made urgent efforts to accelerate the development of HTS cable system, which has been proven through long-term research and demonstration projects. The following is an excerpt from the author's study[6].

Simultaneously, the promotion of price reduction of HTS cables and the development of HTS cable markets also need to be coordinated. From June 2001, the R&D projects for realizing HTS power system application has been started with the name of Development of Advanced Power system by Applied Superconductivity technologies (DAPAS) Program.

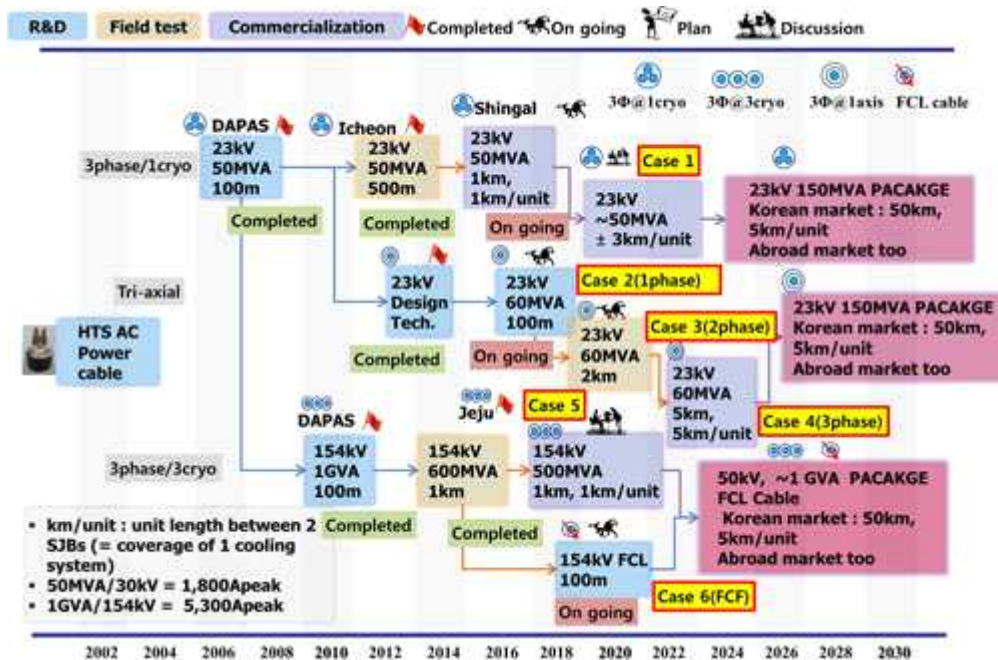


Fig 1.9 Demonstration projects of 23 kV and 154 kV HTS AC power cables and 80 kV HTS DC cables in actual power systems, including the 154 kV Icheon and Jeju substations, were conducted and completed successfully in South Korea

In addition, Since 2008, the pilot demonstrations has been successfully performed through Icheon and Jeju Projects including AC 23 kV and AC 154 kV as well as DC 80kV class HTS power cables [14-19]:

- AC 23kV 50 MVA at Icheon substation
- AC 154 kV 600 MVA and DC 80kV 500MW  
at Superconducting power apparatus center in Jeju

Based on those demonstrations, Korea Electric Power Corporation (KEPCO) which is only electric utility in Korea has launched a plan to commercialize AC 23 kV HTS cables in actual grid, called the Shingal Project. Now, commercial operations are ready to start. In particular, through the Shingal Project, the Korean HTS society is proud to have received the honour of being recognized as the first country in the world to deploy a commercial HTS AC power cable [20-21], and is pursuing the challenge of this new technological expansion as it will have great significance worldwide. Further, the authors expect that the success of this commercial project to contribute greatly to introduce the new trend of superconducting power grid in the future.

In this project, AC 23 kV 50 MVA cable system composed of 1 km long cable, two sets of normal joints and two sets of terminations as well as cryogenic cooling system with 10 kW capacity have been installed between AC 23 kV distribution busbars of 154 kV Shingal and Heungdeok substations, as shown in Fig. 1.10.

Table 1.3 lists the configuration of the 23 kV 50 MVA HTS cable system and triad type HTS cable applied in this project. The 23 kV HTS power cable system in the Shingal Project had a rated a capacity of 50 MVA, rated current of 1,260 A, and nominal voltage of 22.9 kV for the distribution line. This cable was divided by three spans by considering transportation regulation and interval of existing underground structure and approximately 150 km HTS wire has been employed. Especially, at the design stage, two different kinds of HTS wire have been determined to be applied for satisfying manufacturing schedule. For the first and the third span from Shingal substation, the second generation (2G) wires, i.e. ReBCO, and for the middle span generation (1G) wires, i.e.



Fig. 1.10 A 23 kV HTS cable system configuration of the Shingal Project in South Korea

BSCCO, have been employed, as described in Tables 1.3 and 1.4.

Each span of cable have spliced via jointing material inside of normal joint without direct contact of wires of each cable span. Therefore, there was no physical and electrical malfunction to transmit load current in entire length of cable because the ratio between total rated current and critical current is designed to maintain below 50% to reduce in normal condition even though the critical current of two types' of HTS wire is a little different. However, manufacturing process, jointing methods are slightly different. This differences are expected to be a useful comparison in terms of reliability as well as cable maintenance during long term operations.

Table 1.3 The Specifications of 23 kV HTS power cable system of the Shingal Project in South Korea

Items	Unit	Specification
Rated capacity	MVA	50
Rated current /nominal voltage	kA / kV	1.26 / 22.9
HTS power cable type		Triad configuration
Total length of HTS cable	m	1,035
Number of joints	EA	2
HTS tapes		1G / 2G
Total length of the HTS wire used	km	150
Cooling System Design	kW	7.5kW@69 K Turbo-Brayton and decompression
Operation Condition (Temperature and Pressure)	K, bar-g	66~77K, under 10 bar-g
Operation Condition (Mass Flow Rate)	Kg/s	0.4~0.6

Table 1.4 Specification of applied HTS wires

Specification	YBCO (2G)	BSCCO (1G)
Min. DC $I_c$ (@77.3K,sf)	150A	170A
Dimension (W×T) [mm]	4.4 × 0.35	4.4 × 0.35
PLY	3-PLY	3-PLY

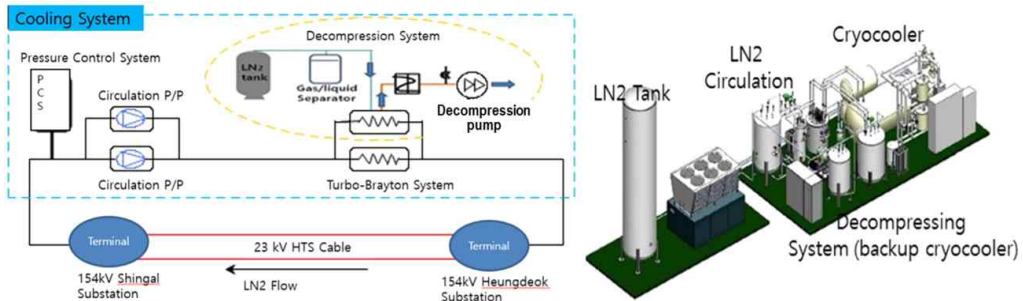


Fig. 1.11 A block diagram and 3D design of the cooling system configuration for the 23 kV HTS power cable in Shingal Project

The cooling system composed of Turbo-Brayton refrigeration system with about 10-kW cooling power as a primary use and an open-loop decompression unit as a backup with the same cooling power has been installed to maintain the stable operation of the HTS cable system. Especially, it is the first application of large cooling power system to prepare long distance HTS cable system similar to the conventional cable's application. Fig. 1.11 shows a system composition diagram with instruments and a three-dimensional illustration of the cooling system.

The performance test result on cooling system to verify its the design value of 10 kW at 70 K has been carried out by artificial load test, as depicted in

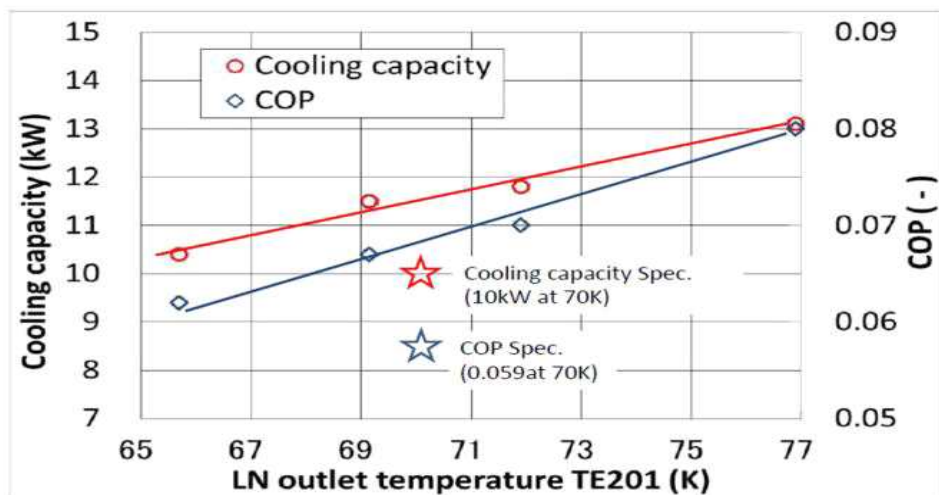


Fig. 1.12 The cooling performance test results of the product refrigerator

Fig. 1.12. In this test, the coefficient of performance (COP) of the refrigerator on the HTS power cable was measured to be 0.059 at 70 K.

After starting the construction of the cooling system installation in Oct. 2017 and signing a contract with LS Cable in Mar. 2018, the superconducting cable installation began in Oct. 2018. In Nov. 2018, the cooling system was completed and the test run was conducted. After the bobbin test of the conduit, HTS cables were installed from Dec. 2018. There was an empty conduit along the cable route between the Shingal and Heundeok substations; therefore, no conduit construction cost other than cable installation costs was incurred. Starting in Mar. 2019, the installation and commissioning test of the cooling system monitoring system were conducted, and vacuuming and liquid nitrogen circulation cooling of the cables began. In September 2019, the trial operation for two months was completed successfully. Now, it's in operation.

Figs. 1.13 and 1.14 show the cable, joint boxes and termination installation for the Shingal project. The 23 kV HTS cables can be installed using conventional cable pulling techniques.



Fig. 1.13 A 23 kV HTS cable installation and joint works at Shingal substation (M/H #1 – M/H #3 section)





Fig. 1.14 Normal joint box and termination were installed

### 1.3.3 Commercial operation of 23 kV HTS power cable

Project motivation is briefly described as follows. Shingal is the name of the residential district which is expected getting population in growth. For this reason, KEPCO had to build a new substation in Shingal area to transmit more power to this area because the existing Shingal substation was already full-banked. By contrast, Heungdeok substation around 1 km away from Shingal substation has two extra places for additional transformers.

In this regards, KEPCO considered to apply 23kV HTS cable by connecting 23 kV bus bars between substations instead of conventional 154 kV underground cable by installing a 154k V step-down transformer in Heungdeok substation as a result from the case study between two solutions comparing HTS application and conventional one. By analyzing economic evaluation between two cases, KEPCO figured out that HTS cable application is cheaper than the conventional cable application by cutting the project cost as 15%p and which was the main reason to proceed this project.

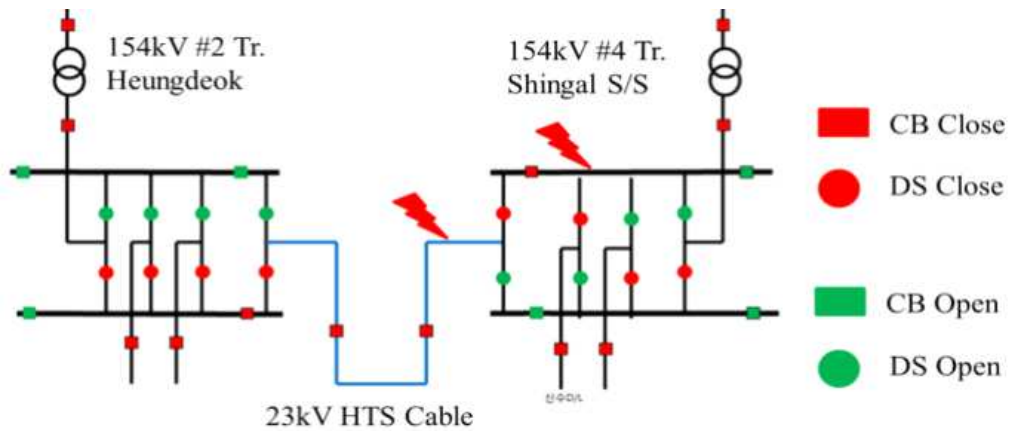


Fig. 1.15 Power system operation and protection schemes were reviewed when the substation was linked with the 23 kV HTS cable

Power system operation and protection schemes has been reviewed when the two substations were linked with the 23 kV HTS cable, as shown in Fig. 1.15. For the reason that the 154 kV Shingal substation has loads of upto 162 MW compared to the 49 MW load of the 154 kV Heungdeok substation, it is expected to share some of the Shingal substation's load through the HTS power cable with the Heungdeok substation. However, considering that this is the first use case of the 23 kV HTS cable in an actual power system and that #4 transformer at Shingal substation has been connected to two feeders and the load of one feeder will first be supplied through the HTS cable and further load sharing will be considered in the future.

Operation measures also have been established for contingency cases of HTS cables, breaker failure, and bus failure. Further, the installation of bus section breakers has been reflected for stable and efficient system operation in case of HTS cable system failure or maintenance.

AC 23kV HTS cable connection is planned to have the effect of sharing the supply capability between the two substations. In addition, emergency supply through the HTS cable will be possible during a complete blackout of AC 154 kV Heungdeok substation. In the past, two simultaneous failures of AC 154 kV transmission lines led to a blackout of AC 154 kV Heungdeok substation,



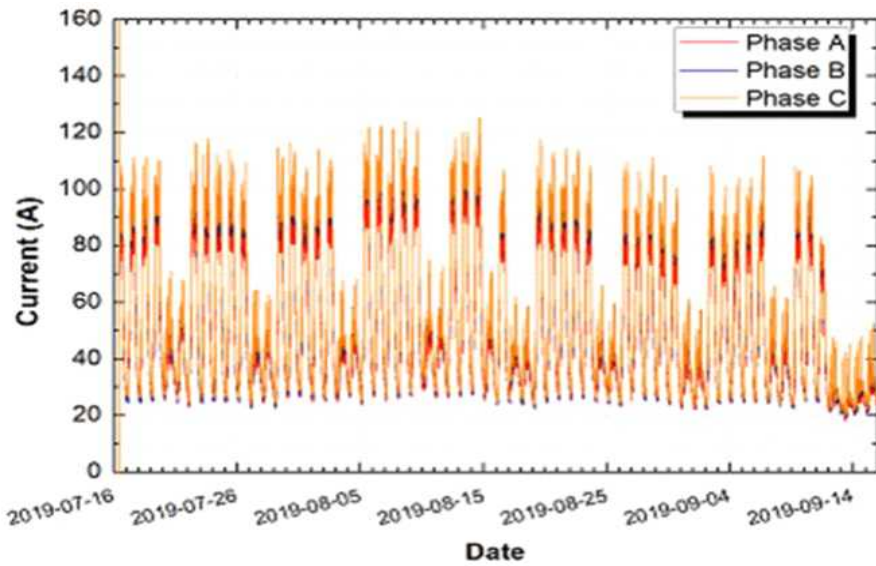


Fig. 1.16 The current curve of the 23 kV HTS power cable in real operation from July 16 to Sep. 14, 2019

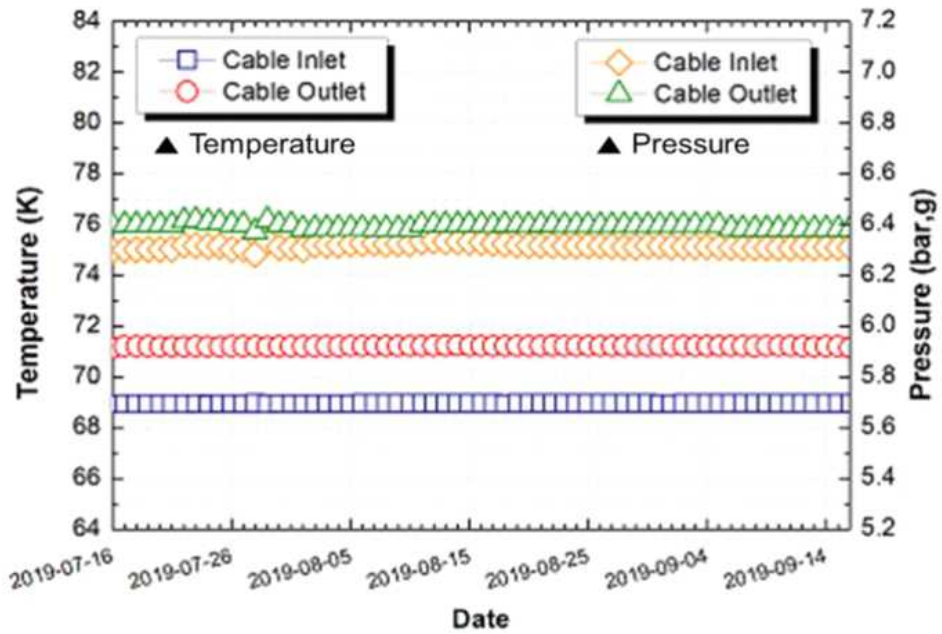


Fig. 1.17 The temperature and pressure of the 23 kV HTS power cable in real operation from July 16 to Sep. 14, 2019

resulting in an outage of up to 49 MW. Now, the system reliability has been greatly improved as power can be supplied through HTS cables before recovering the transmission lines.

The operation current of the 23 kV HTS power cable for 2 months was shown in Fig. 1.16. The temperature and pressure curves were confirmed to be maintained well for over 2 months of test operation, as shown in Fig. 1.17. The inlet and outlet temperatures were measured to be almost 69 K and 71 K, respectively. The inlet and outlet pressures were also stable from 6.3 bar,g to 6.4 bar,g. In terms of the specific heat of LN<sub>2</sub> and mass flow rate of 0.5 kg/s, the temperature differences of 2 K between cable inlet and outlet means a heat loss of 2 kW, therefore it is possible to verify that the system is operating very satisfactorily.

#### **1.3.4 Challenges preventing massive adoption of HTS cables**

Although more than 30 years have passed since the discovery of high temperature superconductor in 1986, many technical challenges remain. Cost and economics are unquestionably the greatest challenges. The basic metric used to assess how cost-effective HTS wires, and consequently, HTS cables, is the cost per kiloampere-meter. This is because higher critical currents result in less HTS wire needed for the same power transfer. For now, HTS cables have cost in the range of a few 100 \$/kAm; this makes HTS solution uncompetitive from cost viewpoint because the corresponding cost for copper and other conventional cabling materials is still a fraction of this value [12][22-23].

The price of cables per unit transmission capacity applied at the actual site seems to be \$3,000 for the 154 kV XLPE cables and around \$19,000 for the CNCE cable, which is most commonly applied as a 23 kV distribution feeder. These values are the average values obtained from KEPCO's purchase statistics. In comparison, the three phase in one cryostat (or triad type) 23 kV HTS cable costs \$110,000; this is around six times higher than the cost of conventional power distribution cables.

The price of superconducting cables, which is an important variable to

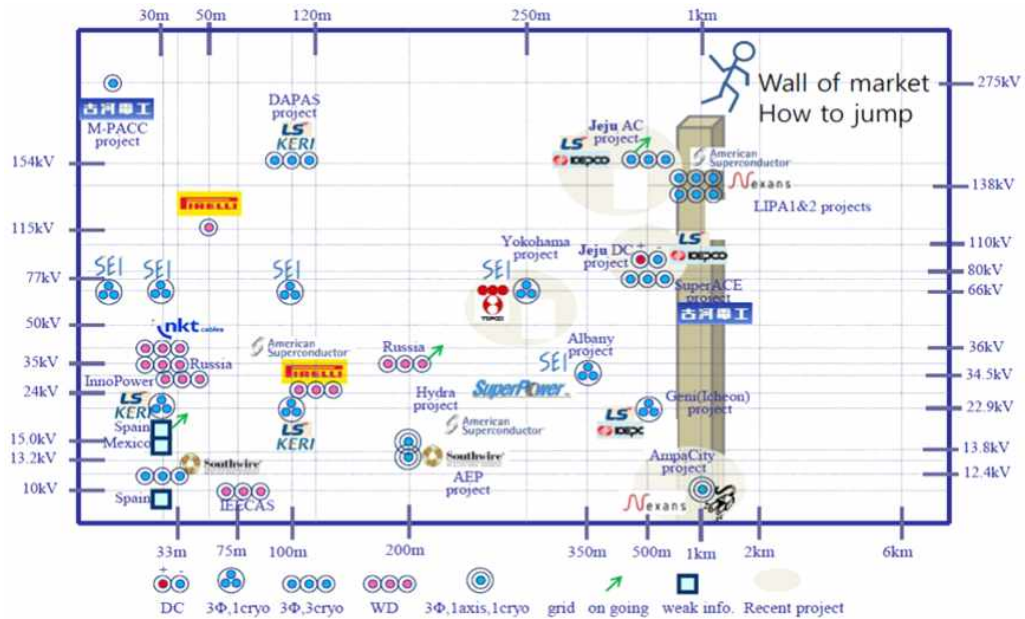


Fig. 1. 18 Projects of HTS power cable (Length vs. Voltage)

determine their economic status, is closely related to the growth of the cumulative sales volume of superconducting cables, and the growth of this market can be expected to fall in the future. For example, data released by the Yano Economic Research Institute in Japan showed that Japan's superconducting cable market is likely to grow rapidly in the future and reach 150 billion yen by 2030. Nonetheless, before market expansion, how to cross the cable length barrier and how much the price of the excessively expensive HTS cable can be lowered remain unclear, as shown in Fig. 1.18 .

Cooling is another significant cost component, even with  $\text{LN}_2$  systems, because cooling requirements and refrigeration costs are high. Although cryogenics has steadily advanced to provide higher efficiency at lower cost, the HTS power industry is still too small to achieve enough manufacturing scale for realizing a significant cost impact [13].

## **1.4 Objectives and contributions of this study**

When constructing a new substation, it is advantageous to construct it at the center of the loads for loss minimization; however, it is not easy to secure a substation site in urban areas with high load density owing to the very high land prices, complex permission processes, and social acceptability issues. This has led to an increase in investment costs, either owing to the failure to construct a substation in a timely manner or the need to relocate the substation outside urban areas.

The advantage of superconducting cables, which have been rapidly developed in recent years, is their capability to transmit 5–10 times more capacity than those of feeders of the same size, making them an excellent means of avoiding building new substations and replacing transmission cables. Given these advantages, studies on how to utilize superconducting cables are required in high load density urban areas where installing new substations and transmission cables is hindered by mounting public opposition.

The author has conducted a study to supply power to urban areas using 23 kV HTS cables and proposes a new power system model called the HTS power platform to prove the method's feasibility. This platform refers to the new configuration of an electric power grid composed of two to three 23 kV switching stations connected with each other by the 23 kV HTS cables in urban areas with high load densities and land costs. The size of the 23 kV switching stations is only 20%–30% of that of the conventional 154 kV substations.

However, the disadvantage of the conventional HTS cable (three phases in one cryostat; triad type) is that it is not easy to utilize further owing to its high investment cost. As an alternative, the development of tri-axial HTS cables without using HTS shield wires, such as those used in the AMPACITY project in Germany, enables cost reductions, but a limitation of the cooling system keeps the HTS cables from exceeding a length of 1 km. Thus, technical improvements in tri-axial HTS cables are needed to configure the HTS power platform.

This study verifies that the cable distance can be increased to 3 km by improving the cooling configuration of tri-axial HTS cables from the conventional internal circulation to an external circulation channel for liquid nitrogen(LN<sub>2</sub>). Consequently, the urban power supply area of the HTS power platform can be expanded with considerable flexibility. In addition, the economic impacts of construction environments, such as land costs, underground structures, and HTS cables were verified by modeling them as mathematical factors. Furthermore, the optimal circuit number and capacity ratings of HTS cables are presented through the design algorithm development of the 23 kV HTS cable system, which is a key facility for the HTS power platform. This enabled a detailed verification for the installation of an HTS power platform in a real grid in consideration of the N-1 reliability criteria and resulted in an increased feasibility of the 23 kV tri-axial HTS cables.




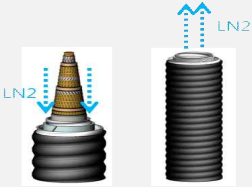
As KEPCO has been increasing the efficiency of power facility investments and operations by standardizing the capacity of substations and power transmission lines, it is expected that standardization can be used to form a superconducting power platform through the relationship between 23 kV switching station capacity and cable capacity rating derived through this study. In the near future, the demonstration of the 23 kV 60 MVA HTS power platform will be carried out in an actual power grid between the 154kV Munsan and Sunyou substations.

## CHAPTER 2

### CONFIGURATION OF 23 kV TRI-AXIAL HTS POWER CABLES

#### 2.1 Comparison of various types of HTS power cables

Table 2.1 The structures of superconducting cables according to their specifications including the tri-axial HTS cable with an external return pipe

Configuration Type	Usage	Structures
Single core HTS cable (single phase in one cryostat)	High capacity High voltage ( $\sim 138$ kV)	
Three-core HTS cable (three phases in a common cryostat or triad type)	High capacity Mid voltage ( $\sim 70$ kV)	
Three-phase concentric HTS cable (tri-axial type or three concentric phases in one cryostat)	Mid capacity Mid voltage, low voltage (13.8 – 50 kV)	
Improved tri-axial cable (three-phase concentric HTS cable with an external return pipe for LN <sub>2</sub> )	Mid capacity Mid voltage (22.9 kV)	

The superconducting cable mainly consists of core parts and cryostat parts, as shown in Fig. 2.1. The cable core consists of formers to support the winding of superconducting wires and bypass fault currents, superconducting wire layers, PPL paper insulation layers, and shield layers. The cable cryostat consists of an internal tube that circulates liquid nitrogen for cable cooling, an outer tube with a vacuum insulation layer, and a jacket to prevent corrosion of the cryostat and protect the cable. The superconducting cable for transmission voltage is similar to the conventional cable with a single-phase cable structure, whereas the superconducting cable for distribution-class voltage is divided into three-phase in one cryostat type or concentric tri-axial type considering its insulation characteristics. Tri-axial superconducting cables, such as those used in the German Ampacity Project, have the advantage of significantly lowering the price of superconducting cables because the shield layer does not need HTS wires. However, the cooling channel consisting of two inner and outer cryostats in the cable indicates that the temperature profile is not uniform, making long distance transmission difficult. In this study, the HTS cable configuration was improved by installing an external return path of  $\text{LN}_2$  separately to enable long distance cables. Specific details are described in the following subsections. Table 2.1 shows the structures of superconducting cables according to their specifications including the tri-axial HTS cable with an external return pipe.

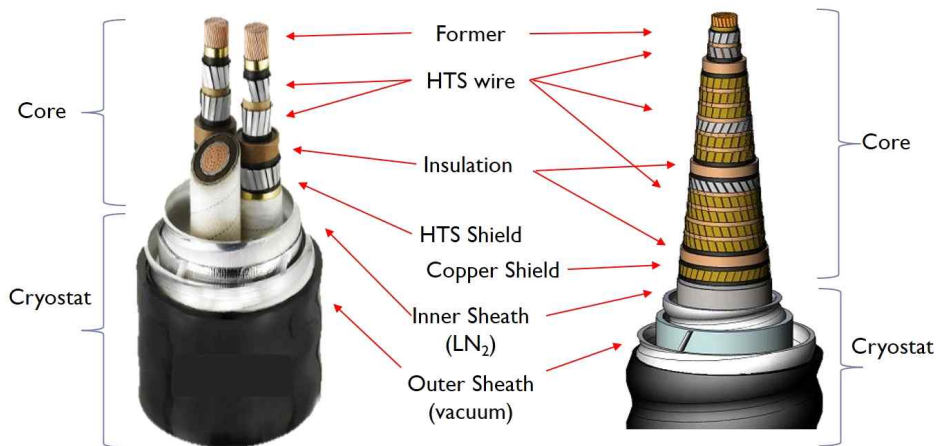


Fig. 2.1 The structure of three phase in one cryostat type and tri-axial type of distribution HTS cable

## 2.2 LN<sub>2</sub> circulation method for tri-axial cable structure

### 2.2.1 Design consideration of core structure

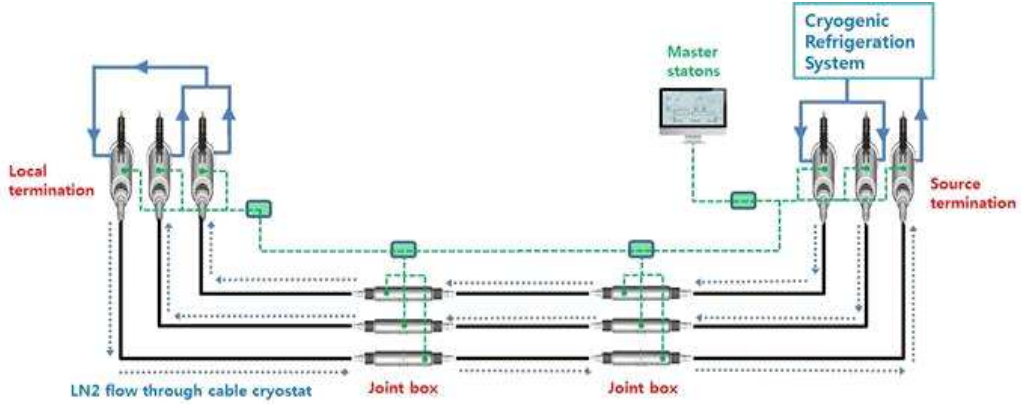


Fig. 2.2 Cooling system configuration of AC 154 kV HTS cables (single phase in one cryostat) demonstrated in Jeju, Korea

LN<sub>2</sub> circulation forms the basis for core design. Because a transmission voltage superconducting cable consists of three single-core types, it is possible to apply either two phases as an inlet and the other one phase as a return outlet (2-Go 1-Return type) or one phase as the LN<sub>2</sub> inlet and the other two phases as the LN<sub>2</sub> return path (1-Go 2-Return type) without the need for a separate cooling path. In this case, the maximum temperature is seen at the cable outlet. In comparison, it is common for distribution voltage superconducting cables to place three phases in a common cryostat, as it is easy to secure insulation performance due to the low voltage. If we examine the structure of the distribution superconducting cables, it can be divided into triad type, which is arranged in three phases in one cryostat, and tri-axial type, which is arranged in a concentric configuration. The triad type requires a separate LN<sub>2</sub> circulation pipe, in which case the temperature calculation simply follows Eq. 1.

$$Q = mC_p\Delta T \quad (1)$$

where  $m$  is the mass flow rate (kg/s);  $C_p$ , the specific heat of LN<sub>2</sub>; and  $\Delta T$ ,



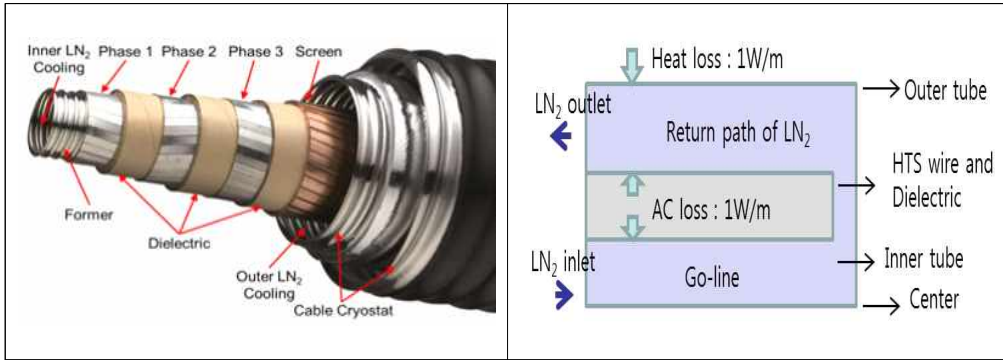


Fig. 2.3 View of the tri-axial HTS cable where the cooling is done within the innermost cryostat and an outer cryostat

the temperature change[°K].

By contrast, temperature profiles should be considered for tri-axial HTS cables. As shown in Fig. 2.3, heat exchange occurs between the inner tube (or center tube) and the  $\text{LN}_2$  flowing through the outer tube, and thus, the temperature distribution varies. Therefore, the maximum temperature of  $\text{LN}_2$  is not likely to occur at the cable outlet. Assuming heat loss and AC loss of 1 w/m, flow rate of 0.4 kg/s, and cable length of up to 1.5 km, Figs. 2.4 and 2.5 show the highest temperature of  $\text{LN}_2$  according to cable length. For example, if the cable length is 800 m, the maximum temperature of  $\text{LN}_2$  appears at  $\sim 700$  m. In addition, the  $\text{LN}_2$  flow between the inner tube and the outer tube shows that the use of the inner tube as Go ( $\text{LN}_2$  inlet) can lower the maximum temperature.

Therefore, the effect of increasing the cable length was checked by using the inner tube as Go. To increase the length required for cable cooling, the most important factors are to increase the heat resistivity or increase the  $\text{LN}_2$  flow rate; however, as thermal resistivity increases, materials such as polypropylene laminated paper and the cable thickness should be changed, and increased  $\text{LN}_2$  flow rate requires an increased external diameter of the cable owing to increased differential pressure. The effects were reviewed by varying the maximum length of the cable as 1, 2, and 3 km. It is assumed that heat

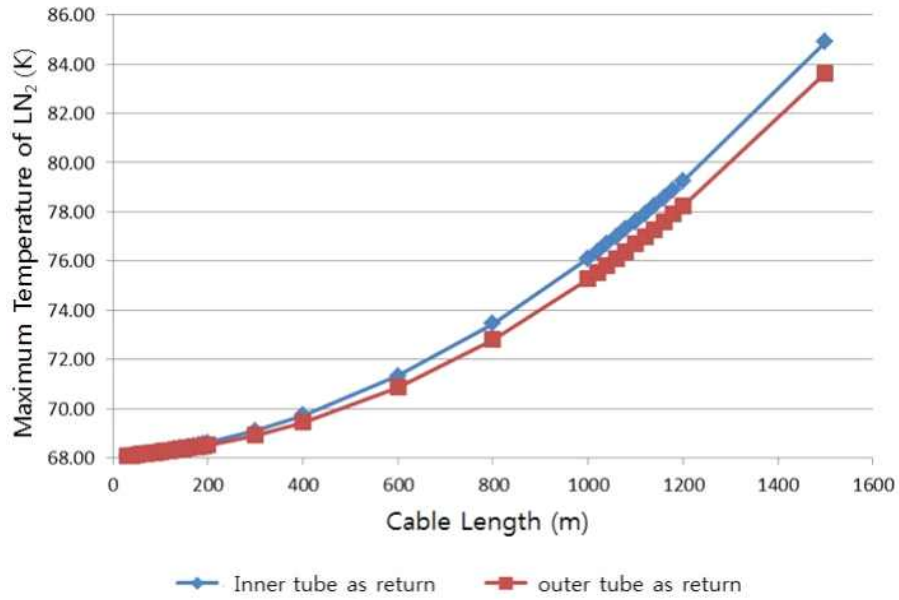


Fig. 2.4 Maximum temperature of LN<sub>2</sub> along the cable length

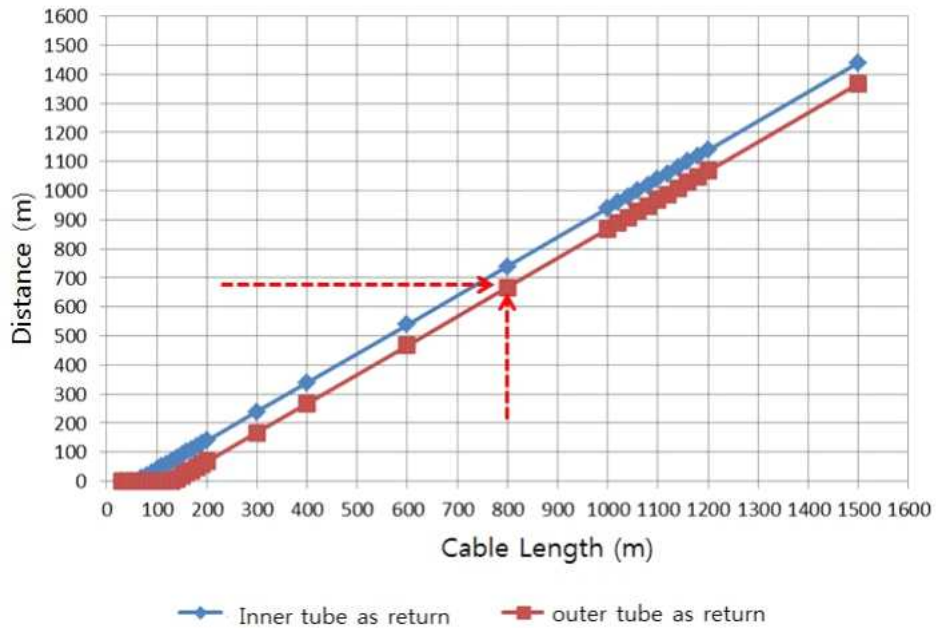


Fig. 2.5 Distance where the maximum temperature of LN<sub>2</sub> occurred by the cable length

loss and AC loss are kept the same as before at 1 W/m and that the outer tube is used for the return path of  $\text{LN}_2$ , starting with an initial flow rate of 0.5 kg/s and controllable according to the differential pressure. The heat resistance of the junction box and terminal is not considered. Figs. 2.6(a), (b) and (c) show the analysis results for this case. When considering the cryostat specifications by distance up to 3 km, the thermal resistance requires six times more insulation. In addition, the only material with a thermal resistivity of more than six times is air, and a flow rate of more than 1 kg/s requires a significant increase in external diameter owing to differential pressure. As a result, because the technical limitations have been identified, a separate return path of  $\text{LN}_2$  for tri-axial cable cooling should be considered for long-distance cooling [24].

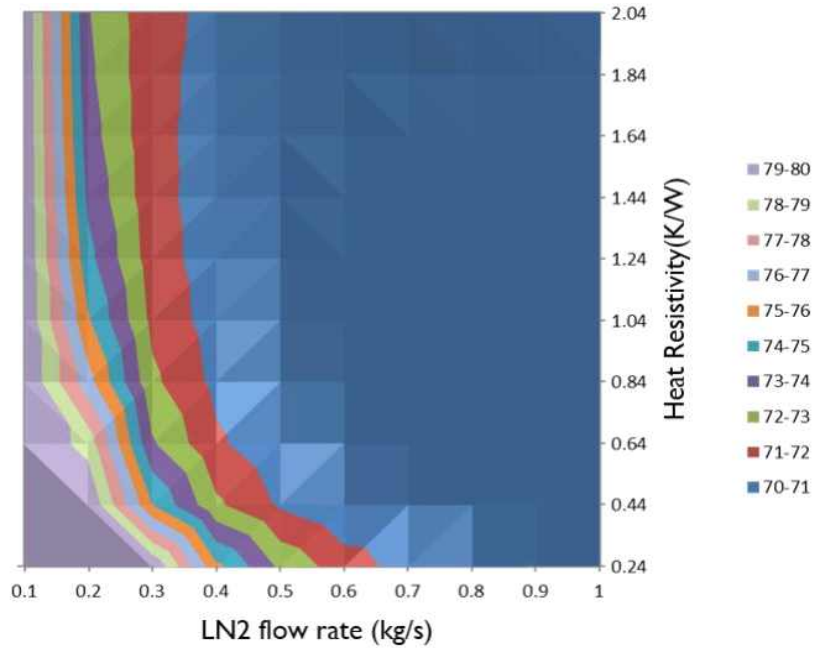


Fig. 2.6 (a) The maximum temperature effects of the cable length as 1 km by  $\text{LN}_2$  flow rate and heat resistivity

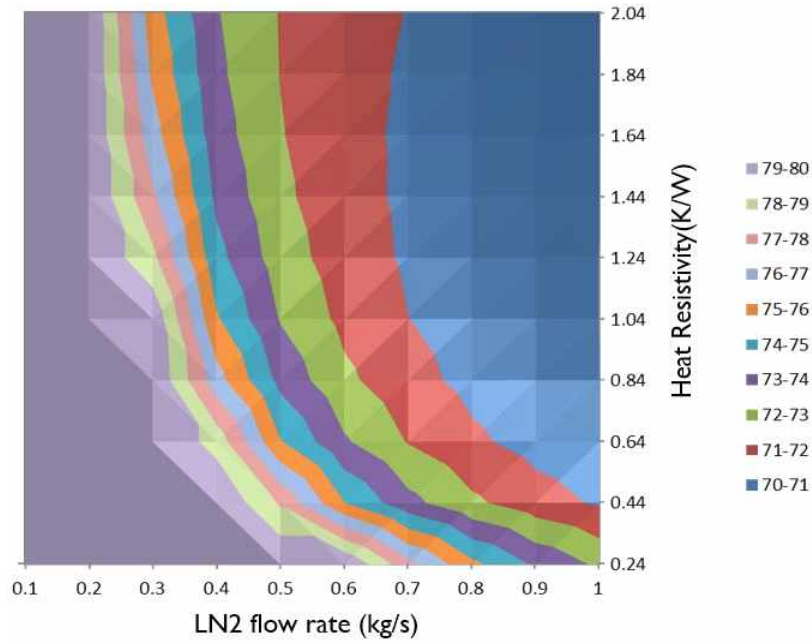


Fig. 2.6 (b) The maximum temperature effects of the cable length as 2 km

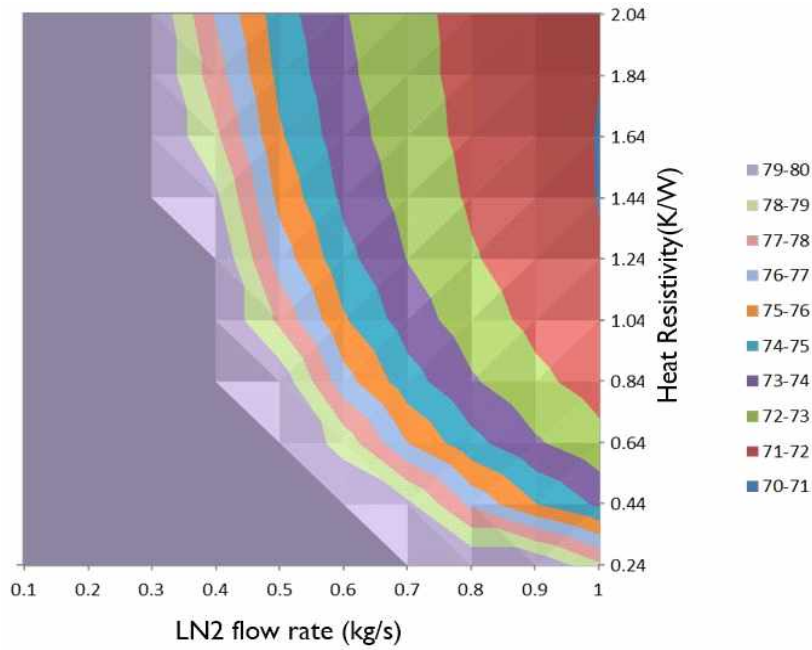


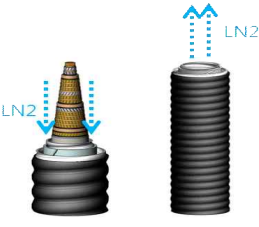


Fig. 2.6 (c) The maximum temperature effects of the cable length as 3 km

### 2.2.2 Tri-axial cable structure by LN<sub>2</sub> circulation method

Table 2.2 Tri-axial HTS cable structure by LN<sub>2</sub> circulation method

	Circulation method	Advantages	Disadvantages
Case 1 (internal Sheath as GO → center tube as Return)		<ul style="list-style-type: none"> <li>- no external return pipe</li> <li>- one conduit for one cable</li> </ul>	<ul style="list-style-type: none"> <li>-larger cable diameter</li> <li>- bad temperature profile</li> <li>- higher temperature than that in Case 2</li> </ul>
Case 2 (center tube as GO → internal sheath as Return)		<ul style="list-style-type: none"> <li>- no external return pipe</li> <li>- one conduit for one cable</li> </ul>	<ul style="list-style-type: none"> <li>-larger cable diameter</li> <li>- bad temperature profile</li> <li>- poor performance for long-distance cooling</li> </ul>
Case 3 (internal sheath as GO → external pipe as Return)		<ul style="list-style-type: none"> <li>-smaller cable diameter</li> <li>-good temperature profile</li> <li>- longer distance of cooling possible</li> </ul>	<ul style="list-style-type: none"> <li>-external return pipe necessary (two conduits for one cable and one return pipe)</li> </ul>

As shown in Table 2.2, the site applicability of the three types of tri-axial cables according to their  $\text{LN}_2$  circulation structure is reviewed. The analysis conditions were the same as before, namely, AC loss and heat loss of 1 W/m, terminal loss of 500 W each, and junction box loss of 20 W. The flow rate is also set at 0.5 kg/s and the initial inlet temperature is set at 68 K. Considering the duct pipe construction conditions, the outer diameter of the cable shall not exceed 153 mm when using an corrugated hard polyethylene pipe (ELP) of 200-mm diameter and not exceed 131 mm when using an ELP of 175-mm diameter. The temperature range of 68–77 K and pressure of 6–17.5 bar G are set.

Table 2.3 summarizes the temperature and pressure changes, indicating that the maximum temperature in Case 1 is always higher than that in Case 2. Case 2 may be appropriate at 500 m or 1 km but was shown to exceed the design margin at 3 km. In comparison, Case 3 with an external separate return pipe shows that the temperature and pressure met the criteria even at 3 km and that the external diameter can be installed easily in 175-mm ELP distribution conduits. It has been shown that the external return path of  $\text{LN}_2$  should be installed separately. Subsequently, all tri-axial superconducting cables in this study will be based on tri-axial cables using an external return pipe. It is also confirmed that there is an advantage to sharing one external return pipe with up to two lines of tri-axial HTS cables rather than using one external pipe per cable, because there is room for cooling capacity when using an external pipe.

Table 2.3 The temperature and pressure difference by LN<sub>2</sub> circulation method and cable length of tri-axial HTS cable

Case	Temperature and pressure difference	unit	0.5 km	1.0 km	3 km
Case 1	$\Delta T$ (min – max)	[K]	4.0	9.3	54.6
	$\Delta T$ (inlet – outlet)	[K]	2.1	3.2	7.7
	$\Delta P$ (diameter: 134 mm)	[bar G]	4.5	9.1	27.1
	$\Delta P$ (diameter: 151 mm)	[bar G]	1.2	2.4	7.2
Case 2	$\Delta T$ (min – max)	[K]	3.0	7.8	51.1
	$\Delta T$ (inlet – outlet)	[K]	2.1	3.2	7.7
	$\Delta P$ (diameter: 134 mm)	[bar G]	4.5	9.1	27.1
	$\Delta P$ (diameter: 151 mm)	[bar G]	1.2	2.4	7.2
Case 3	$\Delta T$ (min – max)	[K]	2.1	3.2	7.7
	$\Delta T$ (inlet – outlet)	[K]	2.6	4.2	10.7
	$\Delta P$ (diameter: 134 mm)	[bar G]	1.8	3.6	11

### 2.3 Engineering factors of 23 kV tri-axial HTS cable

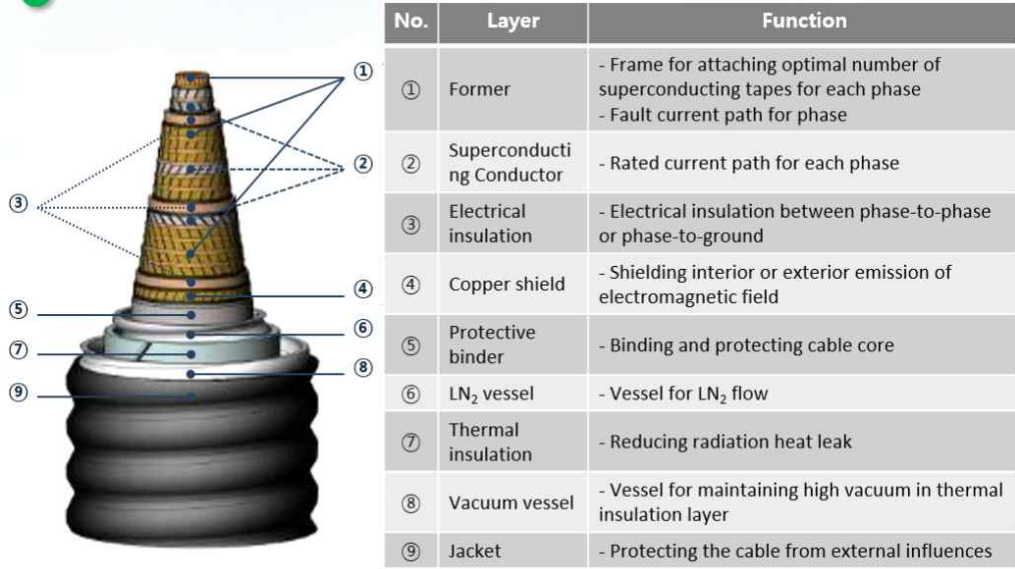


Fig. 2.7 Function of layers of tri-axial HTS cable

In addition to the external return pipe of tri-axial HTS cables, other engineering factors to be considered are explained in this subsection. Fig. 2.7 illustrates the component-specific functions of tri-axial superconducting cables. The innermost former not only retains the shape of the superconducting cable but also has a structure for layering the superconducting wire. It also acts as a bypass if a fault current occurs, and the temperature rise of LN<sub>2</sub> due to Joule heat needs to be kept below the design value. If the temperature of LN<sub>2</sub> rises above its vaporization temperature, the internal pressure will rise owing to phase transition from the liquid phase to the vapour phase and the insulation performance will be destroyed. The former cross section is designed such that LN<sub>2</sub> remains below its vaporization temperature, as shown in Eq. 2, even at the system's highest fault current of 25 kA for 0.5 s.

$$T_{MAX} + \Delta T \leq T_{LN2} \forall P_{MIN} \quad (2)$$



where  $T_{MAX}$  is the maximum temperature of  $LN_2$  ;  $\Delta T$ , the temperature increase; and  $T_{LN_2}$ , the vaporization temperature of  $LN_2$  at the minimum operation pressure

The number of tapes varies depending on the cross sectional area of the former. So, the former size, which should be the starting point for number of tapes calculation, is determined by the size that limits the amount of heat generated by a fault current to within 20 degrees of  $LN_2$  temperature change. Heat generation due to the fault current of 25kA for the braking time of 0.5 second should equal or be lower to heat loss attributed to the temperature change 20 K for keeping  $LN_2$  from evaporation, as described in Eqs. 3 and 4.

$$I_f^2 R t / 4.2 \leq m C_p \Delta T \quad (3)$$

$$R = \frac{\rho l}{A}, m = D_c A l, \quad (4)$$

where,  $I_f$  is a fault current of 25 kA,  $\rho$ ;  $1.72 \times 10^{-8} \Omega m$ ,  $D_c$ ;  $8.94 \text{ g/cm}^3$ .

Combining Eqs (3) and (4) result in the cross-sectional area of former, as shown in Eq. 5.

$$A \geq I_f \sqrt{\frac{\rho t}{4.2 D_c C_p \Delta T}} \quad (5)$$

The final value obtained is  $282 \text{ mm}^2$ . This equation shows that the crss sectional area of the former is dependent on the fault current and braking time but, not the length of the cable.

Superconducting wires have thresholds for current, temperature, and magnetic fields that affect each other. In particular, if the temperature decreases by 1 K, the critical current increases by 8%–9%, and when tha cable is exposed to external magnetic fields, the critical current decreases. As a result, tri-axial type cables can be affected by the magnetic field of each phase of HTS wires; therefore, impedance balancing is considered very important, and each phase has a different radius and should be designed accordingly. In doing so, the magnetic fields of each phase are offset to minimize the induced current in the external sheath, thereby avoiding the need for superconducting shield layers in tri-axial cables. In addition, AC losses show a nonlinear

increase with the ratio of maximum operating current to critical DC current; the number of HTS wires is determined by considering the range of linear segments within 50% – 60% [25-27].

With regard to insulation characteristics, the insulation thickness is determined by comparing the AC withstand voltage criterion, impulse withstand voltage criterion, and partial discharge generation withstand voltage criterion, which is the same as the general AC cable insulation design. The two phases within the core should consider the phase-to-phase voltage between adjacent phases such as A and B wires or B and C wires and the phase-to-ground voltage between phase C and the outer sheath and between phase A and the former.

With regard to shielding characteristics, the introduction of an imbalance current from the system should be considered. This reflects the OCGR single-point operation value of the power distribution network and the 30% reference of the operational capacity current. Because the inner sheath keeps the core of the cable and functions as an LN<sub>2</sub> circulation channel, the maximum operation pressure is calculated by summing the lowest operation pressure and the pressure loss on the outlet side. Further, no LN<sub>2</sub> leakage should occur. Because the pressure loss is proportional to the square of the circulating flow rate, depending on the engineering design conditions, it can be considered unreasonable to determine compliance through absolute criteria. Secondary sheaths are those constructed to form insulation layers to minimize thermal penetration due to convection, conduction, and radiation. The design of insulation structures is optional for the manufacturers; however, these structures should be free from leakage and mechanical damage and should not cause damage or degradation through mechanical stresses accompanying cooling, etc. Considering these engineering requirements comprehensively, the performance verification test items for the cable requirements that can be presented for the utility are summarized as shown in Table 2.4 [28-30].

Table 2.4 Verification tests of HTS cables considering engineering factors

Layer	Engineering Factors	Verification Test
Former	$T_{Max} + \Delta T \leq T_{LN2} \forall P_{Min}$	Short circuit tests
	$N_{wire} W_{wire} \leq L$	Measurement of cable
HTS wires	Measured value of DC $I_C \geq 95\%$ of design value of DC $I_C$	Critical current measurement
	No more temperature increase at rated current	Load cycle voltage test
	AC loss below design value	AC loss measurement
	AC loss below design value under imbalanced current	AC loss measurement
Insulation	Voltage between phase A and phase B, phase C and ground	AC voltage test
	Lightning impulse insulation	Lightning impulse voltage test
	partial discharge	Partial discharge test
Sheath (cryostat)	AC loss from imbalanced current	AC loss measurement
	Vacuum integrity can be judged as undamaged	Pressure test
	No mechanical breakdown of sheath	Pressure test
	Pressure should not be less than the test pressure after 10 min	Pressure test
	The determined leak rate should not be higher than designed value	Vacuum leak test
Commons	No damage from mechanical stress	Thermal cycle test

## 2.4 Configuration of cooling system

Some of the following is an excerpt from the IEA(International Energy Agency) report [12]. One of the critical components of HTS applications is the cryogenic system. These systems operate at the temperature of LN<sub>2</sub> (77 K or - 196 °C). Several types of cryogenic systems are commercially available, including the Gifford McMahon system, pulse-tube systems, Stirling cycle cryocoolers, and turbo-Brayton cryogenic systems. Other cryogenic systems are being applied, such as an open LN<sub>2</sub> tank and circulation system for a cable and fault current limiter project in Essen, Germany. An open system features lower complexity and potentially high reliability; however, it requires the re-filling of a nitrogen storage tank at regular intervals. A closed system only needs electrical power supply after initial filling; however, it requires higher capital investment and specific methods to ensure availability and reliability.

As shown in Fig. 2.8, the design process of the cooling system starts with the review of the basic cable cooling system data including line lengths, operating conditions, cable joint quantities, and LN<sub>2</sub> circulation routes determined for the selection of the target site [31]. Based on these system design conditions, AC loss, heat loss, etc. are calculated and appropriately reflected in the design margin. Because the cable route may not be flat, the site's geographical conditions should be reflected to consider the pressure changes due to the flexion of the cable's passing area, depth of the vertical shafts, etc. The next procedure selects the cooling system type for the determined design cooling capacity. Because a refrigerator-type cooling system is normally used for main cooling, it is necessary to install a decompression-type cooling system as a backup. AC loss and heat loss calculation will be described in subsection 3.2.

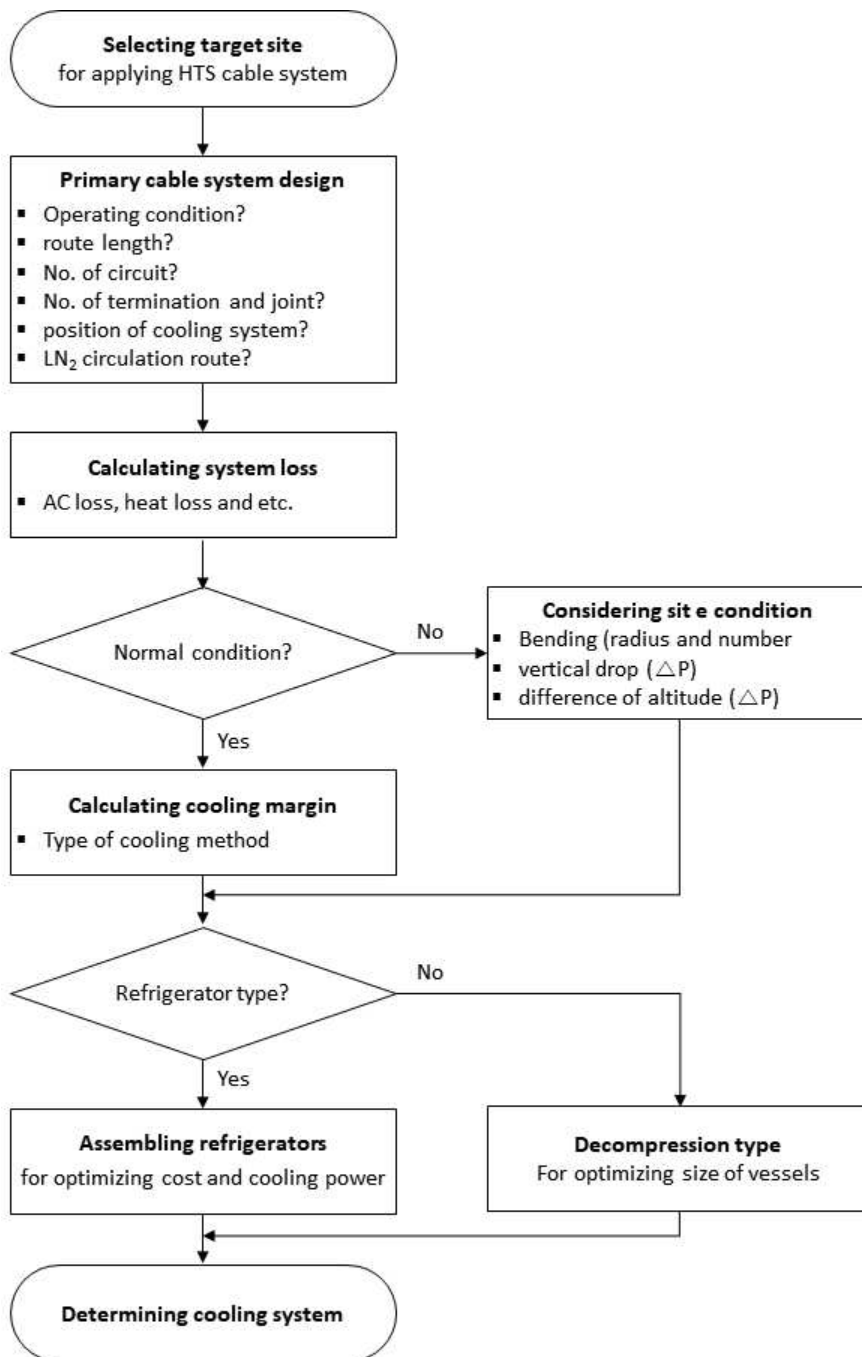


Fig. 2.8 The design process of the cooling system

---

## **CHAPTER 3**

### **DESIGN OF 23 kV HTS POWER PLATFORM FOR URBAN POWER SUPPLY**

---

#### **3.1 Basic data of conventional power system**

In this study, the unit price of conventional power facilities is based on the construction budgetary price of KEPCO in 2018 [32], as explained in following sections.

##### **3.1.1 Construction cost of 154 kV substation**

It is assumed that the new 154 kV substation consists of transformers, gas-insulated switchgear (GIS), other auxiliary devices, and instruments, and it is constructed as a standard type with a building area of 2,500 m<sup>2</sup>. The transformers consist of up to four banks with a capacity of 60 MVA. The GIS facilities include 154 kV GIS Bays for transmission lines and 23 kV GISs for distribution feeders. The total cost of the 154 kV substation facilities is \$4.9 million, including \$3.6 million for the transformers and \$1.3 million for the GIS facilities. Specifically, considering the unit costs, a transformer with a capacity of 60 MVA costs \$0.9 million per bank. One 154 kV GIS bay with a rated current of 2,000 A and a rated short circuit breaking current of 50 kA costs \$0.3 million.

The standard substation building costs around \$2,700 per square meter; therefore, the total cost of a building with area of 2,500 square meters is \$6.8 million. The cost of installing auxiliary facilities and other devices is considered to be 50% of the cost of deploying transformers and GIS, which is

Table 3.1 The total construction cost breakdown for a 154 kV substation with a total capacity of 240 MVA

Required Facilities	Cost (million \$)
Four banks of 154 kV transformer	3.64
Eight 154kV GIS bays	1.32
Building construction (2,500 m <sup>2</sup> )	6.84
Sub total	11.8
Auxiliary facilities and devices (50%)	2.48
Total	14.3

\$2.5 million. As shown in Table 3.1, the total construction cost to build a 154 kV substation with a total capacity of 240 MVA is \$14.3 million. The initial size of the substation is at least two banks of transformers considering the N-1 reliability criteria. Therefore, the load supply capacity of a substation with four banks is considered to be 180 MVA considering the N-1 criteria.

The cost of purchasing the substation site needs to reflect the market price of the land; however, it can be calculated by applying the general guidance of a preliminary feasibility study by the Korean Ministry of Strategy and Finance if the market price is difficult to identify. As shown in Table 3.2, which lists samples of the cost of purchasing substation sites by categories, the large cities applied a market price of \$62.3 million, whereas costs in other areas were calculated by applying the compensation scale for each zoning category of the

Table 3.2 The cost sample of purchasing the substation site by categories

Category	Name of City	Area (m <sup>2</sup> )	Cost (million USD)	Unit cost (\$/m <sup>2</sup> )
Large city	Seoul	1,175	62.3	53,000
New town	Goyang	3,500	6.9	1,970
Small city	Sejong	16,650	4.1	250
Industrial	Incheon	6,601	8.4	1,270

official land price, including \$4.1 million for small cities, \$4.8 million for farming and fishing villages, \$6.9 million for new towns, and \$8.4 million for industrial complexes. The site price range per unit area is very diverse; however, in general, the higher the load density, the higher is the price.

### 3.1.2 Installation cost of 154 kV cables

General underground transmission facilities required to supply electricity from existing substations to new substations have a double circuit of 154 kV XLPE cables with cross section of  $2,000 \text{ mm}^2$ . When installed in duct pipes, the actual transmission capacity is different as the temperature effects on each other vary depending on the number of circuits. In this study, the capacity of conventional transmission cables is assumed to be 240 MVA per circuit considering up to four circuits of cable installation according to KEPCO's planning guideline and construction design standard. The unit price of the 154kV XLPE cables is \$1.13 million per kilometer, \$2.26 million for double circuits, \$4.52 million for 2 km, and \$6.78 million for 3 km, as shown in Table 3.3. It is assumed that all joints and termination fittings related to cable installation are included in the construction. The 23 kV cable used for power distribution feeders is generally 23 kV CNCE  $325 \text{ mm}^2$ , with a price of \$0.21 million per kilometer.

Table 3.3 The cost of the double circuit 154 kV XLPE cables by length

Items (million \$)	1 km	2 km	3 km
154 kV XLPE $2,000\text{mm}^2 \times 2$	2.26	4.52	6.78

### 3.1.3 Construction cost of transmission cable tunnel

As shown in Fig. 3.1, the transmission cable can be installed in a pipe duct(conduits), cable box, or cable tunnel. The direct burial method is not used owing to the need for emergency replacement of cables in case of cable failures. The unit cost of cable box construction is \$6.73 million per kilometer, \$13.45 million for 2 km, and \$20.8 million for 3 km. Generally, the cable box method is applied to high-load-density areas such as large cities and new cities.



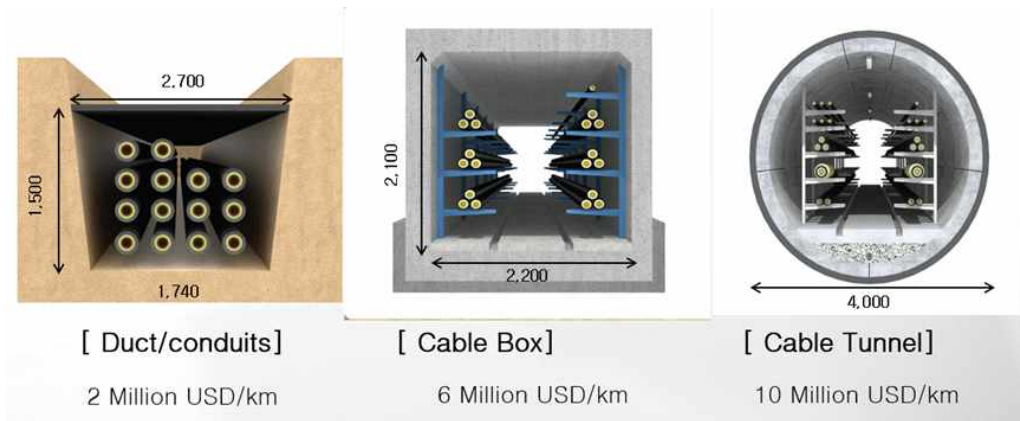
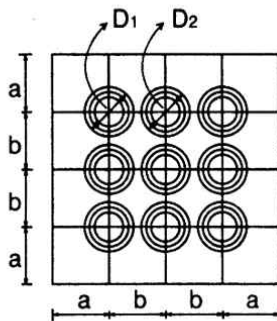


Fig. 3.1 Various types of underground structure including duct pipe, cable box and cable tunnel

#### ► Distribution Ducts

- ELP(Inner Diameter 200mm)
  - Center distance( $b$ )=360mm
  - $b = (D_1 + D_2)/2 + 100\text{mm}$



#### ► Transmission Ducts

- Maximum transmission cables 4 circuits : 12
- Transmission cable 2 circuits and distribution cable 7 circuits : 12

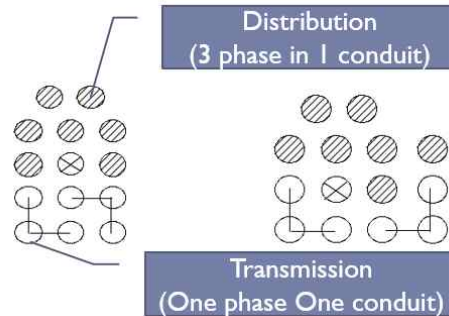


Fig. 3.2 The structural difference between transmission or distribution cable allocation in the pipe duct

The unit price for conduit construction costs \$2.77 million per kilometer, \$5.54 million for 2km construction, and \$8.31 million for 3km construction. The conduit construction method is applied to small towns and industrial complexes that do not require much power transmission capacity because the number of

pipes that can be installed is limited to up to 12. In general, even if construction of conduits is feasible, the cable tunnel system can be applied in downtown areas where traffic is heavy or in areas with river crossings. Unlike conduits for transmission cables, only up to nine conduits for distribution cables will be accommodated, and construction costs will be reduced to less than a quarter of the construction cost for transmission, which will help reduce investment costs even more. Fig. 3.2 shows the structural difference between transmission or distribution cable allocation in the pipe duct [3].

In particular, cable tunnels cost much more than cable boxes because the construction method should use a shield TBM, and construction depth is  $\sim 50$ – $60$  m below ground level. The construction cost of the cable tunnel per kilometer is \$11.5 million, but \$7.3 million should be added to build two vertical shafts with a depth of 50 m or more, as shown in Table 3.4. KEPCO statistics show that  $\sim 20\%$  of the underground cable installation has been built with cable tunnels.

Table 3.4 The construction cost of various underground facilities by distance

Items (million \$)	1 km	2 km	3 km
Cable tunnel	18.82	30.32	41.82
Cable boxes	6.73	13.45	20.18
Duct pipe (conduits)	2.77	5.54	8.31

### 3.2 Cost calculation of 23 kV tri-axial HTS cable system

Superconducting cable systems can be classified into superconducting cables and cooling systems, and detailed material costs can be divided by cable, junction box, LN<sub>2</sub> circulation system, and cooling system. For example, a 23 kV tri-axial HTS cable system with 120 MVA capacity costs \$25.8 million, including \$15.3 million for the superconducting cables, \$3.6 million for the joint and terminations, \$0.36 million for the LN<sub>2</sub> circulation systems, and \$6.46 million for cooling systems.

In the same configuration, the cost of 2 km and 3 km of the 23kV superconducting cable system is \$43.4 million and \$63.0 million, respectively, as shown in Table 3.5.

Table 3.5 Cost breakdown of 23 kV tri-axial HTS cables(120 MVA, 3 CCTs)

Items (million \$)		1 km	2 km	3 km
HTS cable		153.6	307.3	460.9
NJ		12.0	24.0	42.0
Termination		24.0	24.0	24.0
Circulation system	Return pipe	2.0	4.0	6.0
	Joint kit	0.8	1.6	2.8
	Termination kit	0.8	0.8	0.8
Sub total		3.6	6.4	9.6
Cooling system		64.6	72.7	93.8
Total		257.8	434.4	630.3

#### 3.2.1 Cost calculation procedure of 23 kV tri-axial cable

The data on the materials cost of power facilities, construction cost, and maintenance cost were sufficient. However, superconducting cables are still

being developed, and no price information is available for various capacities through market procurement. Because market information for superconducting cables and cooling systems is limited, the investment cost is estimated by calculating the required amount of superconducting materials and cooling capacity by distance.

Therefore, the prices of tri-axial HTS cables were estimated in the following ways, as shown in Fig. 3.3. It shows the procedure for designing the HTS cable to calculate the number of HTS tapes. Unlike conventional power cables, HTS cables still do not have a standardized capacity or design. Therefore, it is common to first select the candidate site for HTS cable application, starting with the design for the HTS cable system. Once the target candidate site is decided, basic system specifications such as the cable length, rated current, temperature and flow rate of cooling, and DC  $I_c$  value of applied HTS tapes are given.

Then, the next process is to calculate the quantity and length of HTS tapes to satisfy these design conditions. It is common for HTS cables to keep the power loss value lower than the design value; therefore, the ratio between DC  $I_c$  and the maximum operation current is kept within 40%–60% as given by the Norris equation. More detailed engineering characteristics should be considered when designing with multiple layers to ensure the capacity required in this process. It also reflects design margins, which vary from manufacturer to manufacturer, but are generally more than 20%. It is also desirable to minimize the gap between tapes considering power losses; however, the design should also consider other effects, such as cable fabrication and tension during the installation process. At the same time, the HTS tape length as well as the mechanical and tri-axial cable characteristics that appear during the wire winding process should be calculated by considering the impedance matching.

The feasibility of fabrication and on-site installation in the process of making cables is reviewed considering the conduit size and site condition. Because the diameter of transmission ELP conduit is only 200 mm, the cable's outer diameter should not exceed 150 mm given the tensile load or bending

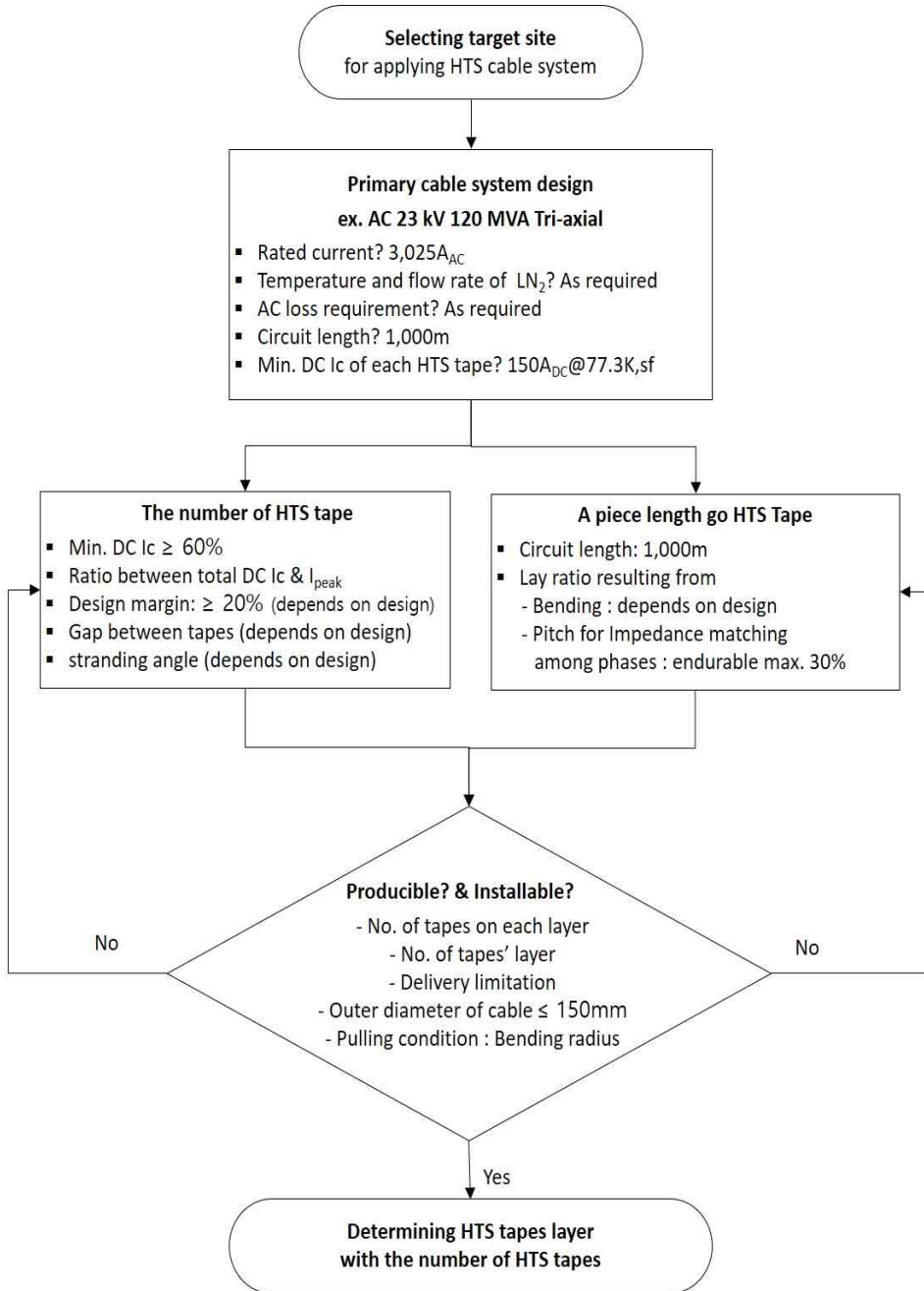


Fig. 3.3 The procedure for designing the HTS cable to calculate the number of HTS tapes

conditions.

As shown in Fig. 3.4, the HTS tapes for phase A is wound around the former and covered with an insulation layer, then wrapped with former, HTS tapes and an insulation layer for phase B, and finally wrapped with HTS tapes for phase C. Fig. 3.5 shows the number of HTS tapes corresponding to HTS cable capacity by considering the size of the former and the HTS tapes. Even at capacities of up to 200 MVA, the outer diameter of the cable does not exceed the maximum of 150 mm.

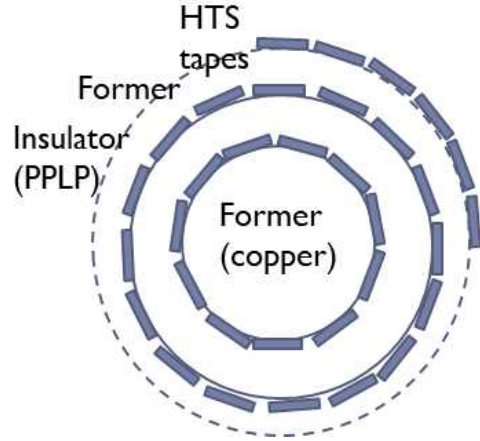


Fig. 3.4 The structure of HTS cable core

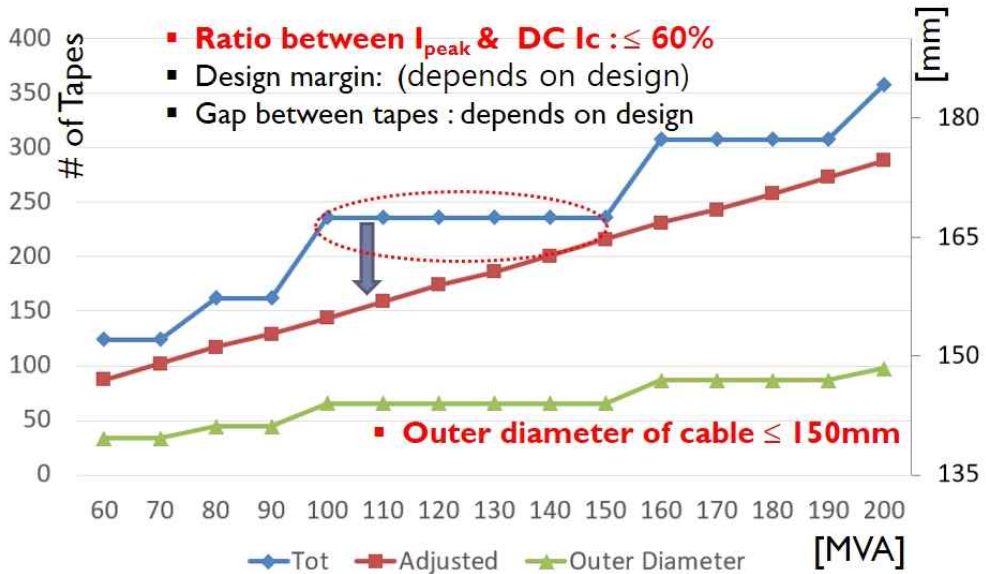


Fig. 3.5 The number of HTS tapes by cable capacity considering the size of formers, HTS tapes, and vacuum insulation layers with outer cryostat and jacket

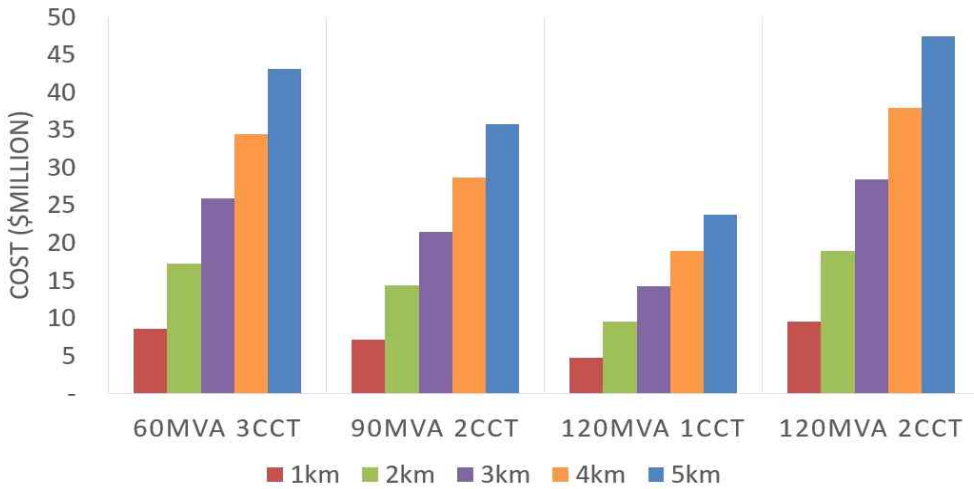


Fig. 3.6 The price of the HTS cables by capacity and by distance

number of HTS tapes and the number of layers. The amount of the HTS tapes is the main factor affecting the price of superconducting cables that will eventually be installed at the target site. Although many other factors need to be considered in the design of tri-axial HTS cables, such as insulation and impedance matching, the fact that no HTS wires for shield layer compared to triad-type HTS cables contributes greatly to the economics of tri-axial HTS cables. Fig. 3.6 shows the price of the HTS cables by capacity and by distance. As capacity increases, the slope of price by distance becomes much steeper. The prices of normal joint, termination are assumed as \$0.2 million and \$0.5 million respectively.

Previously, the price was estimated by simply calculating the required amount of HTS tapes by considering the design margin and multiplying by the unit price of HTS tape, similar to triad-type HTS cable only considering that the tri-axial HTS cable does not require shield layers consisting of HTS tape. For example, an 23 kV 50 MVA tri-axial HTS cable requires a total of 73 wires considering a current margin of 30% and HTS wires with critical current of 150 A. Then, the price of superconducting cables was calculated based on the \$20/m for the HTS tape and the cabling cost of \$300/m. Fig. 3.7 shows the results of calculating the investment cost of a 23 kV HTS cable and its

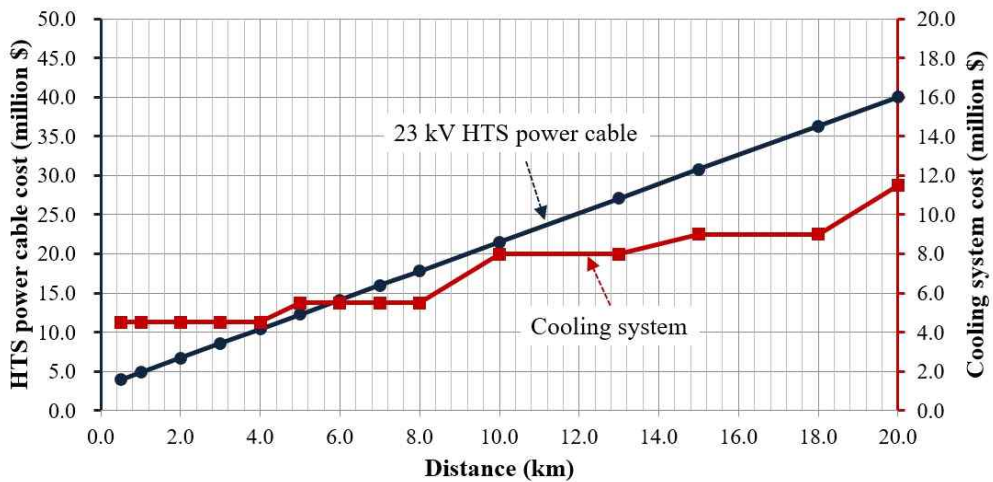


Fig. 3.7 The results of calculating the investment cost of a tri-axial HTS cable and the cooling system by distance.

cooling system by distance [10].

The price of HTS tapes, which are the major component of superconducting cables, is high, making it difficult to achieve economic efficiency compared to conventional cables; however, it is highly encouraging that the current density of HTS tape continues to increase and prices continue to decrease [11].

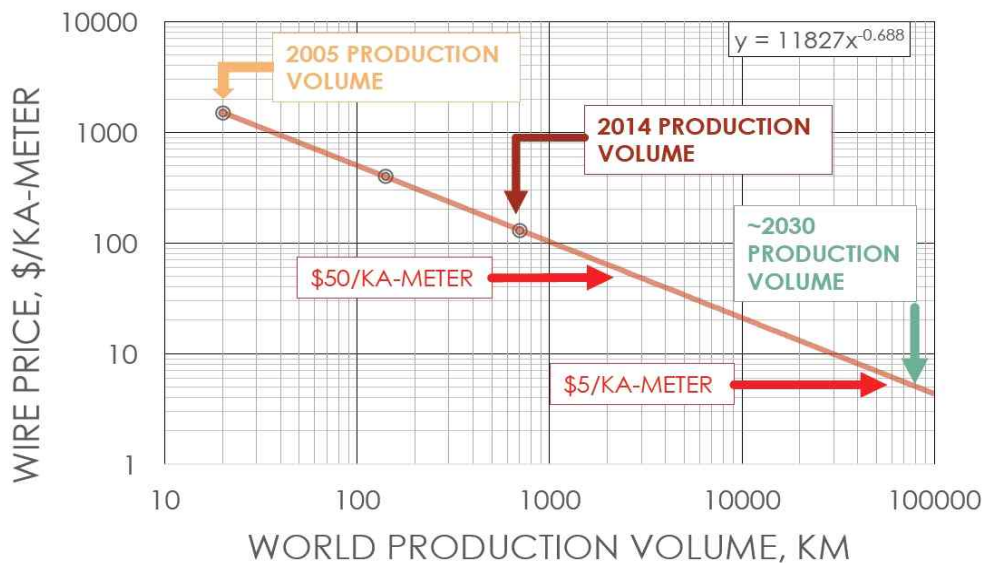


Fig. 3.8 Path for superconducting wire cost reduction by volume



### 3.2.2 Cost calculation procedure of cooling system

The loss of superconducting cables can be largely divided into AC loss and heat loss. In particular, the AC loss is closely related to the ratio of the transport peak current  $I_t$  and DC critical current  $I_c$ , which is expressed as a monoblock Eq. 1 [25–26].

$$P = \frac{f I_c^2 \mu_0}{2\pi h^2} \left\{ \left( 2 - \frac{I_t}{I_c} h \right) \frac{I_t}{I_c} h + 2 \left( 1 - \frac{I_t}{I_c} h \right) \ln \left( 1 - \frac{I_t}{I_c} h \right) \right\} \quad (1)$$

where  $I_c$  is the critical current;  $I_t$ , the peak value of the transport current; and  $f$ , the frequency of the current, and  $h$  is defined as

$$h = \frac{D_1^2 - D_2^2}{D_1^2} \quad (2)$$

where  $D_1$  and  $D_2$  are the outer and inner diameters of the superconducting cylinder, respectively.

It is desirable to control the ratio of the transport peak current and DC critical current in the range of 40%–60% and to control the gap between HTS tapes when embedding them around the copper stranded former because the AC loss appears to be highly affected by the ratio, edge, and layer. The procedure of determining the number of HTS tapes was already explained before.

For the economic simulation in this study, the cooling capacity was calculated by assuming a cable heat loss of 1.5 W/m and a return pipe heat loss of 1 W/m regardless of the capacity of HTS cable. For the AC loss, with the AC loss set to 1 W/m for the HTS cable with 60 MVA capacity, it is assumed that 100% of AC losses at other capacities are only current proportional component, as shown in Eq. 3.

$$Q_{ACloss} = 1.0 \frac{I_{rate}}{I_{60MVA}} \quad (3)$$

where  $I_{rate}$  is the rated current at other cables;  $I_{60MVA}$ , the rated current of 60

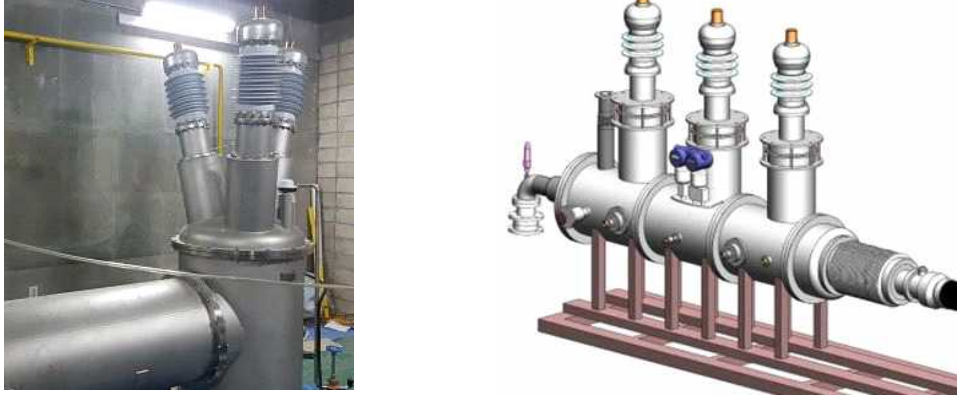


Fig. 3.9 The structure of EBA terminations (a) for three phase in one cryostat HTS cable (b) for tri-axial HTS cable

MVA HTS cable.

The EBA loss for tri-axial cable, as shown in Fig. 3.9, is calculated as

$$Q_{EBA} = 3I^2R + \kappa \frac{3A}{l} \Delta T + \sigma \Delta T^4 \quad (4)$$

where  $I$  is the rated current;  $k$ , the thermal conductivity;  $A$ , the cross section of the copper bar;  $l$ , the length of the copper bar; and  $\sigma$ , the Stefan–Boltzmann coefficient. With respect to the loss calculation for the termination, The first formula of Eq. 4 is directly related to the AC loss, and the second and third formulae correspond to the heat loss. EBA should be designed to maintain a constant temperature gradient at room temperature. Heat-loss-related factors have an inverse relationship with AC-loss-related factors. If the cross-sectional area of the copper bar increases, the heat loss increases whereas ac loss decreases. This in turn means that EBA loss can be optimized depending on how the copper bar and other geometrical shapes are designed.

For the economic simulation in this study, with the EBA loss set to 200 W for the HTS cable with 60 MVA capacity, it is assumed that 75% of the EBA losses at other capacities were current proportional components and 25% were fixed values, as shown in Eq. 5.

$$Q_{EBA} = 150 \frac{I_{rate}}{I_{60MVA}} + 50 \quad (5)$$

The cooling system comprises a combination of 5 kW, 10 kW, and 20 kW considering the market practice that it is not supplied with the exact design capacity. For example, if 9 kW cooling capacity is required, manufacturers would supply a 10 kW cooling system rather than two small 5 kW cooling systems. The investment cost of cooling system was assumed based on a combination of 5 kW and 10 kW cooling systems that were verified in the HTS cable demonstration projects, as shown in Fig. 3.10. The cost required for terminations and joints were considered. In addition, an external return path for two tri-axial HTS cables was applied.

Fig. 3.11(a) shows the results of the cost estimates of the cooling system by the 23 kV tri-axial HTS cable capacity. The length of the tri-axial HTS cables seems to be stable for up to 3 km by simply installing a cooling system on either side of the substation or switching station considering the  $LN_2$  flow rate, temperature, etc. It can be increased up to 6 km by installing cooling systems at both the substations and the switchgear. In this case, stop joint is required in the middle. Beyond that, it might be necessary to install cooling systems at regular interval along the cable route; however, this would

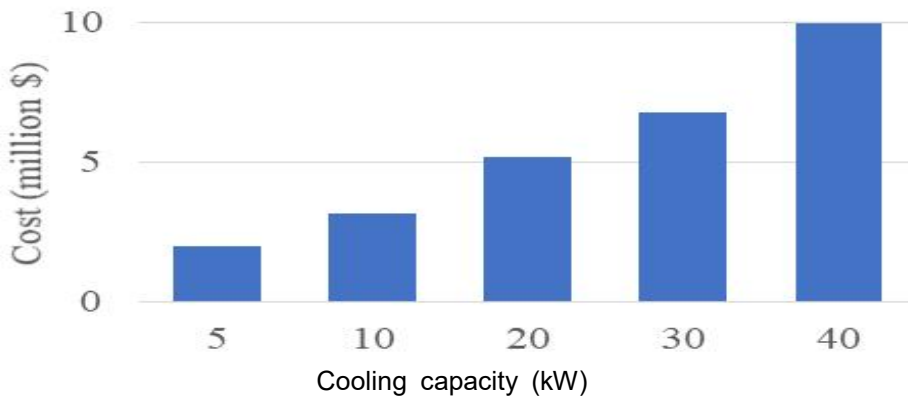


Fig. 3.10 The investment cost of cooling system by cooling capacity based on a combination of 5 kW and 10 kW cooling systems

be difficult in terms of social acceptance and construction permissions.

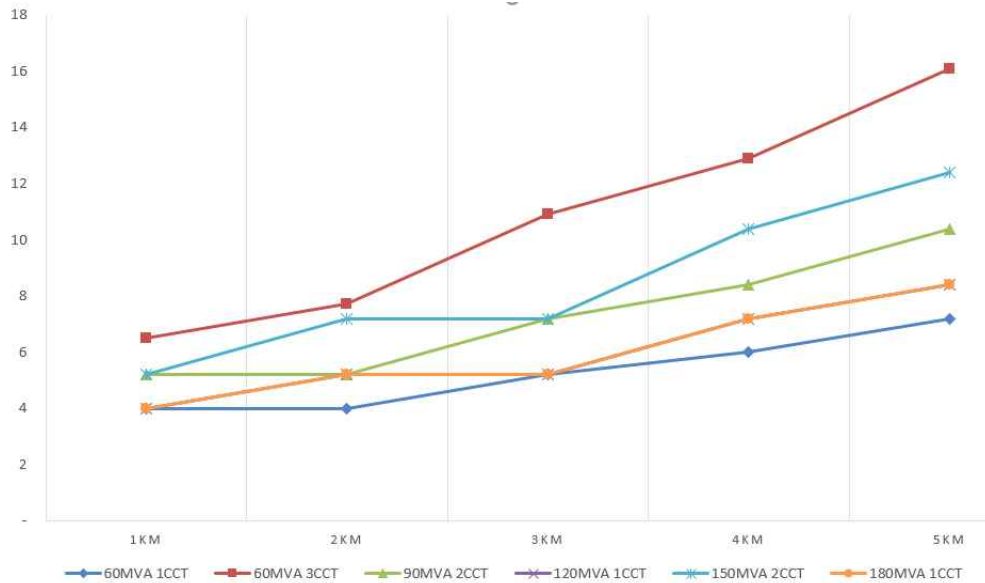


Fig. 3.11(a) The results of the cost estimates of the cooling system by the 23 kV tri-axial HTS cable capacity

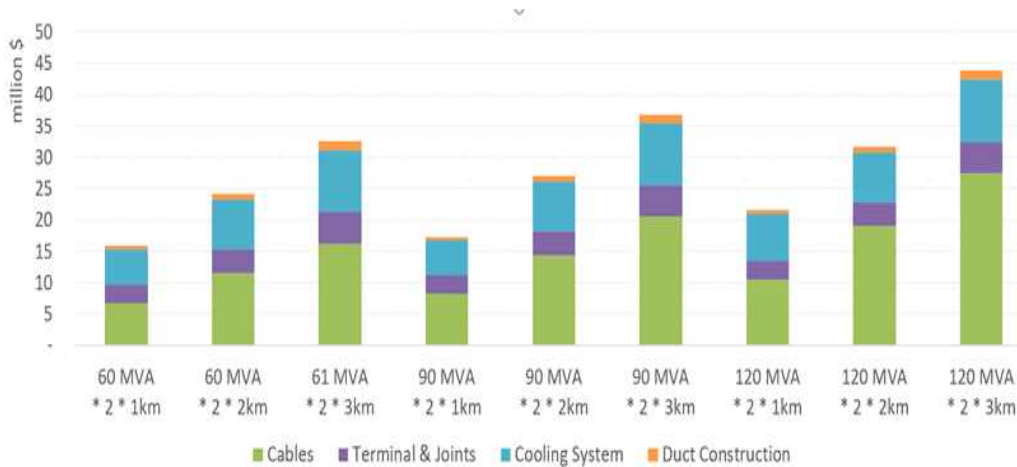


Fig. 3.11(b) The results of the total cost estimation of the HTS cables and cooling system by their configurations

### 3.3 Application design of 23 kV HTS power cables

#### 3.3.1 Hybrid power system with HTS power cables



Fig. 3.12 The conventional method used to install substations in urban areas

Owing to the growth of the economy and of urban districts, new cities have been developed in which industrial and residential complexes are constructed in close proximity. To ensure a reliable supply of electricity, transmission lines and substations should be properly planned and constructed on schedule in these areas; however, opposition from local communities against new substations with extra-high-voltage transmission lines is too severe to build these electric facilities in urban districts. As a result, securing social acceptability during the selection process of cable corridors and substation siting is an important issue [10].

In this respect, 23 kV superconducting cables can be a good alternative to addressing these “not in my backyard” phenomena. The first reason is that there is no or less of a need to construct a substation in urban areas if superconducting cables that can transmit large amounts of electric power at low voltages are used. In addition, owing to the high flexibility of site selection,



Fig. 3.13 The concept of a hybrid power system combined with 23 kV HTS power cables.

the substation can be constructed in areas where land prices and complaints are relatively low rather than in urban areas where land prices and complaints are high. Based on the results obtained for the 23 kV HTS cable application, it can be classified into two cases; elimination of 154 kV substations and relocation of 154 kV substations. Fig. 3.12 shows the conventional method used to install substations in urban areas, and Fig. 3.13 illustrates the concept of a hybrid power system combined with 23 kV superconducting power cables.

### 3.3.2 Elimination of 154 kV substation (Case A)

As shown in Fig. 3.14, the conventional method requires the construction of a new 154 kV substation at the center of loads as well as connecting it to the existing substation by installing two circuits of 154 kV XLPE cables in conduits. If the transmission cables are replaced with 23 kV HTS cables, the construction of a substation is not required. Instead, a 23 kV switching station must be installed, which requires much less space compared to a substation. In this subsection, this approach is referred to as Case A, and it is assumed that the initial supply capacity of the new substation is 100 MVA with two 50

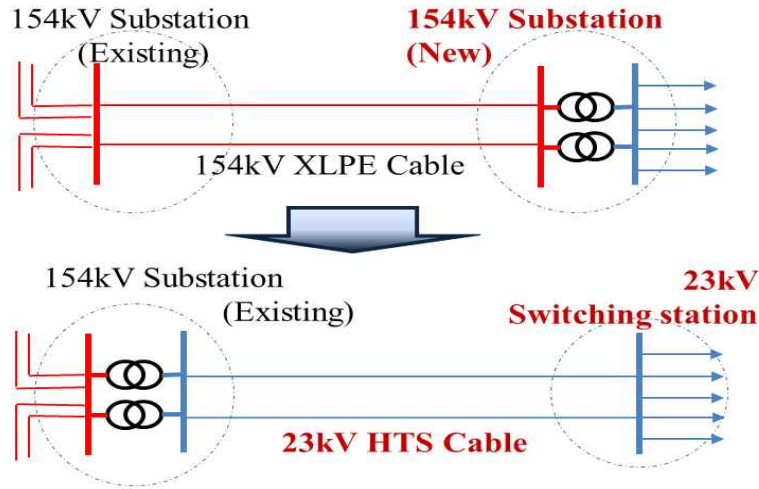


Fig. 3.14 (a) the conventional method requires the construction of a new 154 kV substation at the center of loads (b) the HTS method requires only 23 kV switching stations

MVA transformers. In principle, space must be secured to expand to up to four transformers according to the KEPCO design standard. Further, it is assumed that the total supply capacity of the superconducting cables is the same as that of a substation based on two 50 MVA HTS cables. Generally, transmission lines have a sufficient capacity considering future links with additional substations; however, in this radial configuration, the amount of power supply is confined to the center of loads only, and the necessity of 23 kV HTS cable expansion will be considered separately with the load forecast in the future.

### 3.3.3 Relocation of 154kV substation (Case B)

It is difficult to construct a 154 kV substation in urban areas owing to public objection. Inevitably, the substation site must be relocated to the outskirts of towns, as shown in Fig. 3.15. The distribution HTS cable can play

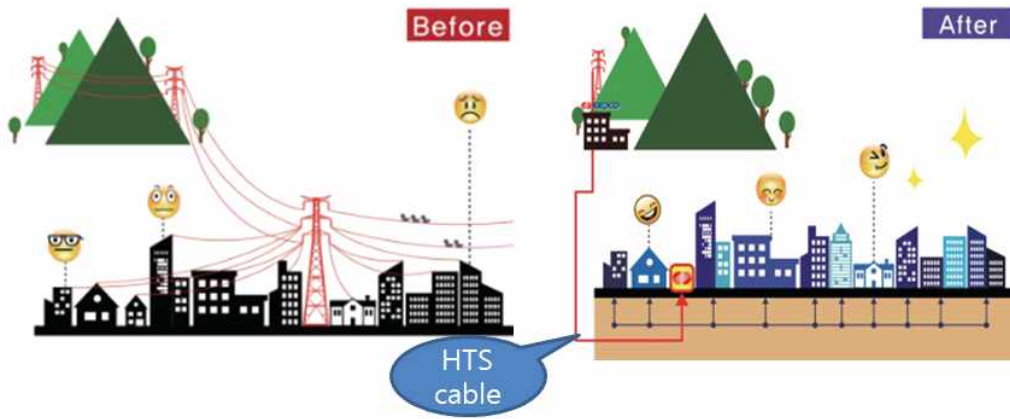


Fig. 3.15 The substation can be relocated to the outskirts of towns by replacing 154 kV cables with 23 kV HTS cables

a important role in this situation.

Fig. 3.16(a) shows a conventional method in which the farther the substation is from the load center, the longer are the distribution feeders and the shorter are the transmission cables. This results in more bundles of distribution feeders on the same corridor from the new substation, which requires the construction of a cable tunnel instead of conduits to accommodate them. Therefore, in selecting the location of the substation, striking a balance between the transmission and the distribution planning organizations is crucial to optimizing the investment cost.

If a superconducting cable is applied, the same capacity can be transmitted with a much smaller number of superconducting cables, which makes it possible to construct less expensive conduits rather than a cable tunnel. Only a 23kV switching station at the center of loads is necessary to link 23 kV HTS cables and to supply power to the load. Fig. 3.16(b) shows a hybrid power system configuration with 23 kV HTS cables in conduits. This results in the reduction of the investment cost owing to the low construction cost of conduits. Case B differs from Case A because HTS cables replace multiple feeders rather than transmission cables, and a new 154 kV substation must still be built whether to link it to the power system by branching from the existing



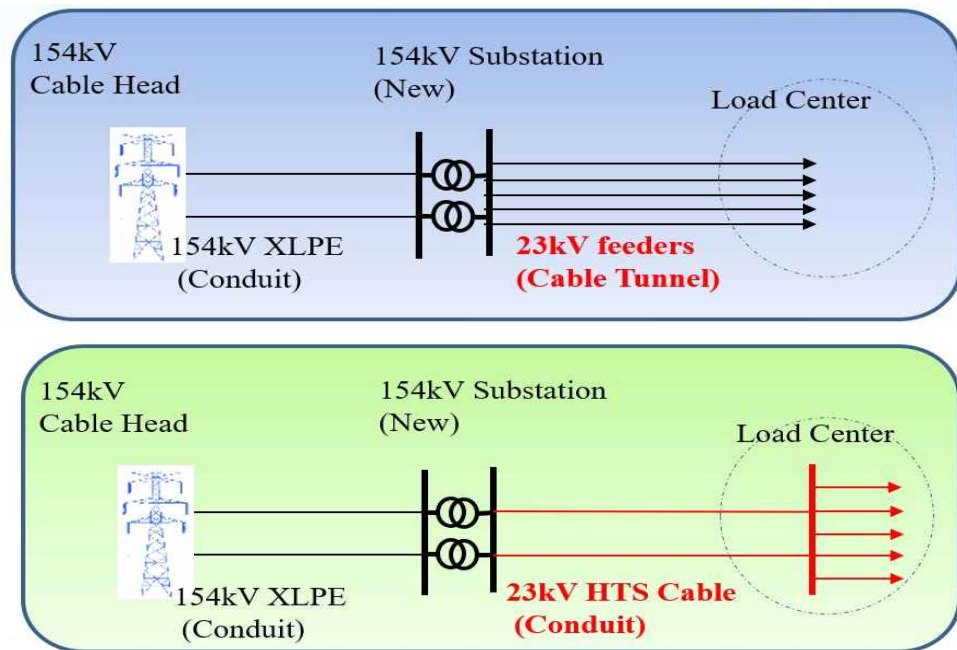


Fig. 3.16 (a) conventional method of substation relocation  
 (b) hybrid power system configuration with 23 kV HTS cables in conduits

154 kV transmission lines or by connecting it with an existing 154 kV substation bus.

### 3.3.4 Other applications of 23 kV HTS cables

In terms of load supply, the application of HTS cables shows a great promise for avoiding building substations or relocating them out of town [33-34]. As shown in Fig. 3.17, the application of HTS cables to connect the power source is also expected to be possible. Because of the need to build distribution feeders to substations in each complex when solar power plants are clustered, more power generation complexes have more feeders, resulting in a lack of routes. Until now, the only method used was to construct a collector substation and send it to a nearby substation after voltage rise. The application of superconducting cables enables the construction of a collector station with

much lower construction costs than the substation to collect power from all feeders and transmitting it together to the substation [35].

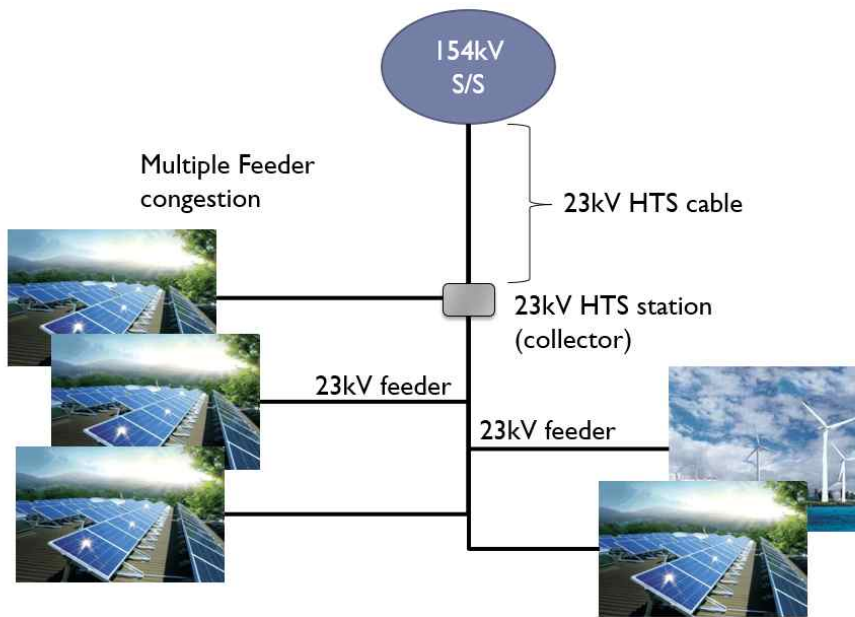


Fig. 3.17 The application of the HTS cables to connect the distributed energy resources(DER) including solar PV farm, wind farm, etc.

### 3.4 New application design of HTS power platform

#### 3.4.1 Description of HTS power platform

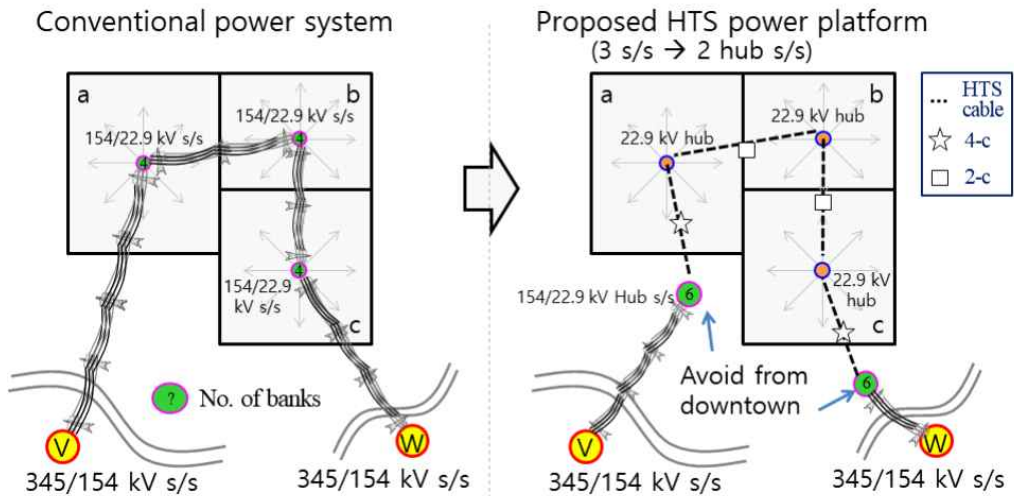


Fig. 3.18 Conceptual diagram of conventional power system and proposed HTS power platform

A 23 kV superconducting cable can transmit much more capacity than a distribution cable of the same size. Therefore, a substation can be installed on the outskirts of downtown areas, and two to three 23 kV switching stations can supply the load in downtown areas, as shown in Fig. 3.18. The connection between the substation and the switching stations can be accomplished by a couple of 23 kV HTS cables rather than a large number of distribution feeders [36-37].

In urban areas where load density is much higher than that in rural areas, the distance between substations is less than 3–6 km, and underground construction is carried out. Fig. 3.19 shows the circuit number of 154 kV underground cables by length in KEPCO's power system, and it can be inferred that the distance between substations in urban areas is within 3–6 km. Fig. 3.20 also shows the load density distribution of substations by supply area. The load density of the urban or industrial complex is as high as 20–

30 MW/km<sup>2</sup>.

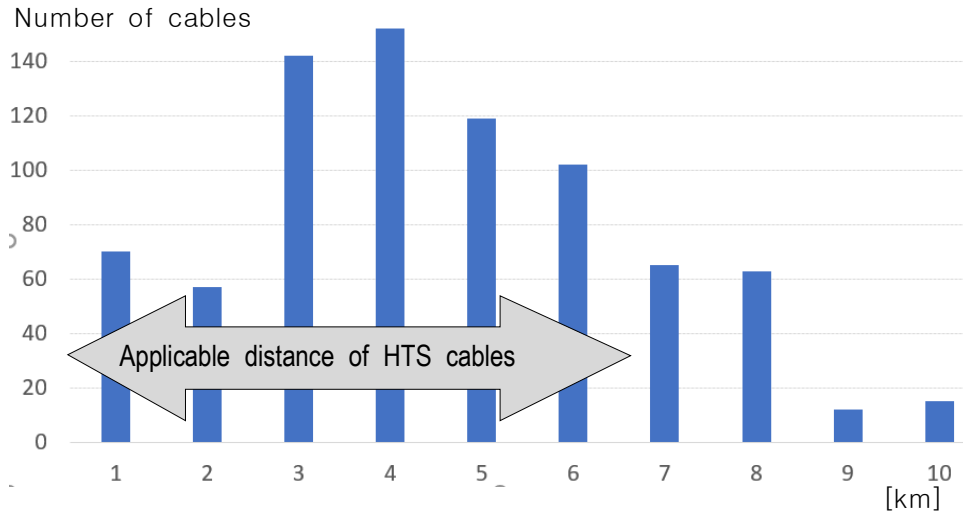


Fig. 3.19 The circuit number of 154 kV underground cables by length in KEPCO's power system

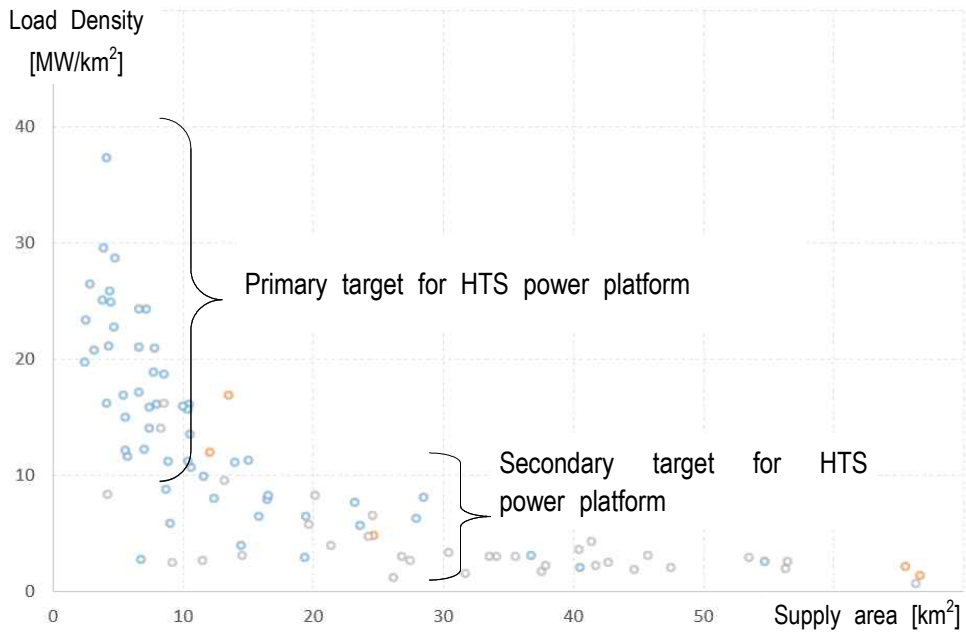


Fig. 3.20 The load density distribution of substations by supply area in KEPCO's power system

It looks appropriate for the HTS power platform to have a total load supply capacity of up to 240 MVA, which is equivalent to two standard 154 kV substations. Considering the load density of 20 — 30 MW/km<sup>2</sup> of developed areas, as shown in Fig. 3.20, it can supply an area of ~10 km<sup>2</sup>. This will be considered as primary target areas for the HTS power platform. Secondary target for HTS power platform can be further expanded to the area of ~30 km<sup>2</sup> when the investment of HTS power platform can be more efficiently justified.

### 3.4.2 Configuration of 23 kV switching station

The 23 kV switching station consists of only superconducting cables and breakers and protective facilities for distribution feeders; therefore, it can be built as a one-story building with underground cable processing rooms. In conventional substations, transformers take up the largest amount of space, making double-story construction inevitable, whereas a very simple configuration can be built without transformers. Figs. 3.21 and 3.22 show a compact substation and one form of a 23 kV switching station. The switching station's

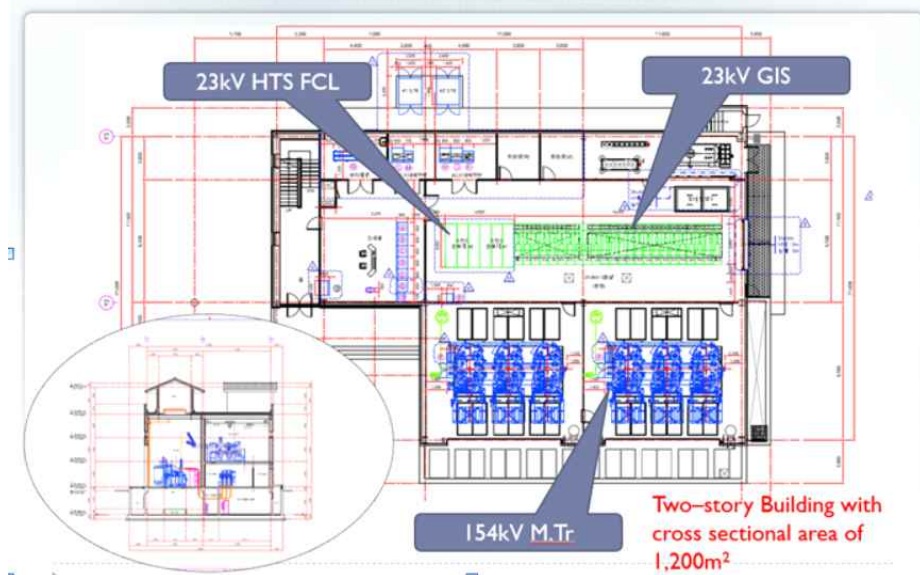


Fig. 3.21 Layout of a small substation with two story building on the cross sectional area of 1,200 m<sup>2</sup>

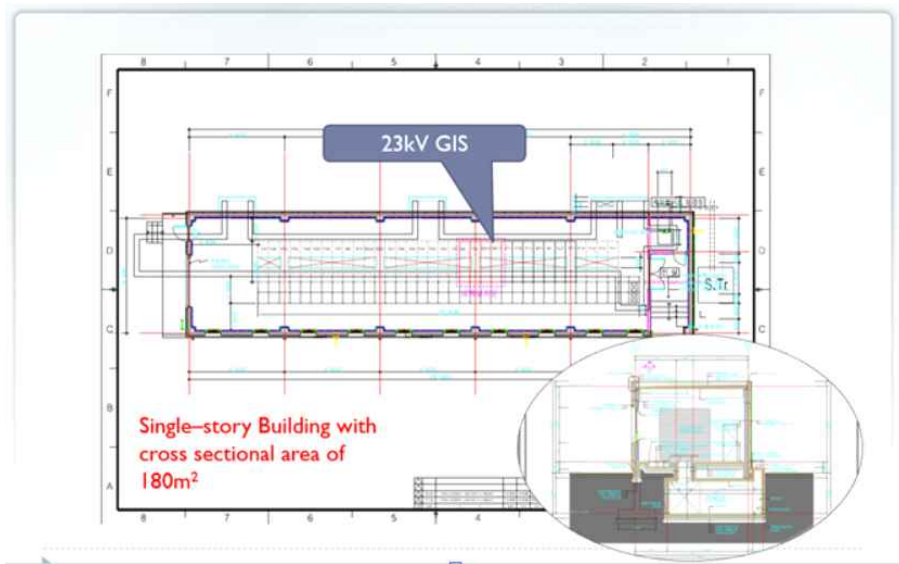


Fig. 3.22 Simplified layout of a 23 kV switching station with single story building on the cross sectional area of 180 m<sup>2</sup>

area can be reduced to 180–500 m<sup>2</sup> with a size of 1/6 to 1/5 of the substation area, compared to an area of 1,200–2,500 m<sup>2</sup> for substations. Further, if necessary, protective equipment such as an superconducting fault current limiter (SFCL) can be installed to reduce the fault current. The use of the 23 kV SFCL in HTS platforms is explained in the subsection 3.4.4.

The installation cost of 23 kV switching stations was calculated by referring to the average cost of the small distribution transformer stations in

Table 3.6 The average construction cost of the small distribution transformer stations in Myeong-dong, Seoul

Name of distribution station	Cost (million \$)
Myeong-dong #1 station	2.05
Myeong-dong #2 station	1.41
Myeong-dong #3 station	2.10
Average cost	1.85

Myeong-dong, Seoul; the construction cost was \$1.85 million per location, as shown in Table 3.6. The area of the 23 kV switching station is estimated to be  $\sim 60\text{--}90\text{ m}^2$ . However, considering the need for space for things other than the power facilities from a conservative viewpoint,  $500\text{ m}^2$  is applied in this study, which is about one-fifth of the area of the 154 kV substation.

### 3.4.3 Detailed configuration of HTS power platform

Figs. 3.23 and 3.24 show the new power system configuration for power supply in urban areas. In this configuration, 2–3 23 kV switch stations are installed near the load center, and they are connected to the 154 kV transformer substations with 23 kV HTS cables. Power is supplied to the individual load through the 23 kV distribution feeders from the substation or station, which is similar to the conventional method. This configuration is called an HTS power platform. The shape can be either ring type or line type. The ring type consists of HTS cable network fed from a single substation and 2–3 switching stations in the middle, as shown in Fig. 3.25, and the line type involves connecting the substations on either side with 23 kV HTS cables and installing switching stations in the middle, as shown in Figs. 3.23 and 3.24.

The conventional method for installing transmission cables requires a cable box or a cable tunnel in urban areas; however, the 23 kV HTS cables can be installed in conduits. This is highly effective in enhancing not only the economics efficiency of the superconducting cable but also the construction workability.

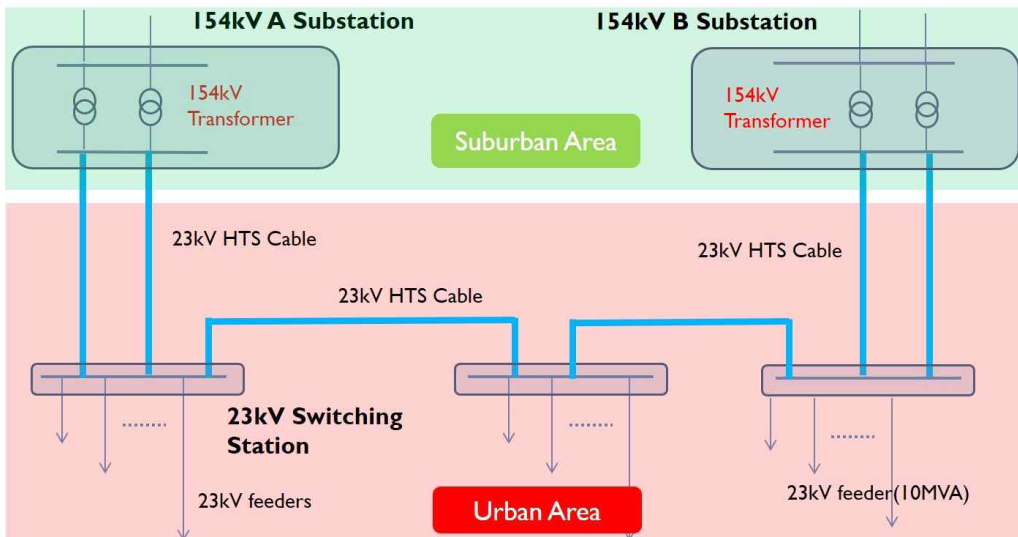


Fig. 3.23 HTS power platform with **three switching stations** linked with 23 kV HTS cables, which is a new power system configuration for power supply in urban areas



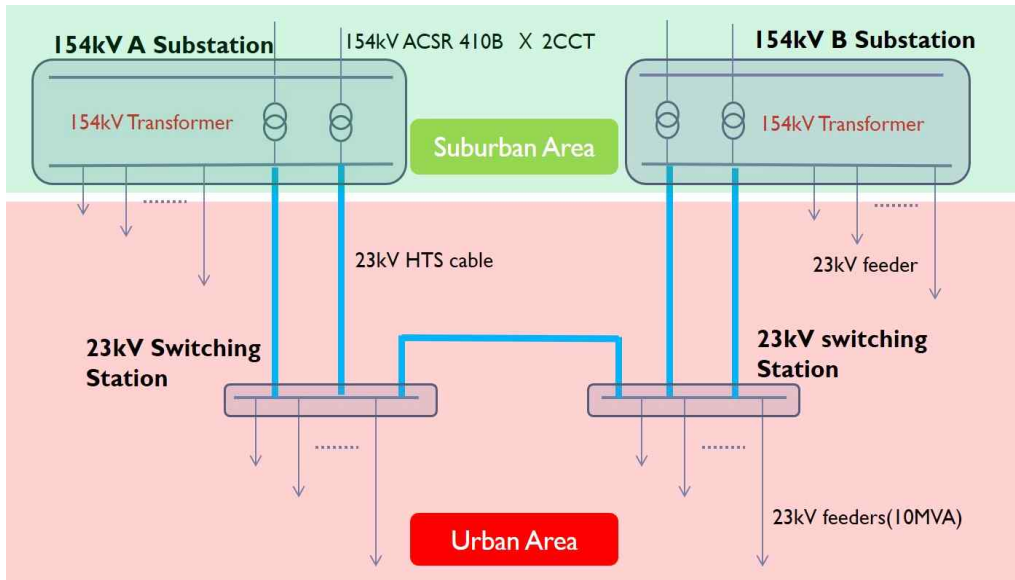
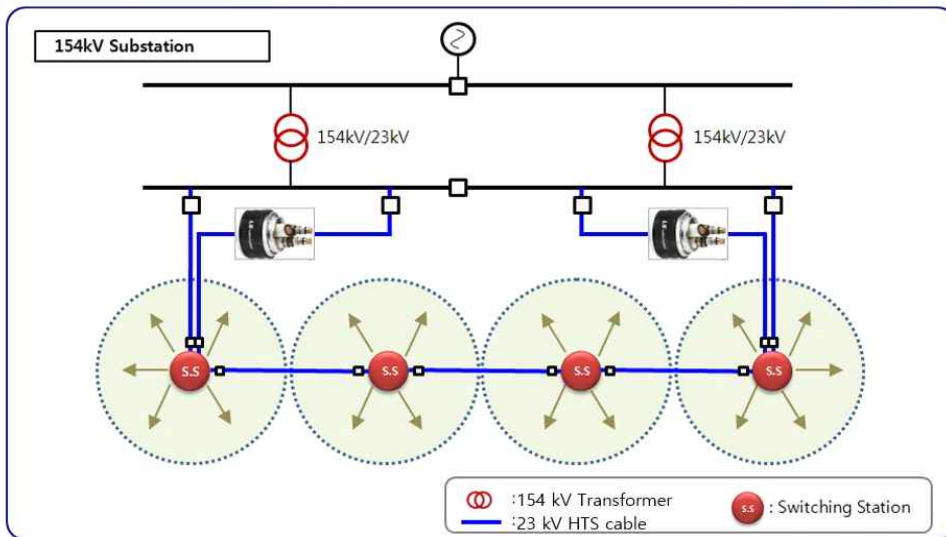


Fig. 3.24 The HTS power platform with **two 23 kV switching stations** linked with 23 kV HTS cables



Figs. 3.25 The shape of an HTS power platform can be either ring type or line type. The ring type consists of HTS cable network fed from a single substation and 2–3 switching stations in the middle

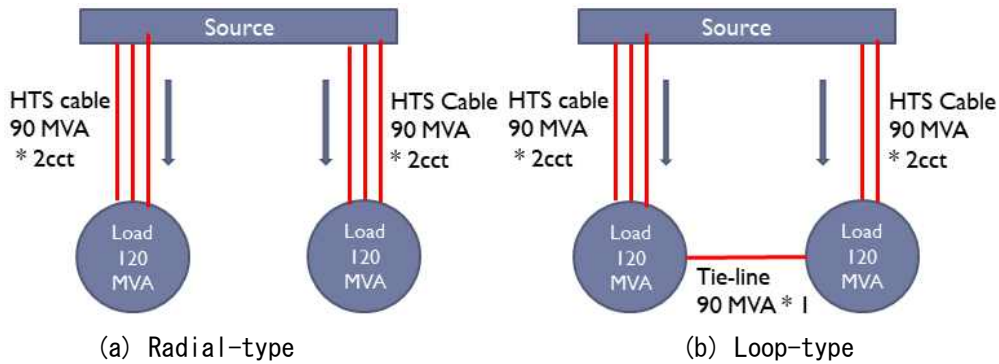


Fig. 3.26 A platform consisting of two stations with 120 MVA load supply capacity each and every HTS cable with a capacity of 90 MVA

While the reliability criteria of the overhead transmission lines are based on the assumption of double circuits for contingency, the reliability criteria of the underground lines only consider the N-1 criteria, which is a single line contingency. This is because a fault of underground cables is more likely to lead to permanent failure as it is mostly damaged by excavation, rather than by a natural disaster such as gusts, lightening.

In a HTS power platform consisting of two stations with 120 MVA supply capacity, as shown in Fig. 3.26(a), if the HTS cable connecting the 23 kV switching stations has a capacity of 90 MVA, a total of six HTS cables are required, with three cables each, to satisfy the N-1 criteria; however, if a route contingency occurs when the switching station has a radial connection, there will be high concerns over power supply. To address this reliability issue, the same number of lines can be maintained while increasing reliability by connecting a tie-line between the two switching stations, as shown in Fig. 3.26(b). On a platform of two stations with 120 MVA capacity, the optimal number of lines that can be considered when interconnected with 90 MVA HTS cables can be five instead of six, as shown in Fig. 3.27. This configuration is also possible if all facilities are built simultaneously; however, in reality, it is common for facility investments to be made sequentially with increasing loads. Therefore, the hypothetical load-increasing model is also considered in this study when reviewing the economics of the platform in

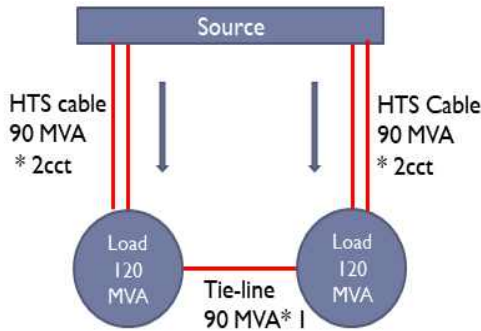


Fig.3.27 On a platform of two stations with 120 MVA capacity, the optimal number of lines can be five, not six

terms of the life cycle cost. If 120 MVA capacity HTS cables are used rather than 90 MVA cables, it consists of four HTS cables, as shown in Fig. 3.28. However, this configuration is based on the assumption that the distance between the two switching stations is the same for the tie-line connection as for the other sections. It is easy to see that the number of HTS cables is very closely related to the load supply capacity of the switching stations and the capacity of HTS cable as well.

Another case is considered in which a 23 kV switching station is newly established between two switching stations, that is, a platform consisting of three switching stations. If there are three switching stations consisting of the same 120 MVA supply capacity, as shown in Fig. 3.29(a), the number of 90 MVA HTS cables considering N-1 criteria will be 10 lines. If 120 MVA HTS cables are applied, the number of lines can be reduced to seven, as shown in Fig. 3.29(b). Furthermore, loop configurations by placing a tie-line between

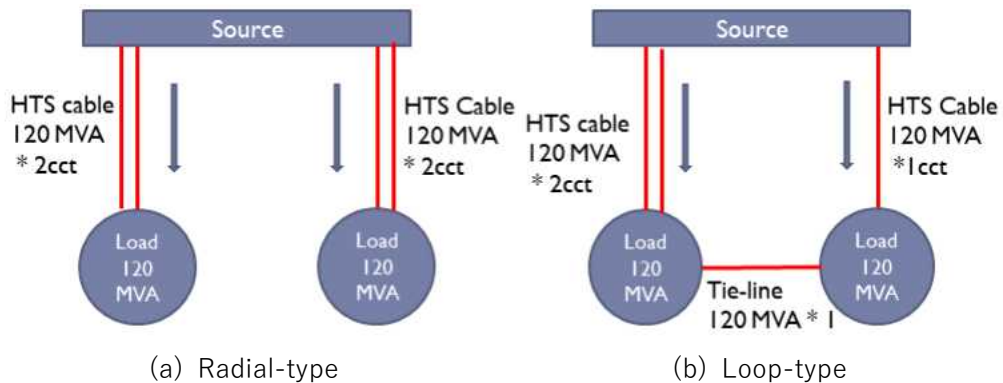


Fig. 3.28 A platform consisting of two stations with 120 MVA load supply capacity and every HTS cable connecting between stations has a capacity of 120 MVA

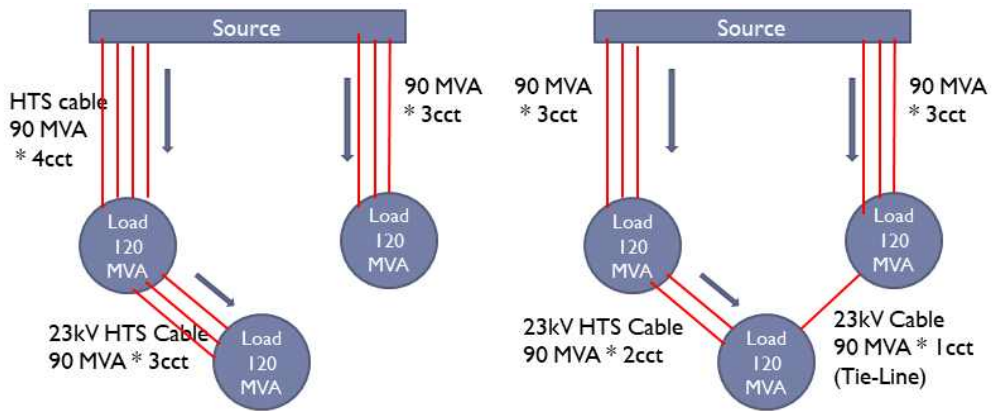


Fig. 3.29(a) A platform consisting of three switching stations with the same 120 MVA supply capacity and with the 90 MVA HTS cables

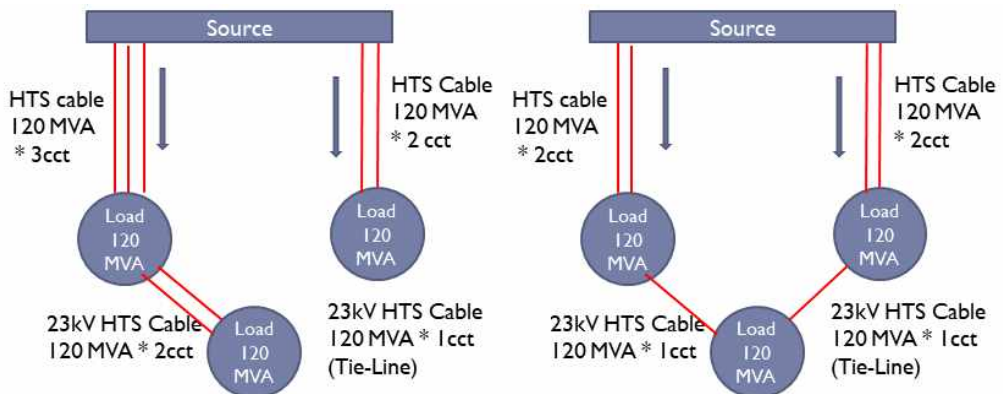


Fig. 3.29(b) A platform consisting of three switching stations with the same 120 MVA supply capacity and with the 120 MVA HTS cables

switching stations can have the effect of increasing reliability while maintaining the same number of HTS cables.

As such, the HTS power platform, similar to the loop-connected transmission system, is capable of forming a loop configuration and has the advantage of maintaining a higher reliability than the radial configuration. However, the installation of SFCLs, which can reduce the fault current of the system within a quarter of a cycle below a certain value, should be considered, because the fault current of the system may increase when the loop configuration occurs. The SFCLs applicable to the platform are described in the following

subsection.

So far, transmission duct pipes are only considered for the HTS power platform. Generally, a distribution duct would be equipped with a maximum of nine conduits. If more than nine feeders are required, cable box construction will be necessary and the construction cost will be much higher. If the 23 kV HTS cable and the distribution feeders are jointly installed in the same route, the number of distribution feeders decreases as the number of HTS cables increases. This means that the load supply capacity is reduced. Therefore, the number of HTS cables is closely related to the substation capacity as well as to the supply capacity of the 23 kV switching stations.

#### **3.4.4 Fault current mitigation**

A larger and more complex power system results in an increase in the fault current. In the event of a system fault, the circuit breaker operation should prevent damage to the power facilities owing to the failure and maintain proper reliability of the power supply. For this purpose, the circuit breakers are given a fault current breaking rating as necessary to accommodate the fault current of the system. However, if the fault current gradually increases and exceeds the breaking capacity of the circuit breaker, it will not be possible to cut off the fault current, which may have a serious effect on the system. Therefore, it is very important to keep the fault current below the proper level. Various methods are applied for this purpose, including the opening of a transmission line from a short-term operation perspective, installation of a current limiting reactor (CLR) to always suppress the fault current, or upgrading the breaking rating of the circuit breaker as a long-term planning perspective. Although system reconfiguration such as transmission line separation is most commonly applied, such approaches have been found to be inherently detrimental to power supply reliability and may lead to fatal human error mistaken by the system operator. The disadvantage of installing the CLR is that inevitably not only causes permanent power loss but also, to some extent, impedes operating

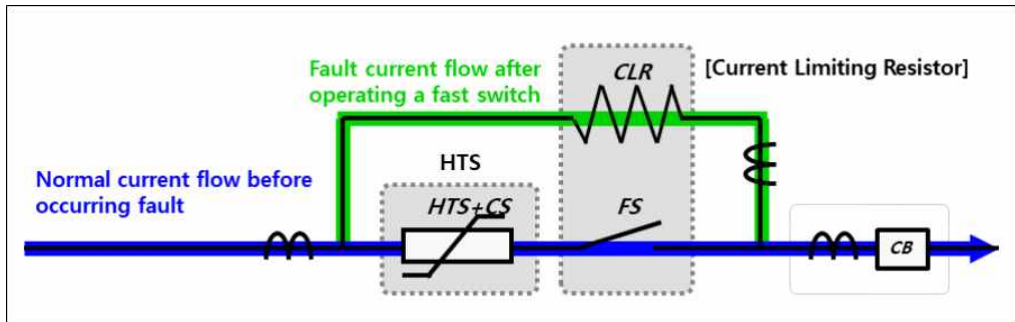


Fig. 3.30 First peak limiting resistor type superconducting fault current limiter (SFCL)

margins such as system transient stability.

In recent years, the rapidly evolving HVDC technology has shown great promise for reducing fault currents. As electrical separation of the two systems takes place around the HVDC, the inflow of fault current is eliminated. In fact, a 500 kV HVDC point-to-point connection with a length of 30 km is being installed in the KEPCO system, because the additional new 765 kV or 345 kV transmission lines cannot avoid the serious effects of the increased fault current. Other new competitively technologies are rapidly emerging to suppress the fault current by using the phenomena of HTS wire's quenching. Technical competition between the two systems, which are largely highlighted as an essential measure to control the fault current, is expected, although it is still not easy to ensure economic feasibility owing to the very high investment costs.

As shown in Fig. 3.30, the SFCL is a power device that reduces the thermal and mechanical stress of the power equipment, and reduces the fault current of the power system to below the certain value within a short duration. During normal operation with an SFCL, there is no impedance at all. In case of a fault, the impedance characteristics shown by the rapid fault detection and quench phenomenon of HTS wires reduce the fault current to a certain extent, and the circuit breakers in between operate to isolate the fault section. The time required for SFCL operation after a fault can be adjusted to within 1/4 to

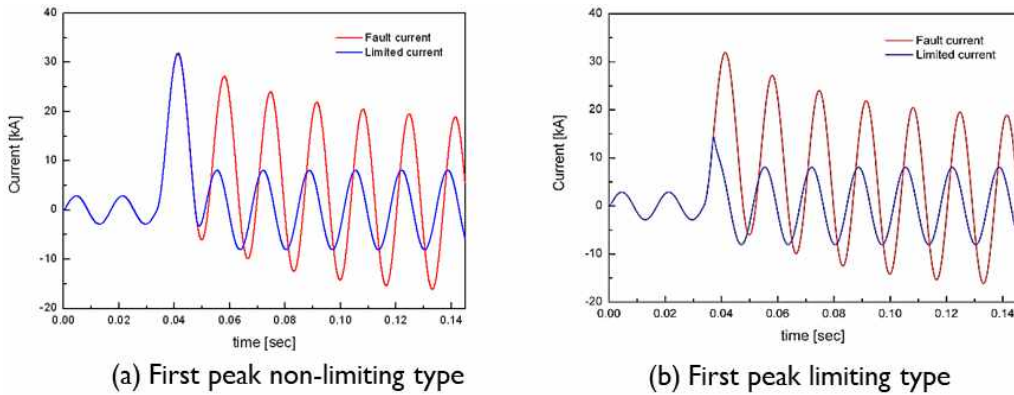


Fig. 3.31 The SFCL can be divided into the first peak limiting type, and the first peak non-limiting type

1 cycle. It is greatly advantageous in maintaining proper system reliability by using existing circuit breakers without upgrading the breaking capacity of the circuit breakers and causing power loss during normal operation [38-40].

The SFCL can be divided into the first peak limiting type, which limits the failure rate within half a cycle immediately, and the first peak non-limiting type, which limits it after one cycle, as shown in Fig. 3.29. Only the first-peak non-limiting type is applied to the power system fault current exceeds the breaking current rating of the circuit breakers. It is desirable to select the SFCL location so as to reduce the fault current; the effective location can be between the 23 kV bus and HTS cables, or near the 154 kV transformers; balanced protection and location optimization need further detailed study.

This study focuses on the configuration of HTS power platforms through the construction of a loop network with 23 kV HTS cables provided that the fault current is properly managed; therefore, no detailed technical review for limiting the fault current is carried out. It is assumed that the 23 kV SFCL is installed in series with a tie-line of the platform to minimize the quantity. The cost of the 23 kV 60 MVA SFCL is assumed to be \$0.4 million, as provided by LS Industrial Systems.

---

## **CHAPTER 4**

### **ECONOMIC EVALUATION OF 23 KV HTS POWER PLATFORM UP TO 300 MVA**

---

#### **4.1 General requirements for economic analysis**

##### **4.1.1 The scope of economic analysis**

The conventional method for an urban power supply is to build a radial substation in the load center and then provide power. The superconducting cable method will build 23 kV switching stations instead of constructing substations to supply loads. This means that superconducting cables will replace transmission cables. Considering the difficult reality of constructing substations in the load center, the substation can be built outside the city, and then power can be supplied with several distribution feeders. Like before, the superconducting cable method builds a 23 kV switching station to supply the load. In this example, however, superconducting cables will replace several power distribution feeders.

The target systems for economic evaluation of 23 kV HTS power platform were largely divided into two types: radial and loop configurations. To compare the economic efficiency of the radial configuration, it was assumed that the distance from the existing substation to the load center could be practically increased by up to 5 to 6 km, which could be fed by superconducting cables, and the load supply capacity of the station varied from 50 MVA up to 120 MVA.



The loop configuration will be utilized when power must be reliably supplied in cities with much higher load densities. The conventional method is to construct two or more new substations connected with existing power grids in loop configuration to feed power. As it is upgraded from a radial substation to a loop-connected substation, it has the advantage of increasing the reliability of the power system supply. On the HTS power platform, a 23 kV switching station will be built instead of a substation to feed loads. In this study, only two to three stations are reviewed because the quantity of switching stations that comprise the platform cannot be effective by recklessly increasing them. Economic evaluations were conducted accordingly by increasing the load supply capacity of an HTS power platform up to 300 MVA. Moreover, as we saw in Chapter 3, the supply area of the platform is closely related to load density, so in a platform consisting of two stations, the distance between the stations or between the existing substations and the station was assessed around the case of 2 km. In the three-stations platform, the distance between stations was reduced to 1 km, and the distance between stations and substations was maintained at 2 km. This is to evaluate how different economic effects can be in a platform with the same load supply capacity when there are two or three stations. The analysis target was selected as an example of the establishment of a 154 kV substation for supplying loads to urban centers or new towns. The 154kV substation consists of two to four transformers with 60 MVA capacity. The total supply capacity of the substation with three transformers is 180 MVA; however, the load supply capacity is generally considered to be 120 MVA, regarding the N-1 reliability criteria. The first study case examines the performance of two 23 kV HTS cables with a capacity of 50 MVA, assuming 23 kV switching stations that supply small loads with 50 MVA capacity. Subsequently, the second case compares the impact by increasing the superconducting cable capacity to 80 MVA, 120 MVA, and 150 MVA.

The traditional method is to install double circuits of 154kV XLPE 2000 mm<sup>2</sup> cables to supply power to a new 154 kV substation linked with a 154 kV substation installed outside the city. The installation of 154 kV cables can

be constructed underground using the cable box or conduit method depending on the region. Comparable superconducting cables are used to connect the 154kV substation installed outside the city to the new 23 kV switching stations in the load center. It is assumed that 23 kV superconducting cables are built using the conduit method to connect to the switching stations. The values discussed in Chapter 3 are used in this study. The values for substation construction are summarized in Table 4.1 as follows.

Table 4.1 Values for 154 kV Substation Construction

Items	Cost (million US\$)
154 kV transformer (four banks, 240 MVA)	3.64
154 kV GIS	1.32
Building construction (2,500 m <sup>2</sup> )	6.84
Auxiliary equipment	2.48
Total	14.28

#### 4.1.2. Analysis method

In general, an economic feasibility analysis estimates the feasibility of costs and benefits by comparing and analyzing them in currency values. A cost-benefit analysis with comparisons on an equal scale leaves little room for evaluators to intervene and assesses economics by calculating the benefit-cost ratio (BCR), net present value (NPV), and internal rate of return (IRR).

The BCR refers to the ratio of the discounted amount to the gross benefit and total cost, as shown in Eq. (1). In other words, the present value of the benefits is divided by the present value of the costs and benefits that will arise in the future. If the  $BCR \geq 1$ , the project is judged to be economically feasible.

$$BCR = \frac{\sum_{t=0}^n \frac{B_t}{(1+r)^t}}{\sum_{t=0}^n \frac{C_t}{(1+r)^t}} \geq 1.0 \quad (1)$$

where  $B_t$  is the benefit at the  $t^{\text{th}}$  period;  $C_t$ , the cost at the  $t^{\text{th}}$  period;  $r$ , the depreciation rate; and  $n$ , the number of periods, that is the analysis period.

The IRR is a discount rate that zeros the NPV of the project by obtaining a discount rate,  $R$ , that equates the present value of benefits and expenses, as expressed in Eq. (2). If the IRR is greater than the discount rate, the project is judged to be economically feasible.

$$\sum_{t=0}^n \frac{B_t}{(1+R)^t} = \sum_{t=0}^n \frac{C_t}{(1+R)^t} \quad (2)$$

$$R \geq r$$

where  $R$  is the IRR.

A cost-benefit analysis can be perceived from various viewpoints. It usually

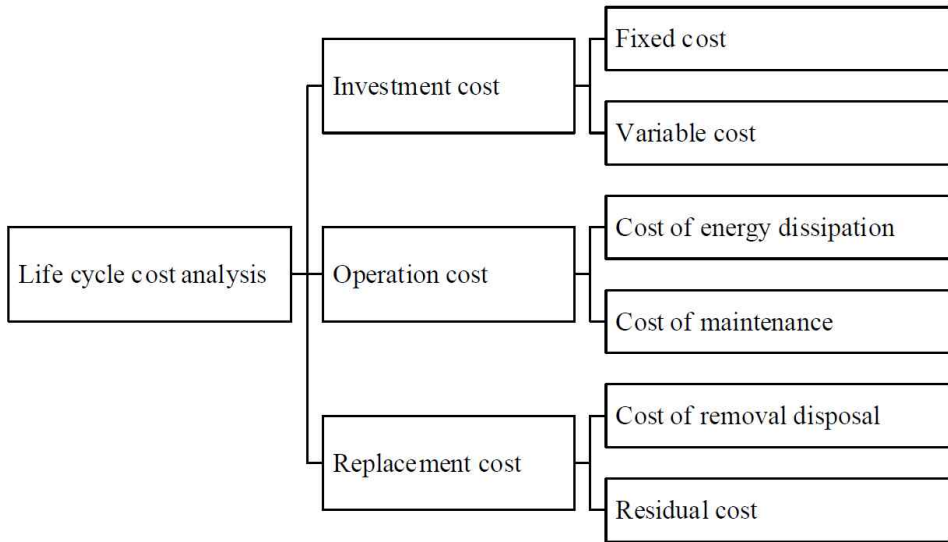


Fig. 4.1 Life-cycle cost analysis (LCCA) includes investment cost, operation cost, and replacement cost

involves the consideration of the service life of a T&D power cable, investment cost, operation cost, and replacement cost, which is called life cycle cost analysis (LCCA) [41], as shown in Fig. 4.1. Although social, planning, and environmental costs may be additional generic costs, they are not discussed in this study.

After applying these derived benefits to the superconducting cable, economic evaluation indicators such as BCR, NPV, and IRR were calculated. In this study, an economic analysis was conducted through the commonly used BCR and IRR indicators among the various economic analysis methods.

The cost and benefits of superconducting cables were assessed for various scenarios by comparing the BCRs and IRRs obtained by calculating the NPV discounted over the project period. Superconducting cables are expected to have a much longer life than conventional power cables because the conductor is in the tube filled with liquid nitrogen, which makes it difficult to exhibit deterioration phenomena unlike conventional cables. Nevertheless, in this study, the analysis period is set at 30 years considering the 30-year accounting life of general power facilities. According to Article 50 (Social Discount Rate) of the Ministry of Strategy and Finance, a social discount rate of 4.5% was utilized [42]. A higher discount rate may give an advantage to a business that generates benefits relatively quickly, and a lower discount rate may give an advantage to a business that generates benefits over a relatively longer future period. In this case, the residual value should also be considered. The residual value is the valuation that exists even after the end of the economic analysis period. The residual value is calculated by applying depreciation methods for buildings or equipment. Land has an indefinitely useful life and is excluded from depreciation. The residual value of land is equal to the cost of land at substations or stations. The residual value of land is reflected in the economic analysis as being returned at the end of the project period. KEPCO's statistics show that the land purchase cost for a standard substation is \$12.5 million in big cities, \$1.4 million in newly developed cities, \$0.8 million in small or medium-sized cities, and \$1.69 million in industrial complexes; this represents a

wide range of price distributions. The residual value of a building is calculated by applying a straight-line method in which the same amount is depreciated each year by applying a 30-year useful life. Generally, the residual value of a building does not exist because it is assumed that the project duration and the useful life of the building are the same.

#### **4.1.3 Calculation of operation costs**

Operation costs consist of maintenance costs and cooling system electrical charges. The electricity charge for the cooling system only applies to the superconducting cables. Of these, maintenance costs are typically calculated by multiplying the cable price or initial investment by a certain percentage each year. The method of multiplying the cable construction cost by the constant ratio was utilized to calculate the maintenance cost. This ratio applies to the average maintenance ratio of 2.28%, calculated from KEPCO's statistics over the past five years. The scope of maintenance costs is utilized differently depending on the characteristics of traditional cables and superconducting cables. Traditional maintenance costs reflect the costs of constructing substations and cable tunnels but not the costs of purchasing land for substations, constructing ducts, procuring cables, and installation. For 23 kV HTS cable applications, only HTS-cable-related operation expenses of the cooling system and the construction cost of the 23 kV switching stations were covered, excluding the cost of cables, land, and duct construction, as before.

Regarding the power loss of the HTS cable system, superconducting cable loss rarely occurs except for AC loss and heat loss and is not influenced by the load factor. Therefore, only the electricity cost for operating the cooling system should be reflected. The annual electricity charges for cooling systems can be calculated using Eq. (3). It was assumed that the consumption power of the cooling system will depend on the cooling capacity and design characteristics of the HTS cable system; however, because the cooling cost accounts for a small proportion of the total cost, the value estimated by calculating the cooling capacity loss in Chapter 3 is utilized considering the

coefficient of performance (COP).

$$AEC = \frac{CP_{cool}}{COP} \times 8760 \times P_{elec} \quad (3)$$

where AEC is the annual electricity charge (\$);  $CP_{cool}$ , the cooling capacity (kW); and  $P_{elec}$ , the electricity charge per kilowatt-hour. In this study, the COP value is assumed to be 10% and the electricity charge is \$0.1/kWh. The annual electricity charges for cooling system with the cooling capacity of 7.5 kW in the Shingal Project is expected to be approximately \$61,000.

#### 4.1.4 Calculation of benefits

Benefits include the contribution of electricity sales revenue, reduction of power loss, and reduction of carbon emissions. The biggest benefit from the establishment of superconducting cable systems is the profit from electricity sales. However, it is very difficult to separately calculate the contribution of HTS cable systems to electricity sales revenue. Therefore, in this study, the electricity sales revenues were considered a benefit under the assumption that the BCR of the conventional method was 1.0 [43]. This assumption was because revenue from regulated industries such as electric utilities ensures adequate returns based on the rate of return to regulatory asset base (ROA). In other words, the construction costs of substations and power lines of electric utilities are deemed to be fully recovered within the project period through proper ROA regulation. ROA regulation is based on the theories of capital asset pricing and cost of capital; however, unlike the weighted average cost of capital (WACC), ROA may be adjusted from a policy viewpoint. Because no additional benefits must be calculated for the conventional method other than electricity sales revenues, the benefits of making the BCR of conventional method 1 are the same as the present value of the total cost. This value does not mean that the total cost and the total benefit are equal but rather that the amount matches the present value of the total cost with the present value of

the total benefit.

Regarding the power loss, superconducting cables have the advantage of having almost zero resistance; therefore, the power loss of superconducting cables is much lower than that of conventional cables of the same capacity. The power loss of the conventional cable is calculated as follows in Eq (4). The difference between the power loss of the conventional cable and the power loss of the superconducting cable can be considered to be the benefit of the superconducting cable.

$$AEC_{loss} = \frac{\sqrt{3}PN_{CCT}}{V\cos\theta} \times Rl \times \theta \times 8760 \times P_{elec} \quad (4)$$

where  $AEC_{loss}$  is annual energy cost of power loss (\$); P, the peak load flow per circuit (kW); V, the rated voltage (kV); R, the resistance of the transmission cable ( $\Omega/\text{km}$ );  $N_{CCT}$ , the number of circuits; l, the cable length (km); and  $\theta$ , the load loss factor.

The resistance of conventional 154 kV XLPE cables is 0.009  $\Omega/\text{km}$  for 2,000 mm<sup>2</sup> and 0.0151  $\Omega/\text{km}$  for 1,200 mm<sup>2</sup>, respectively, and the power loss is calculated at  $\sim 40$  kW/km with a current flow of 1,000 A. From these power loss values, it is expected that, if the length of the transmission cable is increased by several kilometers or more, the power loss will increase proportionally. Thus the power loss savings of the HTS power platform will be sufficient to offset the cooling losses of the superconducting cable. However, it is still necessary to consider the relationship between the load factor and the loss factor of the power transmission lines [44-45].

In addition, one of the benefits of using superconducting cables is the reduction of carbon emissions [46]; however, these are only  $\sim 10\%$  those of the reduced power loss, and therefore, it is difficult to attach significant meaning to these benefits

$$AEC_{CO2} = \Delta P_{loss} * E_{CO2} * EP_{CO2} \quad (5)$$

where  $AEC_{CO_2}$  is annual energy saving cost of  $CO_2$  emission reduction;  $\Delta P_{loss}$ , the power loss reduction;  $E_{CO_2}$ , the amount of carbon emissions per megawatt-hour; and  $EP_{CO_2}$ , the price of carbon emissions per ton. The amount of carbon emission per unit megawatt-hour is based on 2011 data from the Korea Power Exchange, as shown in Table 4.2 and is set as 0.4585 tCO<sub>2</sub>/MWh carbon emission. The greenhouse gas emission costs are \$25/tCO<sub>2</sub> as suggested in the 7<sup>th</sup> Energy Supply Plan of the Korean government. The average emission trading price of the Korea Power Exchange between January and April 2019 is \$26 per ton, as shown in Table 4.3; however, it is utilized based on the above-mentioned value of \$25 because it varies over time.

Table 4.2 The amount of carbon emission per unit megawatt-hour based on 2011 data from the Korea Power Exchange

(Source: <https://www.kpx.or.kr/www/contents.do?key=222>)

Year	Reference Point	Carbon Emission (tCO <sub>2</sub> /MWh)
2008	Generation	0.4494
	Load	0.4682
2009	Generation	0.4515
	Load	0.4707
2010	Generation	0.4517
	Load	0.4705
2011	Generation	0.4415
	Load	0.4585



Table 4.3 The average emission trading price of the Korea Power Exchange between January and April 2019

(Source: <https://www.kpx.or.kr/www/contents.do?key=222>)

Month	Jan.	Feb.	March	April	Average
Price (US\$)	25.1	26.1	26.5	27.6	26.3

## 4.2 Economic evaluation of radial-type 23 kV HTS cable application to replace 154 kV conventional cables

### 4.2.1 Total investment cost of 23 kV HTS cable for substation elimination

As shown in Fig. 4.2, the total investment cost was calculated based on the distance between the existing substation and the load center, in which the new substation or the switching station is located for the conventional method and HTS cable application method using Eq. (6), respectively; however, the land price to secure the substation site or the switching station site was not included to evaluate its economic effect separately.

$$TIC = C_{STA} + L(2C_a + C(1 - \alpha) + T\alpha) \quad (6)$$

TIC: Total Investment Cost (million \$)

$C_{STA}$ : 154 kV Substation or 23 kV Switching Station (million \$)

L: Distance between Substation and Load Center (km)

$C_a$ : 154 kV XLPE or 23 kV HTS Cable (million \$)

C: 154 kV or 23 kV Conduit (million \$)

T: Cable Tunnel (million \$/km)

$0 \leq \alpha \leq 100$  : Percentage of Distance taken up by Cable Tunnel over Entire Transmission Cable Distance (L)

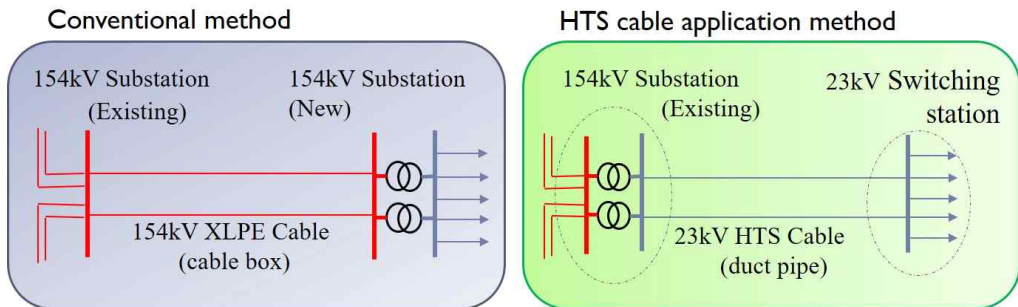


Fig. 4.2 Application of 23 kV HTS cables to replace the 154 kV transmission cables and 154 kV substations

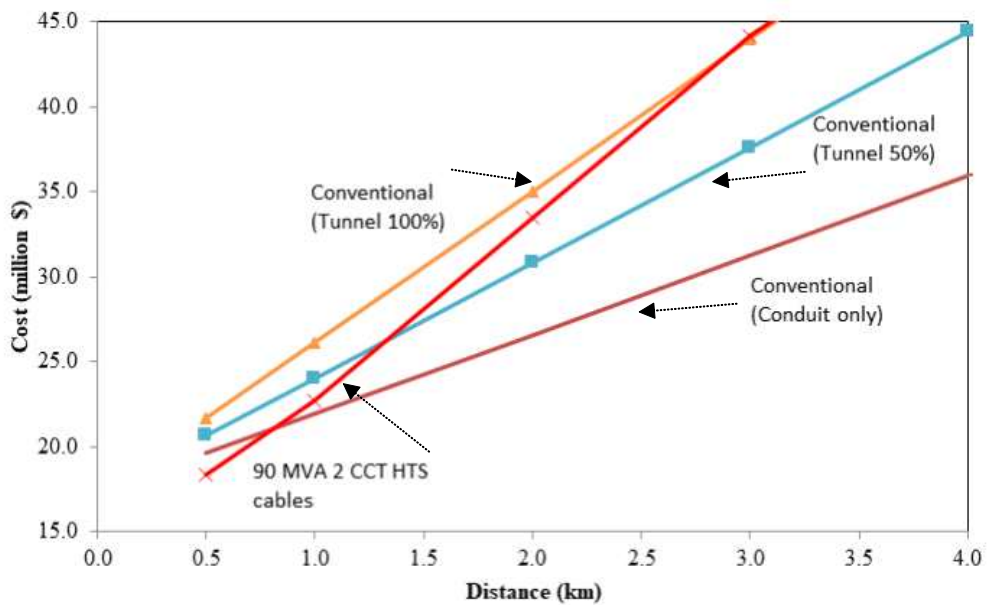


Fig. 4.3(a) The investment cost of the conventional method and 90 MVA HTS cables by distance and the percentage of distance taken up by the cable tunnel

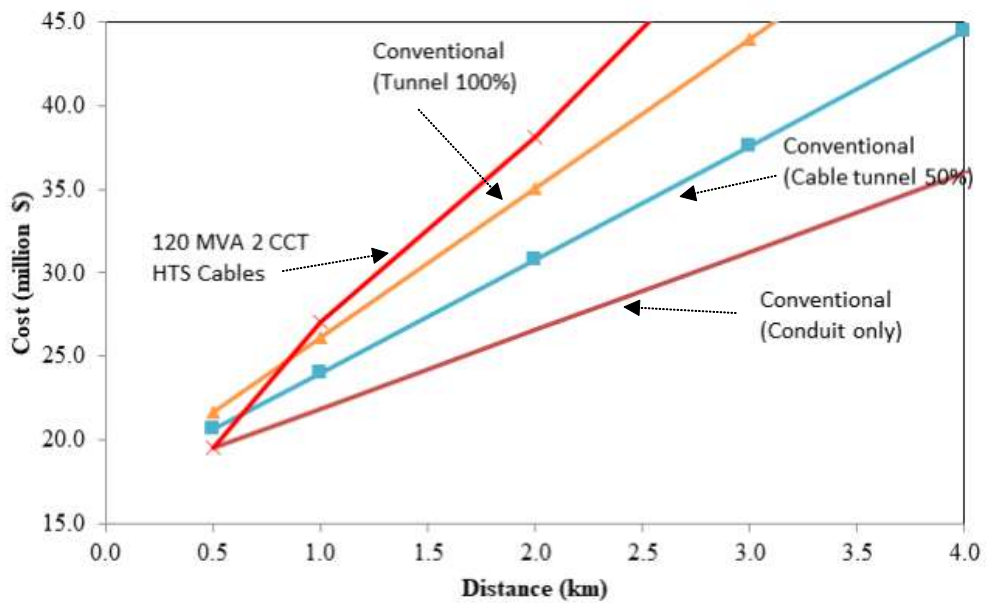


Fig. 4.3(b) The investment cost of the conventional method and 120 MVA HTS cables by distance

Figs. 4.3(a) and (b) show the investment cost by distance and the percentage of distance taken up by the cable tunnel over the entire transmission cable distance when two circuits of 154 kV XLPE cables, 23 kV 90 MVA HTS cables, or 23 kV 120 MVA HTS cables are installed for the conventional method and HTS cable application method respectively. When the distance from the substation is 1 km, the investment cost is calculated as \$21.9 million for the conventional method with conduits only and \$22.7 million for the HTS method. Conversely, if the distance increases to 3 km, the investment cost is \$31.3 million and \$44.2 million, respectively. As the distance from the substation increases, both the conventional and the HTS methods showed an increase in investment cost, and it can be observed that the difference in investment cost between the two methods continued to increase.

In addition, when the change in investment cost by the percentage of distance taken up by the cable tunnel over the entire transmission cable distance was examined, the higher the ratio of the cable tunnel, the steeper was the increase in investment cost. The comparison results of the investment cost indicate that there is a distance for which the investment cost between the conventional and the HTS methods is equal; this is the break-even distance. Fig. 4.3(a) shows that, when the ratio of the cable tunnel is 50%, the investment cost of the two methods is equal at the break-even distance of 1.4 km. Beyond the break-even distance, the HTS application method cannot be economical.

The load supply capacity with a capacity rating of 60 MVA double HTS cable circuits is equivalent to a small 154 kV substation with two transformers with a capacity of 60 MVA, and the 120 MVA rated double circuit is more important because it equals the load supply capacity of the conventional standard 154 kV substation with three transformers. When the distance from the substation is 1 km, the investment cost is calculated as \$24 million for the conventional method with 50% of cable tunnel and \$27 million for the HTS method. However, if the distance increases to 3 km, the investment cost is \$37.6 million and \$51.1 million, respectively, as shown in Fig. 4.3(b).

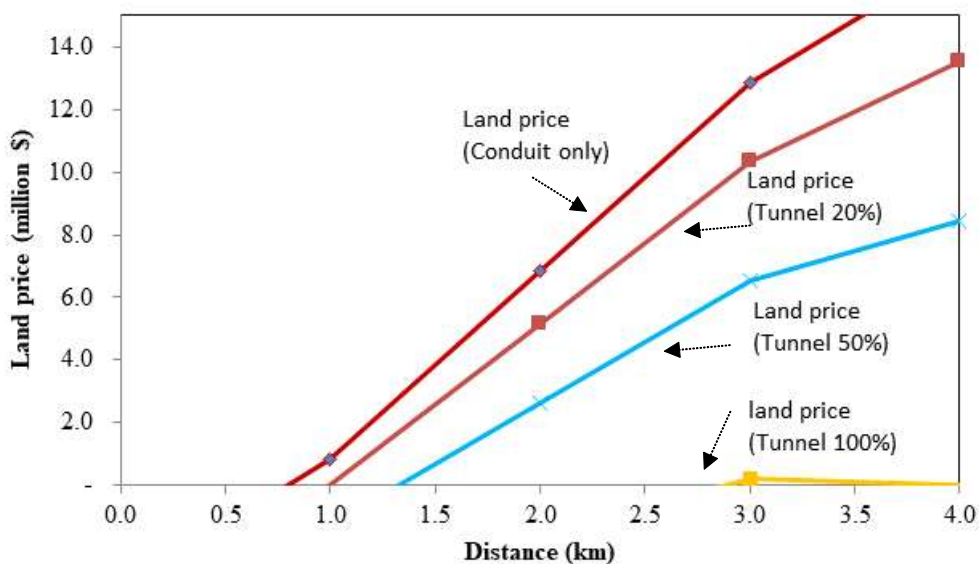


Fig. 4.4 The land price difference that makes the investment cost of the conventional method and the HTS only method the same when two 90 MVA HTS cables are used

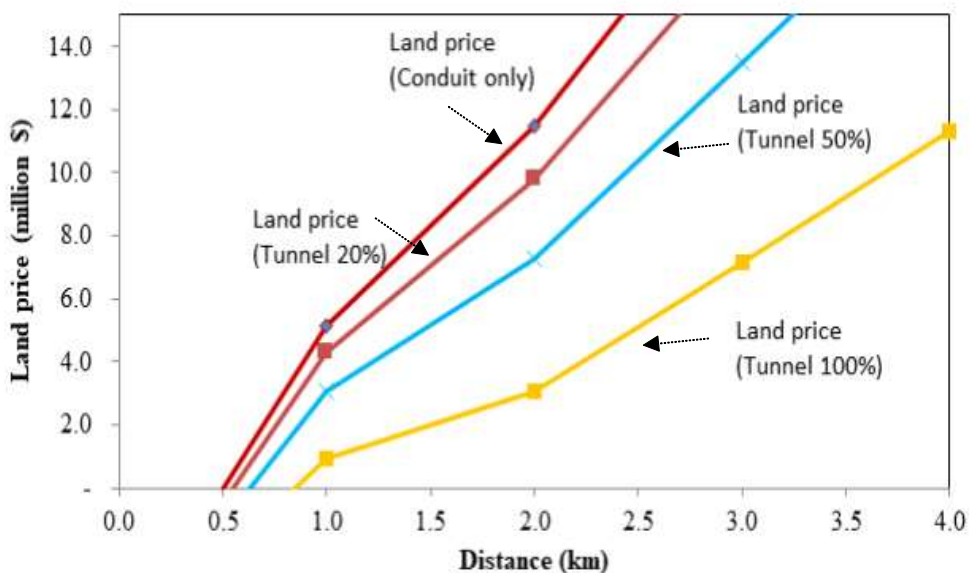


Fig. 4.5 The land price difference that makes the investment cost of the conventional method and the HTS-alone method the same when two 120 MVA HTS cables are used

Fig. 4.4 reveals the results of calculating the land price difference that makes the investment cost of the conventional method and the HTS only method the same. For example, if the difference in land price is \$2.6 million for a cable tunnel percentage of 50%, the break-even distance is  $\sim 2$  km. If the land price is \$8.4 million, it will be about 4 km. This means that, the higher the land price for the substation and the higher the ratio of the cable tunnel, the more economical the HTS application.

Similarly, Fig. 4.5 depicts the land price difference that makes the investment cost of the conventional method and the HTS-only method the same. If the difference in land price is \$3 million with 100% cable tunnel, the break-even distance is  $\sim 2$  km. This means the HTS cable application can be economical up to this distance with 100% cable tunnel. Fig. 4.6 compares the total investment costs including land price with an assumption of 50 % cable tunnel.

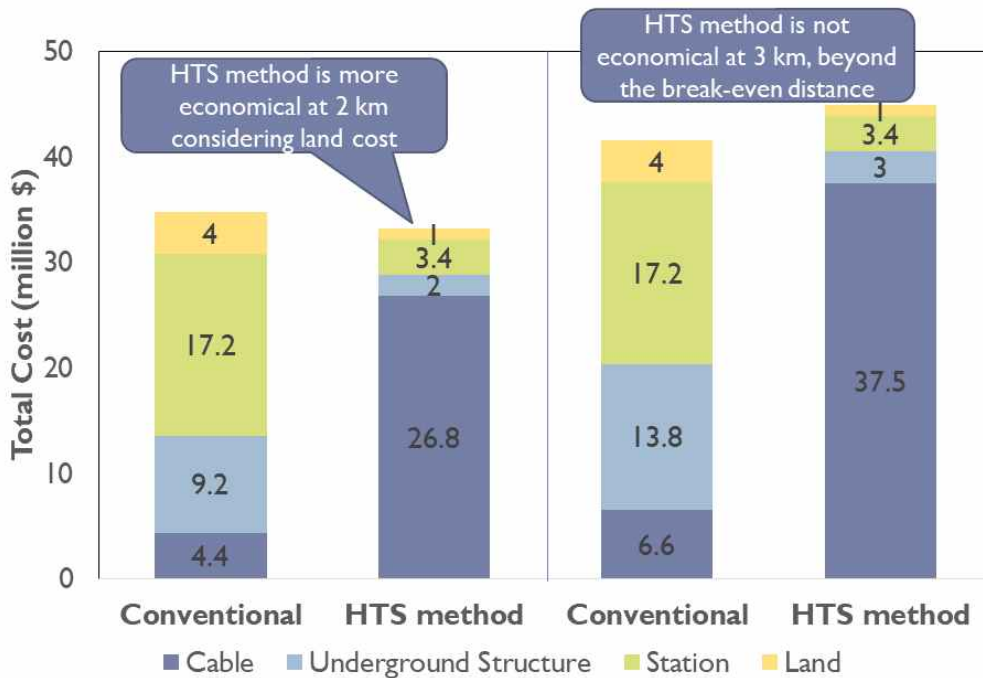


Fig. 4.6 Total investment cost comparison between conventional and HTS cable application method considering the land cost \$4 million of substation (distance 2 km and 3 km, respectively)

#### 4.2.2 Total investment cost of 23 kV HTS cable for substation relocation

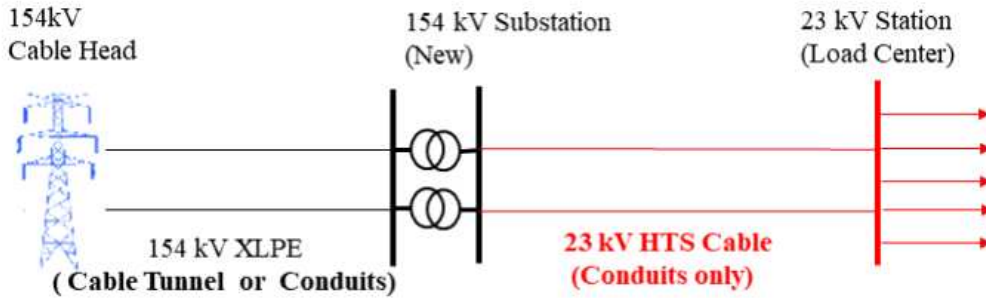


Fig. 4.7 If 23 kV HTS cables are used rather than a bundle of distribution feeders, less expensive conduits can be constructed instead of a cable tunnel

In the conventional method, the farther the substation is located from the load center, the longer the distribution feeders and the shorter the transmission cables. This results in more bundles of distribution feeders on the same corridor from the new substation, which requires the construction of a cable tunnel instead of conduits to accommodate them, as shown in Fig. 3.16(a). If 23 kV HTS cables are used rather than a bundle of distribution feeders, less expensive conduits can be constructed instead of a cable tunnel, as shown in Fig. 4.7. Only a 23 kV switching station at the center of loads is necessary to link 23 kV HTS cables and to supply power to the load. This section shows the results of reducing the investment cost owing to the low construction cost of conduits.

In this analysis, the land price for the new 154 kV substation (and 23 kV switching station) site is included in the total investment cost under the assumption that the land price around the load center is the highest and that it decreases exponentially with the distance from the load center. Furthermore, it was assumed that the minimum cost of land acquisition for the substation was set to \$0.5 million and the full distance from the cable head to the center of loads was 10 km.

The total investment cost was calculated for the conventional method and the HTS hybrid application method using Eqs. (7) and (8), respectively

$$TIC = C_{TS} + (10 - L)(2C_t + C(1 - \alpha) + T\alpha) + L(10C_d + T) + LP(A_s \exp^{-L/1000}) \quad (7)$$

$$TIC = C_{TS} + C_{STA} + (10 - L)(2C_t + C(1 - \alpha) + T\alpha) + L(2C_{HTS} + C) + LPA_{STA} + A_s \exp^{-L/1000} \quad (8)$$

$C_{STA}$ : 23 kV Switching Station (million \$)

$C_{TS}$ : 154 kV Substation (million \$)

$C_t$  : 154 kV Cable (million \$/km)

$C_d$ : 23 kV Distribution Feeder (million \$/km)

$C_{HTS}$ : 23 kV HTS Cables (million \$/km)

$0 < L \leq 10$ : Distance between 154 kV Substation and 23 kV Switching Station or Center of Loads (km)

$LP$ : Land Price at Center of Loads (thousand \$/m<sup>2</sup>)

$A_{STA}$ : Area of 23 kV Switching Station (m<sup>2</sup>)

$A_s$ : Area of 154 kV Substation (m<sup>2</sup>)

Fig. 4.8 shows the results of investment cost by distance when two circuits of 120 MVA HTS cables are installed, where the solid line represents the use of HTS cable and the dotted line, the conventional method using 10 more distribution feeders. As the distance increases, the total investment cost of both the HTS hybrid method and the conventional method decreases for a short distance. This is because under the conventional method, the investment cost of the transmission cables decreases and that of the distribution side increases significantly owing to the construction of the cable tunnel as the distance between the substation and the switching station at the center of loads increases. In addition, the overall change in total investment cost due to land price changes was shown to have a relatively high impact at short distances but not much over longer distances, as shown in Fig 4.9. This is because the closer the distance, the greater the impact of land purchase price.



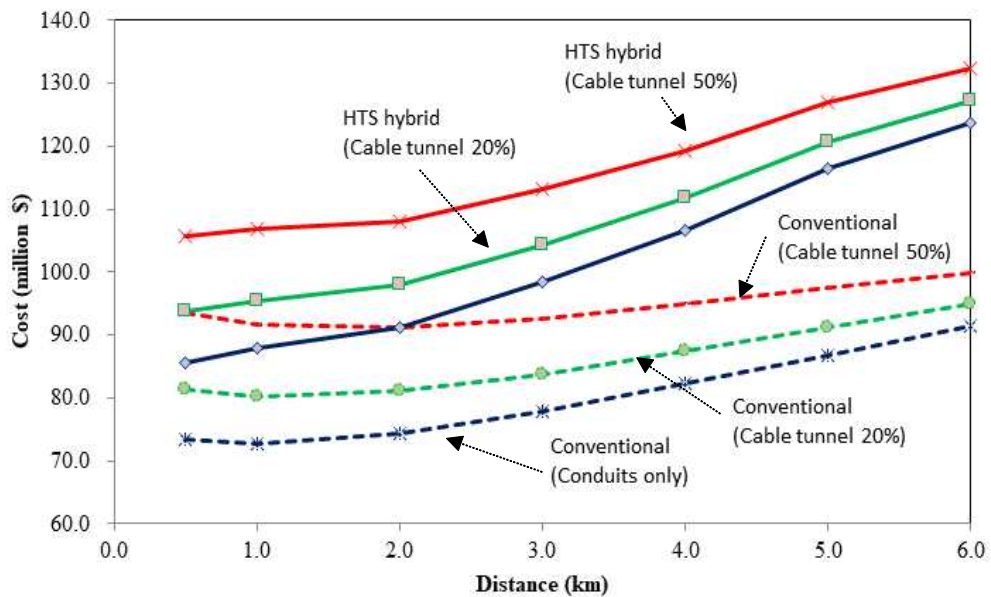


Fig. 4.8 The investment cost by distance when two circuits of 120 MVA HTS cables are installed

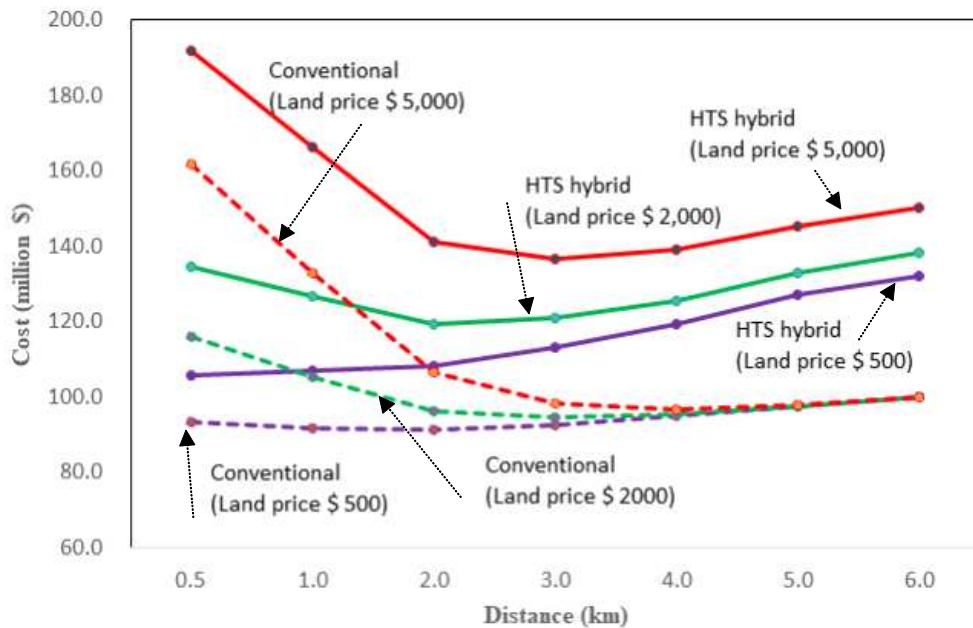


Fig. 4.9 The overall change in total investment cost due to land price changes

Significantly, there is no break-even distance when the HTS hybrid and conventional investments are the same, even with a higher land price. The higher the land price, the larger the spread between the two methods. In other words, it is very difficult to justify the investment of a 23 kV HTS cable application for the replacement of distribution feeders.

#### **4.2.3 Life-cycle cost and benefit of 23 kV HTS cable compared with the conventional method**

Through the review in the previous section, the economics of utilizing 23 kV HTS cables was found to be more reasonable if replacing transmission cables than replacing a bundle of distribution feeders. Thus, the comparative target of life-cycle cost analysis is to be limited to the construction of a radial substation or 23 kV switching station in the load center. The site unit costs were considered for \$2,500/m<sup>2</sup>, \$10,000, and \$25,000. The site unit price of \$2,500/m<sup>2</sup> here means \$6 million for the land purchasing cost of the substation, and as shown in Fig. 4.5 and 4.5, the distance to the load center was subject to review for 2 km where the investment cost of the superconducting cable appeared economically.

When constructing switching stations instead of substations in the center of loads located 2 km from existing substations, the respective economic indicators were calculated for cable capacities of 90 MVA and 120 MVA and summarized as shown in tables 4.4, 4.5 and 4.6. It was assumed that cable tunnels account for 50% of the entire section when applying the conventional method. Table 4.4 presents the cost of making BCR 1.0 from the conventional method as a benefit of electricity sales revenue for the HTS application method.

For example, for the 90 MVA HTS cables, the present value of cost was calculated at \$34.3 million in initial investment including the land cost, \$5.4 million in maintenance, and \$2.9 million in cooling system operation, with the present value of benefits calculated at \$46.8 million in sales revenue, \$1

million in power loss, and \$0.1 million in greenhouse gas reduction.

These results indicate that the economic impact of the initial investment and site costs on the economics of superconducting cables is relatively high. The maintenance cost and effect of reducing power loss do not seem to have much meaning as they are relatively very small. In big cities, the method of installing superconducting cables and small stations was found to be economical up to  $\sim 2$  km compared to purchasing very expensive land and installing substations. Likely, the longer the distance and larger the capacity, the lower the economics; however, the lower the price of superconducting cables, the greater the distance and capacity.

Table 4.4 The economic indicators based on the land price when constructing a substation in the center of loads located 2 km from existing substations

Conventional Method (154 kV Substation )						
Land price (\$/m <sup>2</sup> )	Benefit(million US\$)		Cost (million US\$)		BCR	IRR (%)
	Sum	Present value	Sum	Present value		
2,500	86.1	46.8	58.0	46.8	1.0	4.5
10,000	111.4	60.5	76.7	60.5	1.0	4.5
25,000	162.1	88.0	114.3	88.0	1.0	4.5

Table 4.5 The economic indicators based on the land price when constructing a 23 kV switching station connected with two 23 kV 90 MVA HTS cables

HTS application method (90 MVA cable × 2 CCT)						
Land price (\$/m <sup>2</sup> )	Benefit (million US\$)		Cost (million US\$)		BCR	IRR (%)
	Sum	Present value	Sum	Present value		
2,500	88.3	47.9	50.0	42.6	1.12	5.7
10,000	113.6	61.7	53.7	45.4	1.36	7.6
25,000	164.2	89.2	61.2	50.9	1.75	10.3

At the Table 4.5, the present value of \$47.9 million benefit means electricity sales revenue of \$46.8 million, power loss savings of \$1 million, and carbon emissions reduction of \$0.1 million. The present value of \$42.6 million cost represents the sum of \$34.3 million in investment cost, \$5.4 million in maintenance cost, and \$2.9 million in cooling system electrical charges.

Table 4.6 The economic indicators based on the land price when constructing a 23 kV switching station connected with two 23 kV 120 MVA HTS cables

HTS application method (120 MVA cable × 2 CCT)						
Land price (\$/m <sup>2</sup> )	Benefit (million US\$)		Cost (million US\$)		BCR	IRR (%)
	Sum	Present value	Sum	Present value		
2,500	88.3	47.9	55.4	47.7	1.00	4.4
10,000	113.6	61.7	59.2	50.5	1.22	6.2
25,000	164.2	89.2	66.7	56.0	1.59	8.8

### **4.3 Economic analysis of 23 kV HTS power platform with two to three 23 kV switching stations**

#### **4.3.1 Configuration of HTS power platform up to 300 MVA capacity**

Based on the application of the HTS power platform presented in Chapter 3, cases consisting of two stations and three stations were selected as follows. To compare the total load supply capacity of the platform for 240 MVA and 300 MVA, the load supply capacity of each station of the platform comprising two 23 kV switching stations (two-station platform) was determined to be 120 MVA and 150 MVA, respectively. Similarly, each station's load supply capacity was set to 80 MVA and 100 MVA on a three-station platform. For the two-station platform, the distance between the 154 kV substation and the 23 kV switching station is assumed to be 2 km and that between the two stations is assumed to be 2 km. In the three-station platform, the distance between the 154 kV substation and the 23 kV switching station is 2 km, and that between the station located in the middle and the other stations is assumed to be 1 km each. This configuration was set due to the same geographic characteristics between the two-station and the three-station, because of which the economic comparison could be meaningful. Meanwhile, the additional inflow of fault currents is inevitable with a loop-linked configuration compared to the radial configuration when connecting stations with superconducting cables. To address this issue, it was assumed that the fault current can be controlled by installing 23 kV SFCL devices in a series with the 23 kV tie-line connection breaker.

The initial investment costs were compared at first by considering when a platform was built at once during the economic review process. In this case, the calculation of the present value and the residual value was not considered.

However, it is more reasonable for all 23 kV switching stations on the platform to be built sequentially, rather than simultaneously, in consideration of load increases. To reflect this in the life-cycle cost analysis, a 30-year load increase model was assumed, as depicted in Figs. 4.10 and 4.12. If the load of

the first 23 kV switching station is expected to exceed the station's load supply capacity after the initial construction, the construction of the second station will take place in advance, as shown in Fig. 4.11. Therefore, the timing of the construction will depend on the station's capacity and the demand forecast. The costs are calculated step-by-step for economic review. In this process, the 30-year maintenance and cooling operation costs were calculated. The benefits from the sale of electricity to superconducting platforms were equally applied to cover the total cost of the present value through the conventional method. In this way, the economic indicators of HTS power platforms were calculated.

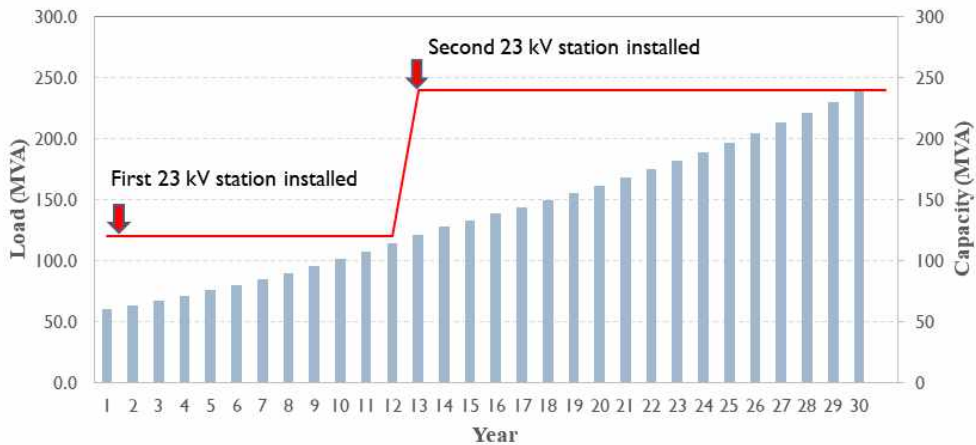


Fig. 4.10 A 30-year load increase model and the sequential installation of a 23 kV switching station for the two-station platform

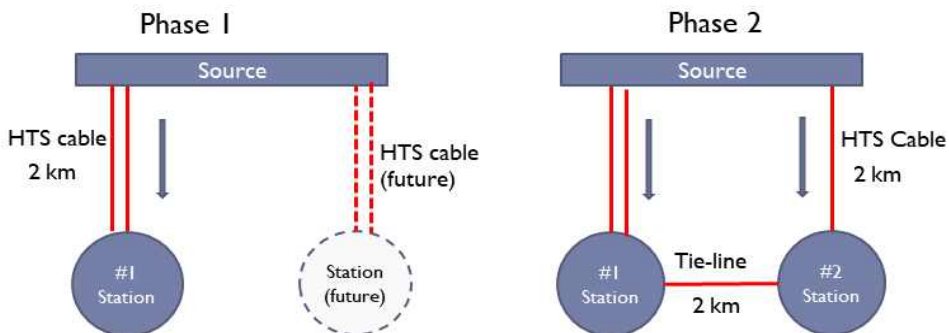


Fig. 4.11 The construction of the two 23 kV switching stations by phases based on the demand forecast for the two-station platform

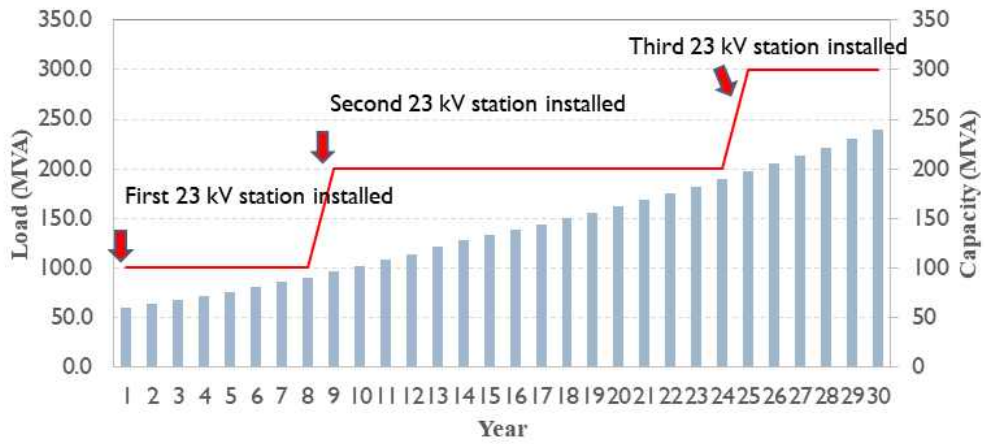


Fig. 4.12 A 30-year load increase model and the sequential installation of a 23 kV switching station for the three-station platform

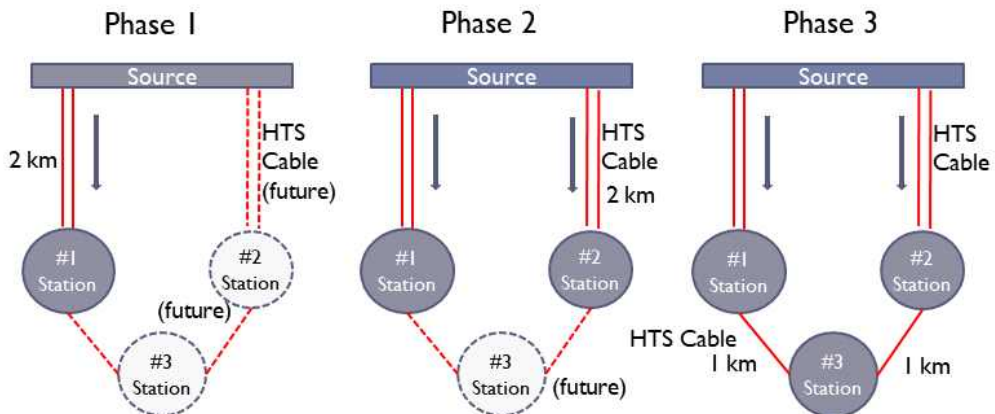


Fig. 4.13 The construction of the two 23 kV switching stations by phases based on the demand forecast for the three-station platform

### 4.3.2 Total investment cost of a 23 kV HTS power platform by load supply capacity and types of radial or loop configuration

When calculating the total investment cost of the HTS power platform, as shown in Fig. 3.24, the number of 23 kV HTS cables has been determined to satisfy the deterministic N-1 reliability criterion, which is widely used in practice for transmission expansion planning. The total investment cost was calculated as the sum of the construction costs of 154 kV substations, 23 kV switching stations, and a 23 kV HTS cable system including the conduits, which is given by Eq. (9).

$$TIC = C_{TS} + C_{STA} + C_{SFCL} + \sum (N_{CCT} C_{HTS} + C_{Duct}) L_i \quad (9)$$

where  $C_{TS}$  and  $C_{STA}$  are the construction costs of the 154 kV substations and the 23 kV switching stations, respectively;  $N_{CCT}$ , the number of circuits of 23 kV HTS power cables;  $C_{HTS}$  and  $C_{DUCT}$ , the costs of the HTS cable system and duct construction, respectively;  $L_i$ , the length of the  $i^{th}$  section of HTS cables between the substations and stations; and  $C_{SFCL}$ , the cost of the 23 kV SFCL.

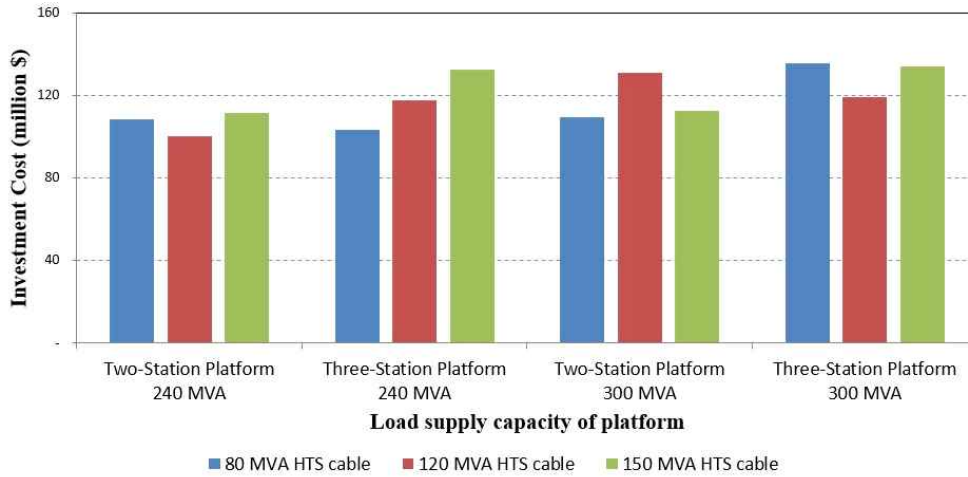


Fig. 4.14 The total investment cost of an HTS power platform based on the load supply capacity and the capacity of 23 kV HTS cables



Fig. 4.14 demonstrates the total investment cost of an HTS power platform based on the load supply capacity and the capacity of 23 kV HTS cables according to the station's capacity. For example, on a two-station platform with a load supply capacity of 240 MVA, the lowest investment cost was achieved when the platform was configured with 120 MVA HTS cables. If the station's capacity is increased to 150 MVA, which makes the load supply capacity of a two-station platform 300 MVA, the capacity of HTS cables was found to be the most economical when configured with 80 MVA double circuits, not 150 MVA or 120 MVA HTS cables. However, if configured as a 150 MVA HTS cable, it appears to be around \$117.8 million, which is 2.5% more expensive than the lowest cost of \$114.9 million for 80 MVA HTS cables. All the detailed information on the investment cost breakdown is listed, as shown in tables 4.7, 4.8, 4.9 and 4.10.

Table 4.11 gives the total investment cost of the three-station platform, which has a 300 MVA load supply capacity and a radial configuration with no tie-line. It has a minimum investment of \$137.1 million when using a 120 MVA HTS cable rating, while a loop-type platform has a minimum investment of \$123.3 million when using the same HTS cable rating. The difference between the two is \$13.8 million, which represents a ~10% change from the total investment cost. This is mainly caused by the different amount of HTS cables besides the SFCL installation cost required for the loop-type platform. Since the difference in investment costs between the radial type and loop type platform can vary depending on configuration and construction environment conditions, either the radial or loop type is not necessarily economical, as shown in Figs. 4.15 and 4.16. Nevertheless, a difference in investment costs is expected to be offset if reliability values are considered because the power supply reliability of the loop-type platform provides a significant improvement in the interconnection between the two stations. By combining these features, the process of selecting the optimum cable capacity for the HTS power platform will be examined in subsection 4.4.

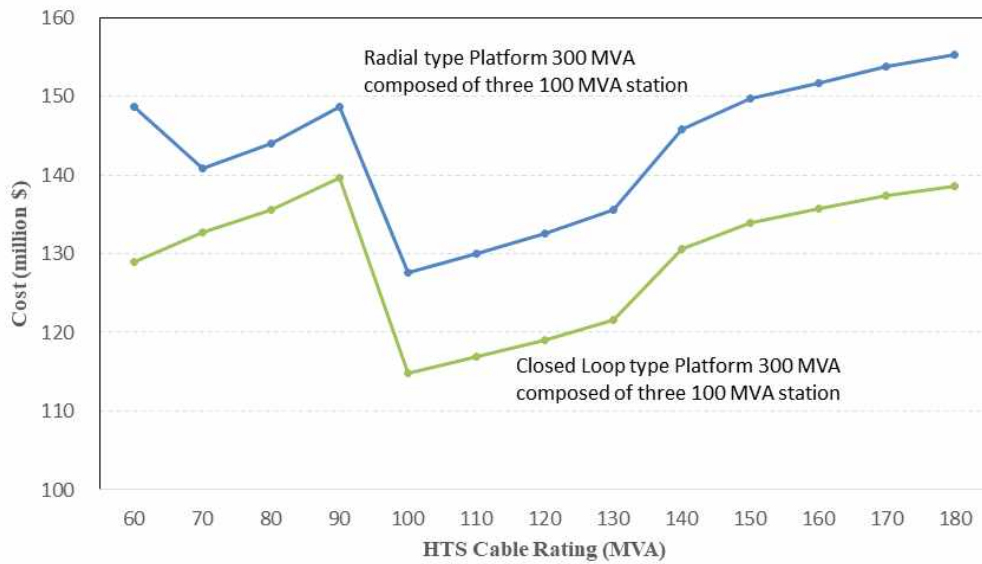


Fig. 4.15 For a three-station platform, a loop-type configuration seems more economical

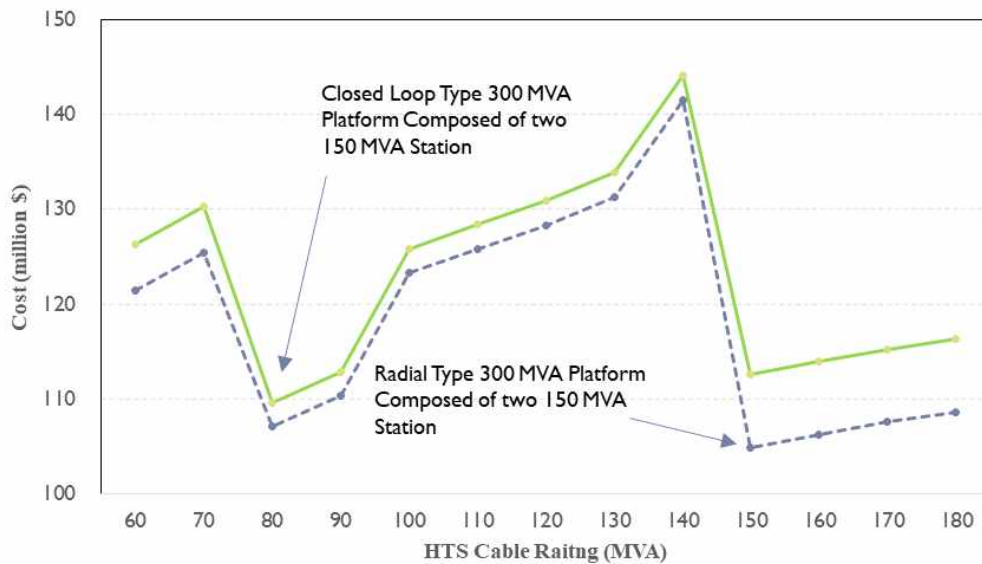


Fig. 4.16 For a two-station platform, a radial-type configuration seems more economical

Table 4.7 The investment cost breakdown of two-station loop-type HTS power platform (120 MVA  $\times$  2 stations)

Type		Two-station platform (loop configuration)		
Total load supply capacity (MVA)		240		
23 kV switching station		120 MVA $\times$ 2 stations		
Capacity of 23 kV HTS cables (MVA)		80	120	150
Minimum required number of circuits		6	4	4
Initial capital cost (million US\$)	HTS cables	51.1	45.5	54.9
	Cooling system	26.2	23.8	25.4
	Duct	2.2	2.0	2.0
	23 kV station	8.8	9.0	9.0
	154kV substation	20.0	20.0	20.0
	Land (\$ 3,000/m <sup>2</sup> )	3.0	3.0	3.0
Total investment cost		111.3	103.3	114.3

Table 4.8 The investment cost breakdown of a two-station loop-type HTS power platform (150 MVA  $\times$  2 stations)

Type		Two-station platform (loop configuration)		
Total load supply capacity (MVA)		300		
23 kV switching station		150 MVA $\times$ 2 stations		
Capacity of 23 kV HTS cables (MVA)		80	120	150
Minimum required number of circuits		6	6	4
Initial capital cost (million US\$)	HTS cables	51.1	68.3	54.9
	Cooling system	26.2	30.2	25.4
	Duct	2.2	2.2	2.0
	23 kV station	10.0	10.1	10.2
	154kV substation	22.4	22.4	22.4
	Land (\$ 3,000/m <sup>2</sup> )	3.0	3.0	3.0
Total investment cost		114.9	136.2	117.8

Table 4.9 The investment cost breakdown of a three-station loop-type HTS power platform (120 MVA  $\times$  3 stations)

Type		Three-station platform (loop configuration)		
Total load supply capacity (MVA)		240		
23 kV switching station		80 MVA $\times$ 3 stations		
Capacity of 23 kV HTS cables (MVA)		80	120	150
Minimum required number of circuits		6	6	6
Initial capital cost (million US\$)	HTS cables	43.7	58.0	69.7
	Cooling system	26.9	26.9	30.2
	Duct	2.0	2.0	2.0
	23 kV station	10.6	10.7	10.8
	154kV substation	20.0	20.0	20.0
	Land (\$ 3,000/m <sup>2</sup> )	4.5	4.5	4.5
Total investment cost		107.8	122.3	137.3

Table 4.10 The investment cost breakdown of a three-station loop-type HTS power platform (150 MVA  $\times$  3 stations)

Type		Three-station platform (loop configuration)		
Total load supply capacity (MVA)		300		
23 kV switching station		100 MVA $\times$ 3 stations		
Capacity of 23 kV HTS cables (MVA)		80	120	150
Minimum required number of circuits		7	6	6
Initial capital cost (million US\$)	HTS cables	65.5	58.0	69.7
	Cooling system	35.8	26.9	30.2
	Duct	2.4	2.0	2.0
	23 kV station	11.8	11.9	12.0
	154kV substation	20	20	20
	Land (\$3,000/m <sup>2</sup> )	4.5	4.5	4.5
Total investment cost (million US\$)		140.0	123.3	138.4

Table 4.11 The investment cost breakdown of a three-station radial-type HTS power platform (150 MVA  $\times$  3 stations)

Type		Three-station platform (radial configuration)		
Total load supply capacity (MVA)		300		
23 kV switching station		100 MVA $\times$ 3 stations		
Capacity of 23 kV HTS cables (MVA)		80	120	150
Minimum required number of circuits		10	7	7
Initial capital cost (million US\$)	HTS cables	74.0	69.4	83.4
	Cooling system	36.3	29.9	33.0
	Duct	2.2	1.9	1.9
	23 kV station	11.4	11.4	11.4
	154kV substation	20	20	20
	Land (\$3,000/m <sup>2</sup> )	4.5	4.5	4.5
Total investment cost (million US\$)		148.4	137.1	154.2

### 4.3.3 Life-cycle cost and benefit analysis of HTS power platform compared with conventional methods

As explained in the previous subsection, it is not easy to extract the benefits from the electricity sales revenue for the HTS power platforms. Therefore, the present value of the cost was reflected as the benefits of the HTS power platform with the assumption that the present value of the investment and maintenance costs for the conventional method could be 100% recovered through the regulated policy for the utilities. Other benefits of HTS power platform includes the savings from the power loss reduction and the greenhouse gas emission reduction. The benefit of the greenhouse gas emission was considered although it was too small. Tables 4.12 and 4.13 summarize the specifications of the conventional method and the HTS power platform with the load supply capacity of 240 MVA and 300 MVA for comparison. The HTS power platform with a 240 MVA load-supply capacity is the same size as two 154 kV substations with three 60 MVA transformers. Similarly, a platform with a load-supply capacity of 360 MVA is the same size as two substations with four 60 MVA transformers or three substations with three 60 MVA transformers. In this study, the number of substations for the conventional method was set to two, because a 154 kV substation with four transformers is considered only for an emergency supply and is not deemed a standard substation.

The present value of life cycle costs and benefits of an HTS power platform is given in Eqs. (10) and (11).

$$PV_{LCC} = TIC_o - (1+r)^{-30} C_{site} + \sum_{i=1}^n (1+r)^{-i} (C_{maint,i} + C_{cool,i}) \quad (10)$$

$$PV_{LCB} = \sum_{i=1}^n (1+r)^{-i} (B_{electricity,i} + B_{loss,i}) \quad (11)$$

where  $PV_{LCC}$  and  $PV_{LCB}$  are the life-cycle costs and benefits;  $r$ , the interest rate;  $i$ , the year; and  $C_{site}$ ,  $C_{maint}$ , and  $C_{cool}$ , the price of land, maintenance cost,



and operation cost of a cooling system, respectively.

Table 4.12 The specifications of the conventional method and the HTS power platform with a load supply capacity of 240 MVA

	Conventional Method	HTS Power Platform	
Load Supply Capacity (MVA)	240	240	240
Specification	154 kV S/S × 2	23 kV 120 MVA Station × 2	23 kV 80 MVA Station × 3
Underground Structure	Cable box	Conduit	Conduit

Table 4.13 The specifications of the conventional method and the HTS power platform with a load supply capacity of 300 MVA

	Conventional Method	HTS Power Platform	
Load Supply Capacity (MVA)	240	300	300
Specification	154 kV S/S × 2	23 kV 150 MVA Station × 2	23 kV 100 MVA Station × 3
Underground Structure	Cable box	Conduit	Conduit

Tables 4.14, 4.15, 4.16 and 4.17 summarize the BCR and IRR of the HTS power platform with a load supply capacity of 240 MVA and 300 MVA, respectively by the loop-connection of the HTS power cable capacity. It was assumed that all transmission cables are installed underground in a cable box when using the conventional method, as before. These results indicate that the BCR for the HTS power platform is less than 1, making it seemingly difficult to achieve direct economic feasibility. Moreover the results show that the economic impact of the initial investment and site costs on the economics of the HTS power platform are relatively high. The maintenance cost and effect of reducing power loss do not seem to have much meaning as they are

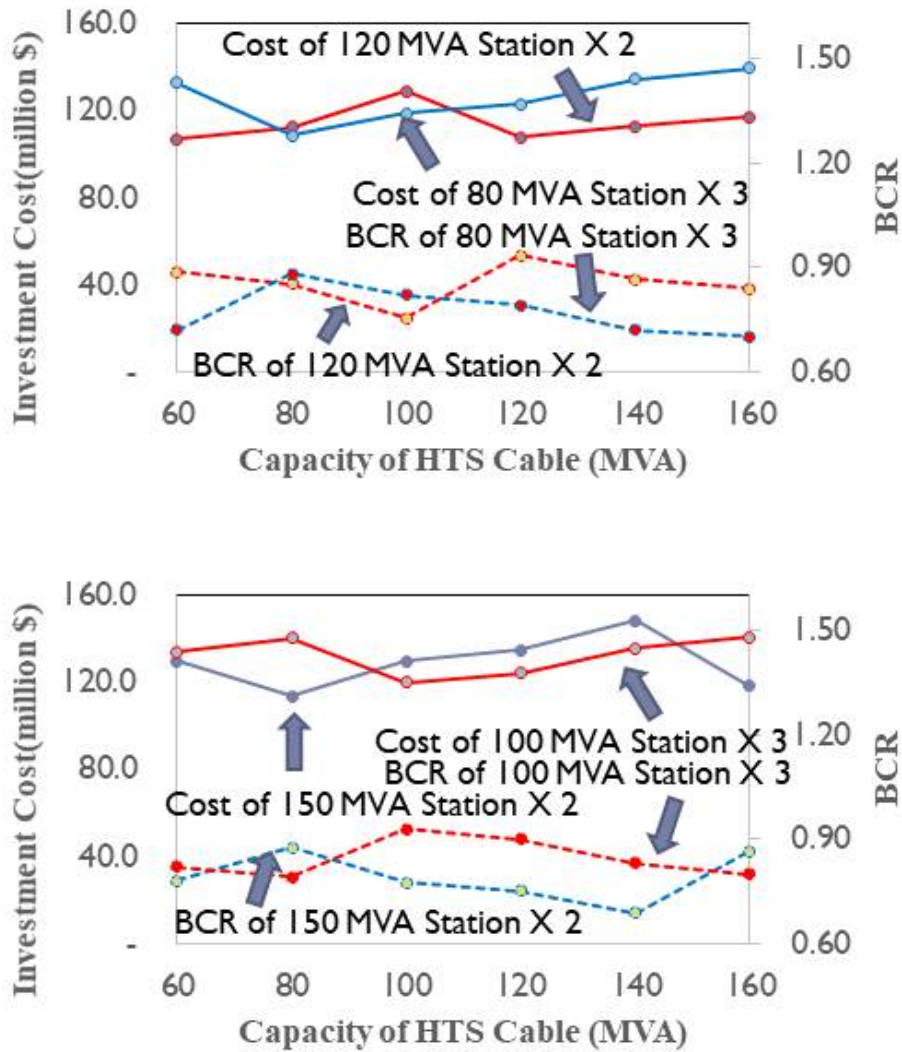


Fig. 4.17 The comparison of the investment costs and BCRs between the two-station or three-station platform with the same load-supply capacity by the HTS cable capacity

relatively very small.

Based on the HTS power platform with the same load-supply capacity, the investment costs and BCRs were compared between two or three switching stations, as shown in Fig. 4.17. It was found that the economics of the platform differed depending on the HTS cable capacity rather than the number

of stations that constituted the platform. It also demonstrates a very close inverse relationship between the BCR and the investment costs of the HTS platform. This means that the economic comparison of the HTS power platform can also be meaningful rather than the life-cycle cost analysis, by simply comparing it with the initial investment cost.

Table 4.14 The BCR and IRR of the two-station HTS power platform with a load supply capacity of 240 MVA

Type	Two-station platform (loop configuration)		
Total load supply capacity (MVA)	240		
23 kV switching station	120 MVA $\times$ 2 stations		
Land price	\$3,000 $\times$ 500 m <sup>2</sup> $\times$ 2		
Capacity of 23 kV HTS cables (MVA)	80	120	150
Minimum required number of circuits	6	4	4
Total investment cost (million US\$)	112.5	104.8	115.9
Cost (million US\$)	100.1	91.3	100.5
Benefit (million US\$)	82.9	82.9	82.9
BCR	0.83	0.91	0.83
IRR (%)	2.16	3.20	2.10

Table 4.15 The BCR and IRR of the three-station HTS power platform with a load supply capacity of 240 MVA

Type	Three-station platform (loop configuration)		
Total load supply capacity (MVA)	240		
23 kV switching station	80 MVA $\times$ 3 stations		
Land price	\$3,000 $\times$ 500 m <sup>2</sup> $\times$ 3		
Capacity of 23 kV HTS cables (MVA)	80	120	150
Minimum required number of circuits	6	6	6
Total investment cost (million US\$)	108.7	123.2	138.1
Cost (million US\$)	96.8	107.8	120.5
Benefit (million US\$)	85.3	85.3	85.3
BCR	0.88	0.79	0.71
IRR (%)	2.58	1.50	0.49

Table 4.16 The BCR and IRR of the two-station HTS power platform with a load supply capacity of 300 MVA

Type	Two-station platform (loop configuration)		
Total load supply capacity (MVA)	300		
23 kV switching station	150 MVA $\times$ 2 stations		
Land price	\$3,000 $\times$ 500 m <sup>2</sup> $\times$ 2		
Capacity of 23 kV HTS cables (MVA)	80	120	150
Minimum required number of circuits	6	6	4
Total investment cost (million US\$)	113.8	135.2	117.1
Cost (million US\$)	97.3	113.8	97.5
Benefit (million US\$)	82.9	82.9	82.9
BCR	0.85	0.73	0.85
IRR (%)	1.22	-1.94	0.98

Table 4.17 The BCR and IRR of the three-station HTS power platform with a load supply capacity of 300 MVA

Type	Three-station platform (loop configuration)		
Total load supply capacity (MVA)	300		
23 kV switching station	100 MVA $\times$ 3 stations		
Land price	\$3,000 $\times$ 500 m <sup>2</sup> $\times$ 3		
Capacity of 23 kV HTS cables (MVA)	80	120	150
Minimum required number of circuits	9	6	6
Total investment cost (million US\$)	140.6	124.4	139.3
Cost (million US\$)	108.6	94.3	105.4
Benefit (million US\$)	85.3	85.3	85.3
BCR	0.79	0.90	0.81
IRR (%)	1.59	3.20	1.94

#### 4.3.4 Economic impact of land price in urban areas

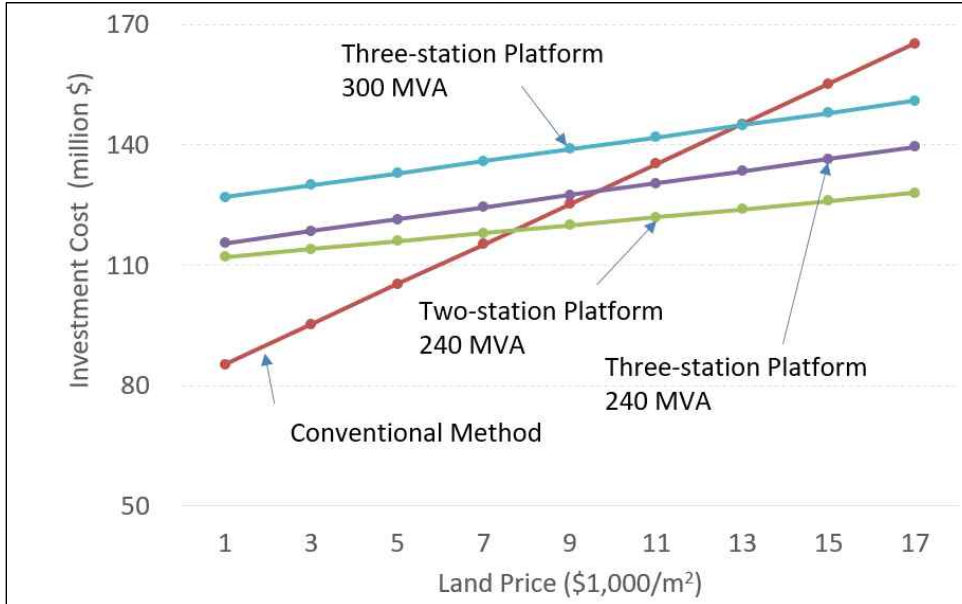


Fig. 4.18 Total investment cost of HTS power platform by land price

To compare the difference in the total investment costs between the conventional method and the HTS power platform, the land purchase cost for the 154 kV substations and 23 kV switching stations was reflected in the calculation of the total investment cost of the HTS power platform. It was assumed that the land price per  $\text{m}^2$  in urban areas could be varied, but that the cost of the substation site on the outskirts would be set at a minimum of \$1 million, which is equivalent to \$400/ $\text{m}^2$ . For a land price of \$1,000/ $\text{m}^2$ , the HTS power platform costs almost 20% higher than the conventional method, as shown in Fig. 4.18. However, if the unit land price is \$8,000/ $\text{m}^2$ , there is a break-even point at which the total investment costs between the two methods are equal.

Encouragingly, the land purchase expenses of the HTS power platform are significantly lower than those of conventional methods due to the much smaller space of 23 kV switching stations. If the number of 23 kV switching stations is two, with 120 MVA or three with 80 MVA, that is the total load supply

capacity of the HTS power platform remains the same, the total investment cost of the HTS power platforms with two stations is relatively more advantageous. Fig. 4.19 shows the comparison of the total investment cost between the conventional method and HTS power platform. The HTS power platform shows the HTS cable cost accounts for the largest share and the cooling system is the second largest.

#### **4.3.5 The cost effects of an external single return path of $\text{LN}_2$**

The 23 kV tri-axial HTS cables used for this economic evaluation study uses a single external pipe as the return path of  $\text{LN}_2$  for two circuits of HTS cables (2-Go 1-Return type). Thermo-hydraulic analysis was performed to determine the operating conditions of 23 kV tri-axial HTS cables considering the allowable operating temperature and pressure drop characteristics. [7]

Fig. 4.20 illustrates the cost effects of an external single return path for  $\text{LN}_2$ . The HTS power platform using the 2 Go-1 Return type rather than 1 Go-1 Return type had an investment cost savings of approximately 7% or more. For example, if two circuits of HTS cable are necessary, a 1 Go-1 return HTS cable system needs a total of four conduits. However, since the 2 Go-1 return uses only three conduits, it has the advantage of one more conduit available for distribution feeders. Moreover, the size of a cooling system and the number of monitoring and control systems can be optimized while maintaining the same reliability. Concerning reliability, it still has the advantage of transmitting the same capacity if one of the two HTS cables is used as a return path for  $\text{LN}_2$ , even with the single contingency of an external return pipe.



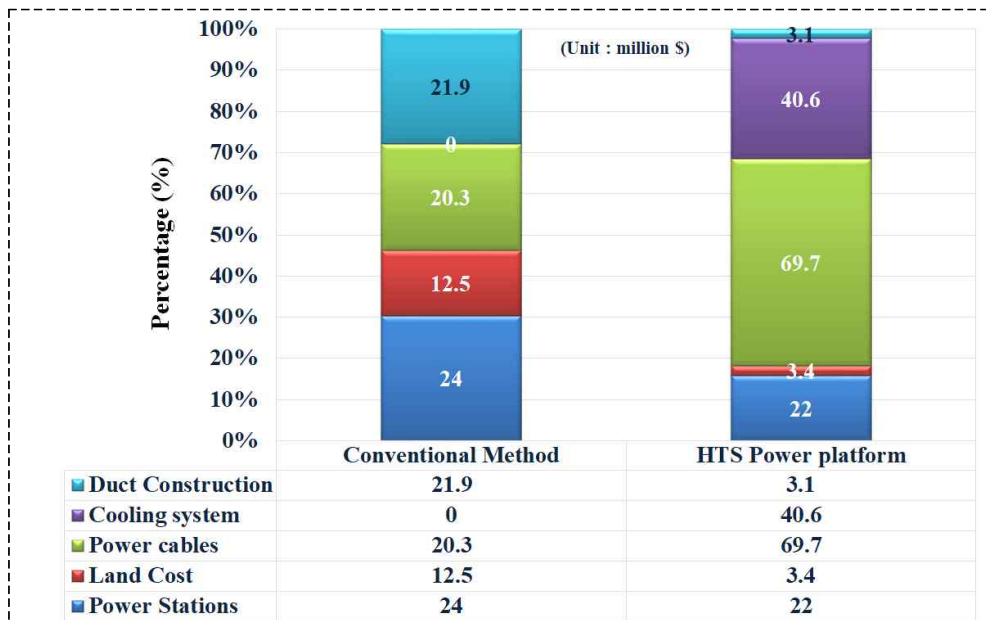


Fig. 4.19 Cost comparison between conventional method and HTS power platform

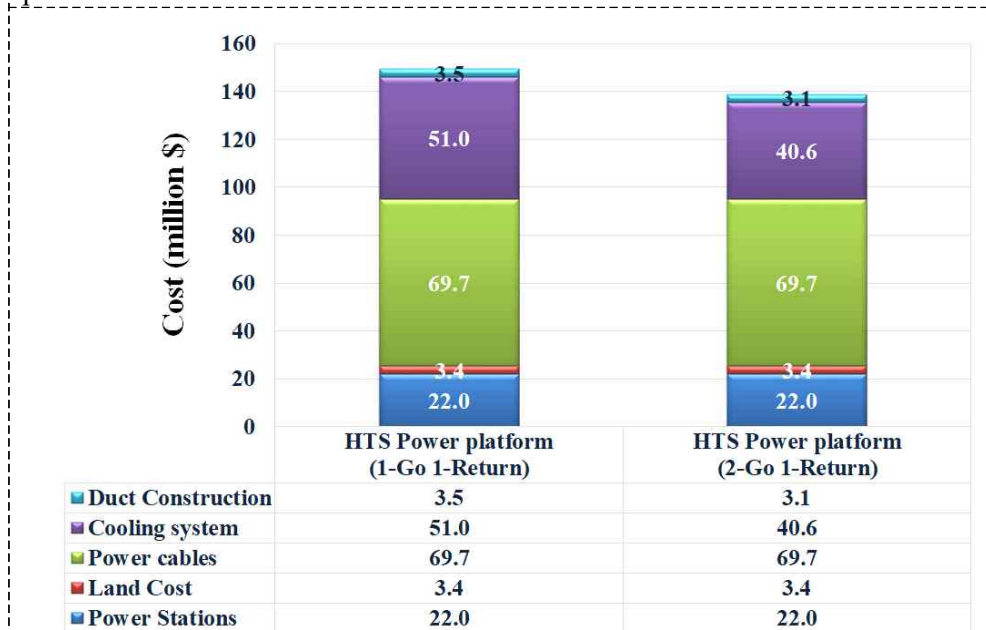


Fig. 4.20 Cost comparison of 1 Go-1 return and 2 Go-1 return

## 4.4 Optimal rating selection of 23 kV HTS power cables for a 23 kV HTS power platform by load supply capacity

### 4.4.1 A 23 kV HTS power cable rating for an HTS power platform comprising two 23 kV switching stations

Each line in Fig. 4.21 represents the total investment cost of a two-station HTS power platform consisting of 90 MVA, 120 MVA, 150 MVA and 180 MVA of 23 kV switching stations by the capacity of HTS cables ranging from 60 MVA to 180 MVA. For example, the middle red line represents the total investment cost of an HTS power platform in case the switching station's capacity is set to 120 MVA. Then, the total load supply capacity of this platform is 240 MVA since there are two switching stations. The HTS power platform appears to be the most economical when configured with HTS cables of 120 MVA. Similarly, for the HTS power platform consisting of two 150 MVA stations, as shown by the green line in the same Fig. 4.21, the lowest

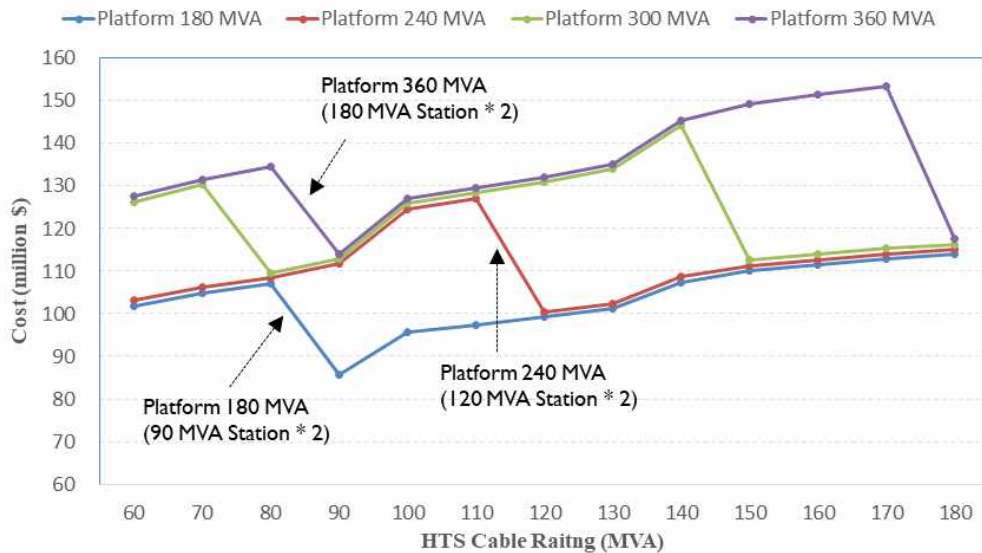


Fig. 4.21 The total investment cost of the HTS power platform based on the load supply capacity and the capacity of 23 kV HTS cables according to the 23 kV switching station's capacity

investment cost was achieved when the platform was configured with 150 MVA HTS cables. Notably, HTS cables of 80 MVA were the second most economical. These results indicate that it is reasonable to select a capacity of HTS cable equal to or equal to half the capacity of switching stations.

#### 4.4.2 A 23 kV HTS power cable rating for an HTS power platform comprising three 23 kV switching stations

Like the previous platform, but adding one more 23 kV switching station between the two stations, the total investment cost of the HTS power platform consisting of three switching stations was summarized, as shown in Fig. 4.22. Similarly, these results indicate that it is reasonable to select a capacity of HTS cable equal to the capacity of switching stations.

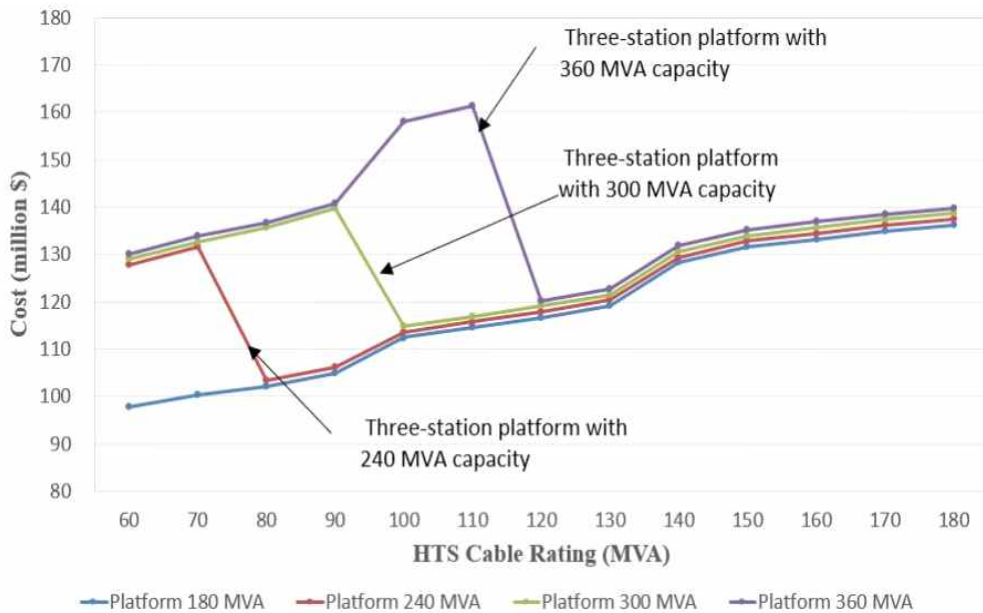


Fig. 4.22 The total investment cost of the three-station loop-type HTS power platform by the capacity of 23 kV HTS cables

Looking at the total investment costs of radial-type three-station HTS power platforms, as shown in Fig.4.23, it represents a somewhat different form of loop type than we have seen before. However, it can still be seen that it is reasonable to apply a cable capacity that matches a station's capacity.

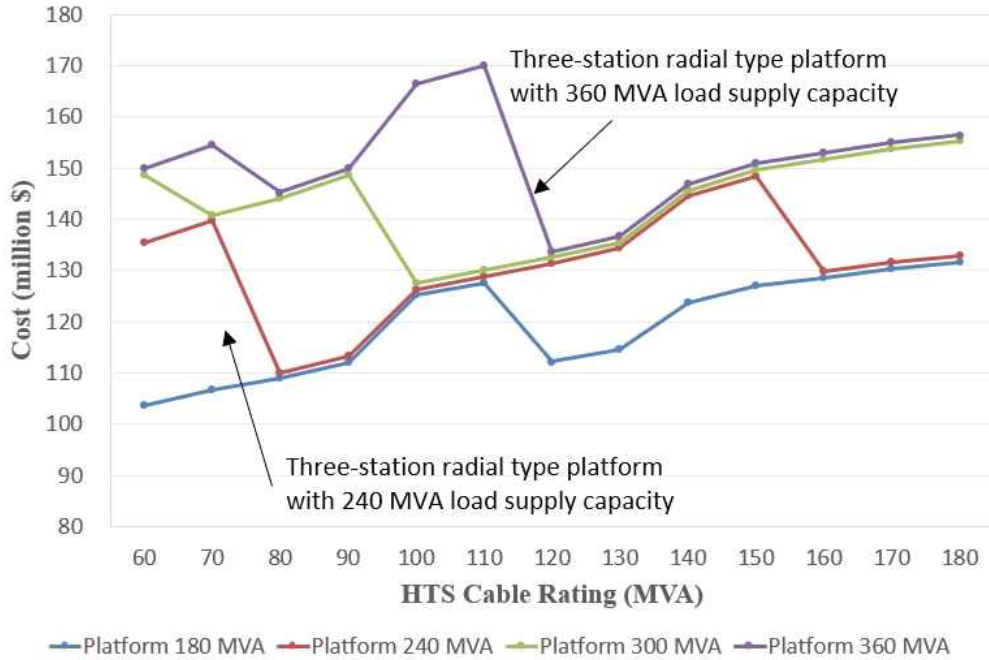


Fig. 4.23 The total investment cost of the three-station radial-type HTS power platform by the capacity of 23 kV HTS cables

---

## CHAPTER 5

### INSTALLATION OF 23 kV 60 MVA HTS POWER PLATFORM IN A REAL GRID

---

As shown in Fig. 5.1, one cell of a 23 kV HTS power platform will be demonstrated between KEPCO's 154 kV Munsan and Sunyou substations. For this purpose, a 23 kV switching station with 60 MVA capacity will be constructed in the middle of a cable route instead of a 154 kV substation and it will be loop connected with 23 kV tri-axial HTS cables to verify their performance, social, and economic effects. In this chapter, the selection of candidate sites and design requirements is described for the use of the 23 kV HTS power platform with the actual power system.

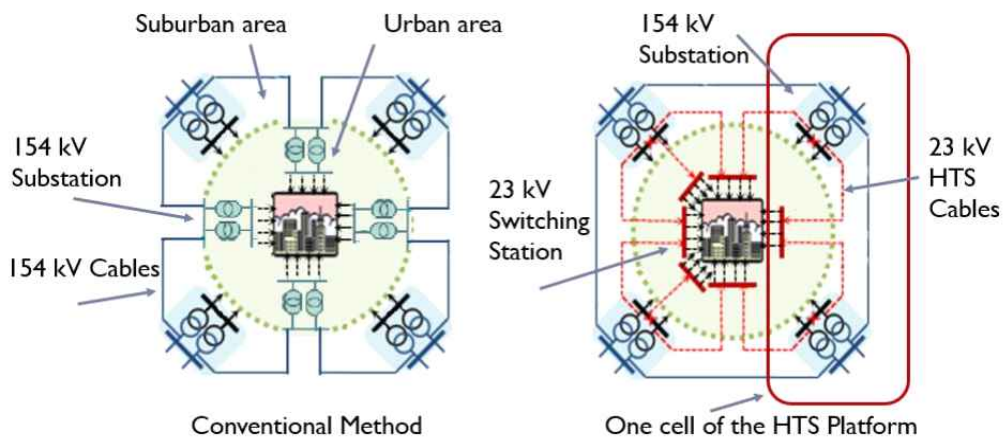


Fig. 5.1 Conventional method and the one cell of the 23 kV HTS power platform

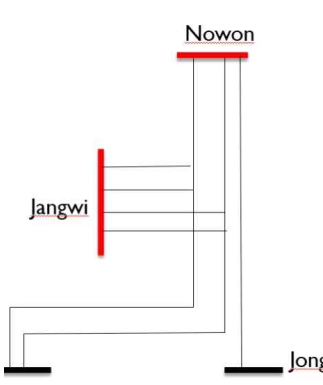
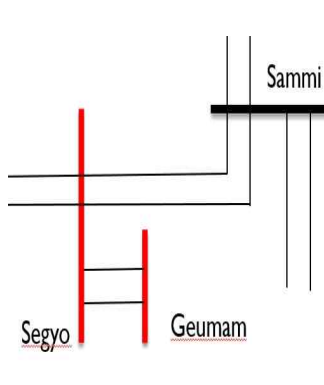
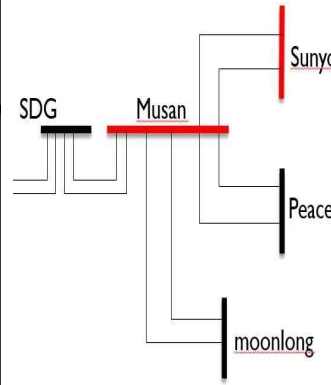
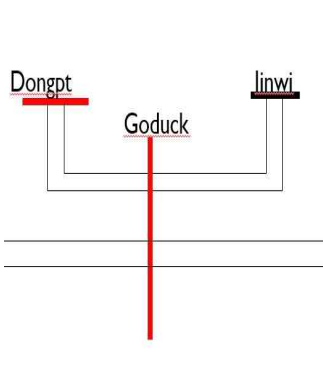
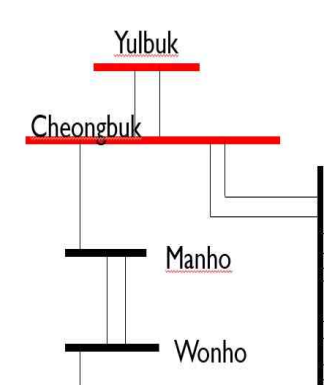
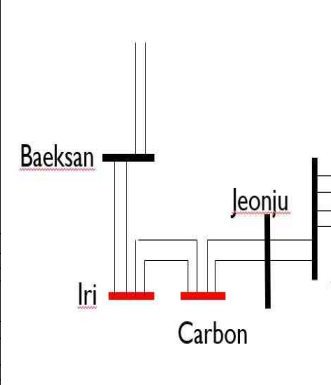
## **5.1 Site selection for the 23 kV 60 MVA HTS power platform**

Following the configuration of the HTS power platform suggested in Chapter 3, Chapter 4 reviewed the economics of the HTS power platform according to the two types: radial or loop configuration. During the review of the HTS power platform comprising up to three 23 kV switching stations, a very close relationship was noted between the load supply capacity of the HTS power platform and the HTS cable capacity. Based on the study results, specific discussions for application with a real system have been initiated. Considering that this demonstration project will be the first case for the new urban power supply configuration, the required specification of the platform was set as a 60 MVA switching station, loop connected with adjacent 154 kV substations through the 23 kV, 60 MVA HTS cable systems.

When selecting a candidate site, several conditions were set as follows: First, the target site should be a downtown power supply facility; therefore, there should be extra space for the expansion of transformers in existing substations that feed power to the platform. Second, considering the cooling capacity, the distance of 23 kV HTS cables should not exceed 3 km. Third, to reduce the burden on system operators because this is their first HTS power platform, areas with relatively less sensitive loads, such as housing, appear more suitable. Finally, power systems seem satisfactory if they have relatively easy loads to transfer to nearby substations in case of a supply emergency.

According to the above-described conditions, six 154 kV substation candidates were derived, as shown in Table 5.1, by reviewing 154 kV substations or 154 kV transmission lines with their construction scheduled until the year 2025 in the long-term transmission expansion plan. The radial 154 kV Sunyou substation, one of the above candidate sites, has two banks of 60 MVA transformers and is connected only to the 154 kV Munsan substation, and 44% of the total load cannot be transferred in case of a double contingency of transformers resulting in a full blackout. From the last three years of load variation profiles from 154 kV Sunyou substations, it can be

Table 5.1 Six 154 kV substation candidate locations derived from the eighth long-term transmission expansion plan of KEPCO

Jangwi S/S (planned)	Geumam S/S (planned)	Sunyou S/S (existing)
Cable length: 2 km	Cable length: 3 km	Cable length: 2 km
		
Dongpt S/S (existing)	Yulbok S/S (planned)	Carbon S/S (planned)
Cable length: 3.5 km	Cable length: 1.5 km	Cable length: 2.5 km
		

confirmed that the Sunyou substation is supplying 40—60 MW, or  $\sim 50\%$ , of the total 120 MVA facility, and that the nearby 154 kV Munsan substation has four banks installed and supplies 90—140 MW. To solve the reliability issue of the radial substation located at the end of the transmission line, the long-term transmission expansion plan aimed to secure a dual power source by

connecting a Sunyou substation with an SDG substation. If a 23 kV switching station is constructed between the Sunyou and Munsan substations and a 23 kV HTS cable is installed, not only is reserve power shared between the two substations but also loads can be fed through 23 kV HTS cables in the event of a blackout of the Sunyou substation. In addition, the distance between the new switching station and the Munsan and Sunyou substations is  $\sim 1$  km each. Consequently, all six candidate sites were comprehensively reviewed for load profiles, system operation conditions, and construction conditions. Finally, it was decided to establish an HTS power platform between the Sunyou and the Munsan substations, with the capacity of the platform set at 60 MVA, as shown in Fig. 5.2.



Fig. 5.2 The demonstration project of a 23 kV 60 MVA HTS power platform between KEPCO's 154 kV Munsan and Sunyou substations



## 5.2 Configuration of 23 kV 60 MVA HTS power platform

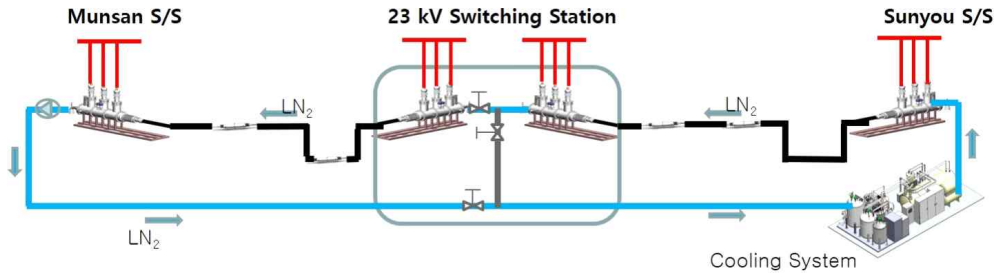


Fig. 5.3 The configuration of a cooling system installed in the Sunyou substation to cool the superconducting cables on both sides together

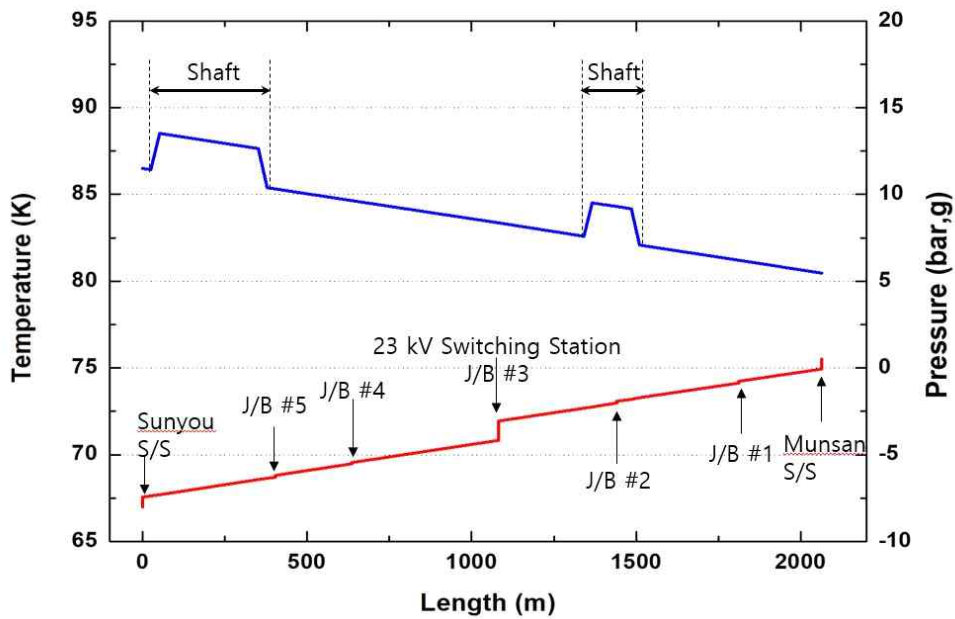


Fig. 5.4 The temperature and pressure profiles of a cooling system installed in the Sunyou substation

The load supply capacity of the 23 kV switching station is set to 60 MVA, corresponding to a substation with two banks of transformers. The 23 kV tri-axial HTS power cable with the same 60 MVA capacity is installed. One is from the 23 kV switching station to the 154 kV Munsan substation, and the other is to the 154 kV Sunyou substation. If the capacity of the 23 kV switching station is

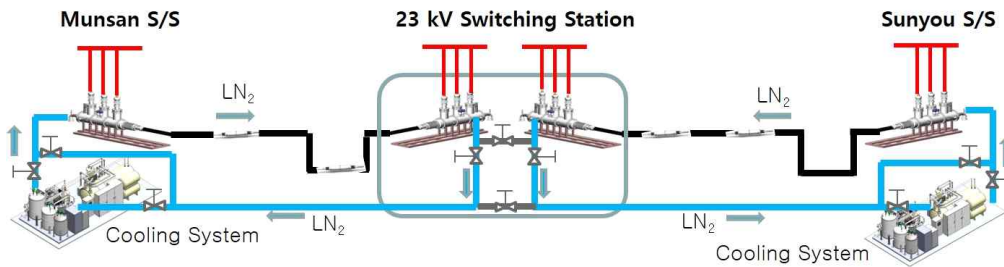


Fig. 5.5 The configuration of the cooling systems installed separately in the Munsan and Sunyou substations to achieve a more reliable power supply

increased to 120 MVA, the load supply can be easily and flexibly attained merely by adding one more line of superconducting cables.

Concerning the configuration of the cooling system, it is possible to install a cooling system in one of the Sunyou or Munsan substations to cool the superconducting cables on both sides together, as shown in Fig. 5.3, and to install the cooling systems separately in both substations, as shown in Fig. 5.5. If it is installed at only one location, the initial investment cost will be lower, making it more economical; however, the separate independent operation of each cable might be impossible, which could make both cables inoperable in case of a fault. Conversely, if separate cooling systems are installed, the initial investment cost will be high; however, each cable has the advantage of being operable separately. Accordingly, the separate installation method was considered more desirable for achieving a more reliable power supply. Figs. 5.4 and 5.6 demonstrate the temperature and pressure profiles of the cooling system.

The 23kV switching station for the HTS power platform will be developed into a disguised station, like buildings for houses and cafes, to harmonize with the surrounding environment. It is expected that not only the building's energy efficiency system will be improved by installing solar panels on its roof but also the building's exterior will be constructed with harmonizing landscaping and relaxation areas to enable it to be used as a new technology exhibition hall or superconducting public relations center, besides its original function to supply energy to nearby areas.

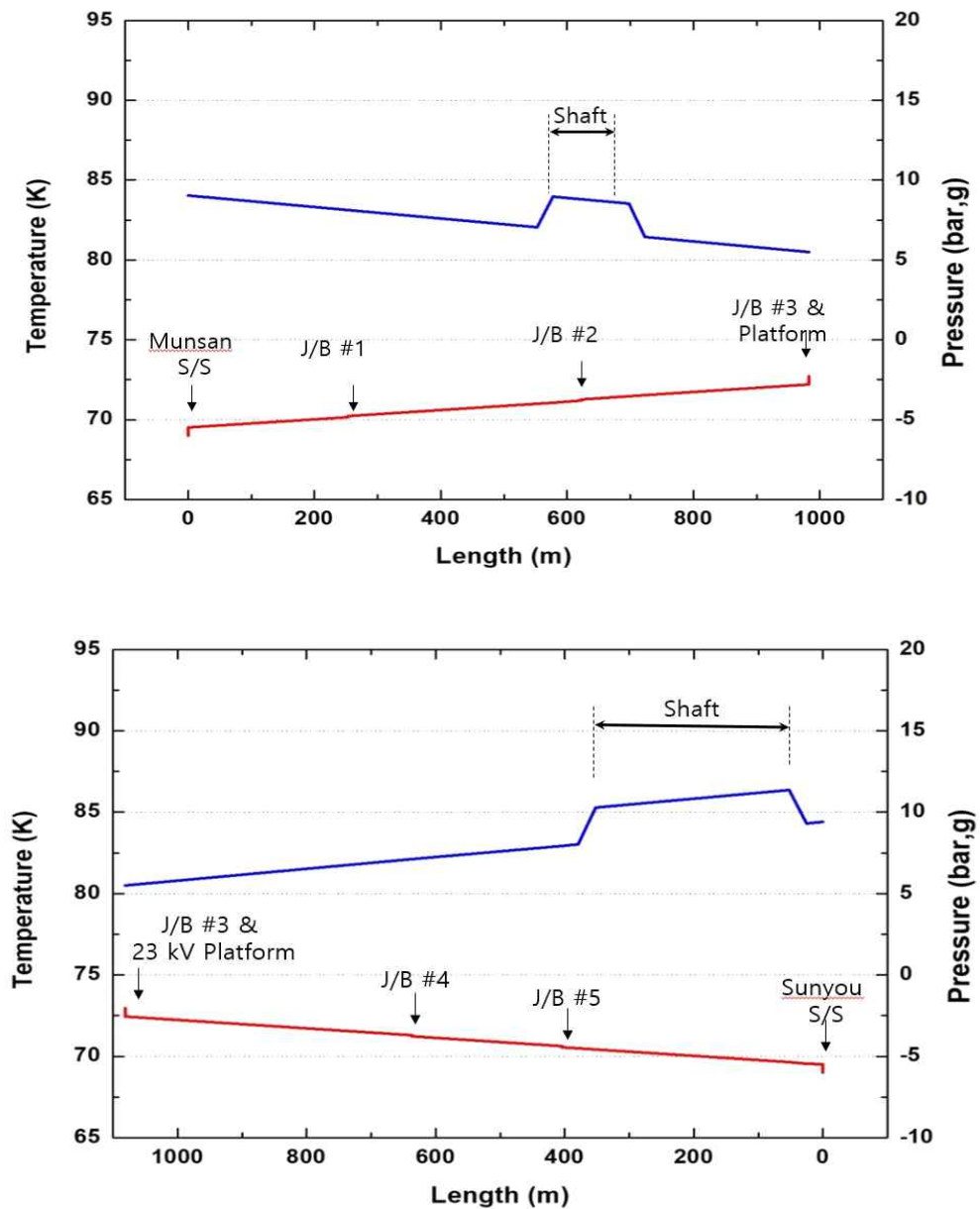


Fig. 5.6 The temperature and pressure profiles of the two cooling systems installed separately in the Munsan and Sunyou substations



Table 5.2 The results of the load flow analysis for the HTS power platform

Year	Facility	Normal Operation	Contingency Analysis (MW)			
			Case 1	Case 2	Case 3	Case 4
2021	Munsan-Sunyou	21×2(8%)	29×2(11%)	14×2(5%)	43×1(16%)	-
	Munsan-Station	14×1(24%)	-	30×1(53%)	14×1(24%)	57×1(112%)
	Sunyou-Station	16×1(28%)	30×1(52%)	-	16×1(28%)	27×1(55%)
2024	Munsan-Sunyou	12×2(6%)	19×2(9%)	4×2(4%)	22×1(12%)	-
	Munsan-Station	14×1(24%)	-	30×1(53%)	14×1(24%)	15×1(25%)
	Sunyou-Station	16×1(28%)	30×1(52%)	-	16×1(28%)	15×1(27%)
2031	Munsan-Sunyou	11×2(6%)	18×2(8%)	4×2(3%)	21×1(11%)	-
	Munsan-Station	14×1(24%)	-	30×1(53%)	14×1(24%)	15×1(25%)
	Sunyou-Station	16×1(28%)	30×1(52%)	-	16×1(28%)	15×1(27%)

In case of a two-line fault(or double contingency) of the 154 kV Munsan-Sunyou transmission lines in 2021, overloading of the 23 kV Munsan-Superconducting ST HTS cable may occur. However, that is very unlikely, because this condition considers the two-line fault of the underground transmission cables. Even if the fault occurs, it can be resolved by switching the loads of the platform to the 154 kV Munsan substation. After 2024, the above overload problem does not occur after the construction of the 154 kV SDG-Sunyou transmission lines. However, without the HTS power platform, it would be disadvantageous for the system operation because the 154 kV Sunyou substation is radial until the construction of the 154 kV SDG-Sunyou transmission line. Consequently, HTS platforms contribute to enhancing the system's reliability.

The fault current was also reviewed for the cases before and after the installation of the HTS power platform. Originally, the 23 kV bus fault current was 6.7 kA at Munsan substation and 7.2 kA at Sunyou substation, respectively; however, the fault current increased to 13.2 kA after a loop connection with 23 kV HTS cables. This value of fault current still satisfy the criteria since it's below the breaking current of 25 kA for a circuit breaker. This result means the loop-connected HTS power platform can be feasible as long as fault current is properly managed.

It might always be possible to open the circuit breakers and then close them in an emergency to transfer loads if fault current is expected to be over 25 kA; however, a temporary power outage is inevitable. Therefore, just in case, the installation of SFCLs can be considered, as described in Chapter 3. With the installation of SFCL in series with the HTS cable, fault currents were reduced to 7.54 kA at Munsan substation and 8.0 kA at Sunyou substation, respectively, which showed excellent performance. This study did not consider additional measures to address the fault current issue; however, doing so including identifying the optimal location and current limiting resistance value of the SFCL seems worthwhile.

Table 5.3 The fault currents before and after the installation of the HTS power platform

HTS power platform	Substation name	Year 2021	Year 2024	Year 2031
Before HTS Platform	Munsan	6.71	6.73	6.73
	Sunyou	7.19	7.21	7.21
HTS Power Platform without an SFCL	Munsan	13.26	13.33	13.33
	Sunyou	13.29	13.36	13.36
HTS Power Platform wiith an SFCL	Munsan	7.54	7.56	7.56
	Sunyou	8.02	8.05	8.05

---

## CHAPTER 6

### CONCLUSIONS

---

When installing a new substation, it is advantageous to construct it at the center of loads for loss minimization; however, it is not easy to secure a substation site in urban areas owing to high land prices, complex permission processes, and increasing social acceptability issues. The use of distribution superconducting cables has been actively promoted as a technological solution. KEPCO initiated the Shingal Project to utilize the 23 kV triad-type HTS cable with an actual system, and it started its commercial operation in 2019.

However, the disadvantage of the triad type superconducting cable is that it is not easy to utilize it further owing to high investment costs. As an alternative, the development of tri-axial cables at the distribution voltage level without using HTS shield wires, such as those used in the Ampacity project in Germany, resulted in cost savings, but the limitations of the cooling system kept the superconducting cable from exceeding a length of 1 km.

This study shows that the distance can be increased up to 3 km by improving the cooling configuration of the tri-axial HTS cables from the two channels in the same cryostat to an external separate circulation channel for liquid nitrogen(LN<sub>2</sub>). With the use of 23 kV tri-axial HTS cables with radial power systems, the economic effects were compared with the conventional method. If the HTS cable is used, a 154 kV substation can be eliminated or relocated far from urban areas depending on how the 23 kV HTS cable connection is implemented into the existing power system. In addition, the higher the land price, the smaller the economic gap between the HTS

application and the conventional method.

Moreover, as a new configuration of an electric power grid for urban power supplies, an HTS power platform for using 23 kV tri-axial HTS power cables was presented. In an HTS power platform, two to three 23 kV switch stations are installed near a load's center, and they are loop connected to the 154 kV transformer substations with 23 kV HTS cables to satisfy the N-1 reliability criteria. Individual loads can be fed through the 23 kV distribution feeders from the 23 kV switching station. It is appropriate for the HTS power platform to have a total load supply capacity of up to 300 MVA including the substation capacity, which is equivalent to two fully equipped 154 kV substations. Considering the load density of  $4.5 \text{ MW/km}^2$  in the newly developed area, it can supply an area of  $\sim 80 \text{ km}^2$ .

Therefore, consideration should be given to the proper load supply capacity of 23 kV switching stations and the circuit configuration of 23 kV HTS cables that link the switching stations in urban areas with substations outside the load center. In particular, for determining economic feasibility, construction environments of power system, as well as HTS cables should be considered carefully among the various alternatives being compared. Construction environments include underground construction methods, land prices, and corridor constraints, which can affect economic feasibility. In view of these circumstances, the economic effects of the HTS power platform are compared with those of the conventional method. The HTS cable application can be more economical than the conventional method to a certain distance, although the economics, such as BCR and IRR, may show different values depending on the construction conditions. As a result, it was confirmed that the high investment cost of superconducting cables can be offset by the effects of land acquisition, cable tunnel construction, and the price reduction of the tri-axial HTS cable itself.

One cell of the 23 kV HTS power platform will be installed in an actual power system between KEPCO's 154 kV Munsan and Sunyou substations. A 23 kV switching station with a 60 MVA capacity will be constructed in the



middle of the cable route instead of a 154 kV substation, and it will be loop connected with the 23 kV tri-axial HTS cables to verify their performance, social, and economic effects. This study also showed the fault current issue of the loop-type HTS power platform can be addressed by installing SFCLs.

The author would like to explain some implications of this study. It was considered that the larger the capacity of the distribution voltage HTS cable, the better it was. However, it depends on their own configuration philosophy such as the number of substations, load supply capacity, the size of supply area, reliability level. Those HTS cables which blends harmoniously with conventional power facilities will not compromise the reliability and efficiency of the energy network. This innovation will have a great synergy effect when HTS technology works together with HVDC, energy storage technologies which are at the forefront of the paradigm change in energy. Additionally, HTS cable enables us to focus on eco-friendly, high-capacity transmission. However, the application of HTS cables can be feasible only for short distances for the time being. A significant price reduction in HTS wires and cooling system will further increase the feasible distance. As KEPCO has been increasing the efficiency of power facility investments and operations by standardizing the capacity of substations and power transmission lines, it is expected that standardization can be established to form an HTS power platform based on this study's results.

## REFERENCES

- [1] KEPCO, “The 8<sup>th</sup> long term transmission expansion plan(2017—2031),” July 2018.
- [2] H. Oh, Y. Won, J. Hwang, “The long-term transmission & substation plan in Korea power system,” 2009 Transmission & Distribution Conference & Exposition: Asia and Pacific, Oct. 2009.
- [3] KEPCO, “The design standard on the underground transmission,” Design standard of KEPCO (DS6002), Jan. 2015.
- [4] Korean act, “The act on compensation and support of areas around transmission line and substation facilities,” law no. 14994, Oct. 2017.
- [5] KEPCO, “The design standard on the 154 kV hub-type substation construction in the high-load density area,” Apr. 2006.
- [6] C. LEE, H. Son, Y. Won, Y. Kim, C. Ryu, M. Park, and M. Iwakuma, "Progress of the first commercial project of high-temperature superconducting cable by KEPCO in Korea," *Supercond. Sci. and Technol.*, vol. 33, no 4, Feb. 2020
- [7] M. Stemmler, F. Merschel, M. Noe, A. Hob, and N. Lallouet, “Ampacity project - advanced superconducting 10 kV system replaces conventional 110 kV cable system in city center,” in *Proc. CIGRE*, 2014.
- [8] H. J. Kim, K. Hur, “Expanded adoption of HTS cables in a metropolitan area and its potential impact on the neighboring electric power grid,” *IEEE Trans. Appl. Supercond.* vol. 22, no. 3, Jun. 2012.
- [9] J. Yoon, S.R Lee, and J.Y.Kim, “Application methodology for 22.9 kV HTS cable in metropolitan city of south Korea,” *IEEE Trans. Appl. Supercond.* vol. 17, no. 2, Jun. 2007.
- [10] C. Lee, H. Yang, J. Choi, M. Park, M. Iwakuma, “Economic evaluation of 23kV tri-axial HTS cable application to power system”, *IEEE Trans. Appl. Supercond.* vol. 29, no. 5, Aug. 2019.
- [11] S. J. Lee, M. Park, I. Yu, Y. Won, Y. Kwak, C. Lee, "Recent status and progress on HTS power cables for AC and DC power transmission in

- Korea", IEEE Trans. Appl. Supercond., vol. 28, no. 4., Jun 2018, Art. no. 5401205J.
- [12] B. G. Marchionini, Y. Yamada, L. Martini, H. Ohsaki, "High-temperature superconductivity: A roadmap for the electric power sector applications, 2015-2030", IEEE Trans. Appl. Supercond. vol. 27, no. 4, Jun. 2017.
  - [13] D. I. Doukas, "Superconducting transmission systems : Review, classification, and technology readiness assessment", IEEE Trans. Appl. Supercond. vol. 29, no. 5, Aug. 2019.
  - [14] S. Sohn, H.Y. Yang, J. Lim, S. Oh, S. Yim, S. Lee, H. Hang, and S. Hwang, "Installation and power grid demonstration of a 22.9 kV , 50 MVA, high temperature superconducting cable for KEPCO," IEEE Trans. Appl. Supercond. vol. 22, no. 3, Jun. 2012.
  - [15] B. Yang, J. Kang, S. Lee, C. Choi, and Y. Moon, "Qualification demonstration of a 80 kV 500 MW HTS DC cable for applying into real grid," IEEE Trans. Appl. Supercond. vol. 25, no. 5, Jun. 2015.
  - [16] H. S. Yang, D. L. Kim, S. H. Sohn, J. H. Lim, et.al., "Long term performance test of KEPCO HTS power cables," IEEE Trans. Appl. Supercond. vol. 19, no. 3, 2009.
  - [17] C. Ryu, H. Jang, C. Choi, Y. Kim, and H. Kim, "Current status of demonstration and commercialization of HTS cable system in grid in Korea," in Proc. 2013 Int. Conf. IEEE Appl. Supercond. Electromagn. Devices, Oct. 2013.
  - [18] S. R. Lee, J. J. Lee, J. Yoon, Y. W. Kang, and J. Hur, "Impact of 154 kV HTS cable to protection systems of the power grid in south Korea," IEEE Trans. Appl. Supercond. vol. 26, no. 4, 2016.
  - [19] S. Kim, S. Ha, J. Kim, et. al., "Development and performance analysis of a 22.9 kV /50 MVA tri-axial HTS power cable core," IEEE Trans. Appl. Supercond. vol. 23, no. 3, Jun. 2013.
  - [20] IEA HTS TCP, "Energy efficiency, resilient electric systems, and transportation applications using high-temperature superconductivity," A publication of the IEA's technical collaboration program on

- high-temperature superconductivity, July 2019.
- [21] D. Koo, Y. Won, C. Ryu, et al., “World’s first commercial project for a superconducting cable system in Korea,” CIGRE 2018, B1-303, Aug. 2018
  - [22] S. Wimbush, N. Strickland, “A public database of high-temperature superconductor critical current data,” IEEE Trans. Appl. Supercond. vol. 27, no. 4, Jun. 2017.
  - [23] W. H. Fietz, M.J. Wolf, A. Preuss, R. Heller, and K. Weiss, “High-current HTS cables: Status and actual development,” IEEE Trans. Appl. Supercond. vol. 26, no. 4, 2016.
  - [24] C. Lee, D. Kim, et. Al., “Thermo-hydraulic analysis on long three-phase coaxial HTS power cable of several kilometers,” IEEE Trans. Appl. Supercond., vol. 29, no. 5, Aug. 2019
  - [25] N. Amemiya, Z. Jiang, M. Nakahata, et al., “AC loss reduction of superconducting power transmission cables composed of coated conductors,” IEEE Trans. Appl., vol. 17, no.2, Jun. 2007
  - [26] S. Fukui, J. Ogawa, N. Suzuki, et al., “Numerical analysis of AC loss characteristics of a multilayer HTS cable assembled by coated conductors,” IEEE Trans. Appl. Supercond., vol. 19, no. 3, Jun. 2009
  - [27] S. Kim, K. Sim, J. Cho, H. Jang, M. Park, “AC loss analysis of HTS power cable with RABiTS coated conductor,” IEEE Trans. Appl. Supercond., vol. 20, no. 3, Jun. 2010
  - [28] KEPCO, “23 kV Superconducting cable and accessories,” General Technical Specifications of KEPCO(GS) 6145-0088, Nov. 2015.
  - [29] CIGRE, “Recommendations for testing of superconducting cables,” TB 538, 2013.
  - [30] IEC 60840, “Power cables with extruded insulation and their accessories for rated voltages above 30 kV up to 150 kV- Test methods and requirements,” 2011.
  - [31] KEPCO, “Cryogenic refrigerator and cryogenic cooling system for superconducting cables,” General Technical Specifications of KEPCO(GS).
  - [32] KEPCO, “Budget standard unit price in the construction sector,” Budget

- guideline of KEPCO, Mar. 2019
- [33] W. Yuan, S. Venuturumilli, Z. Zhang, Y. Mavrocostanti, and M. Zhang, "Economic feasibility study of using high temperature superconducting cables in UK' electrical distribution networks,"IEEE Trans. Appl. Supercond.,vol. 28, no. 4, Jun. 2018, Art. no. 5401505.
  - [34] M. Elsherif, P. Taylor, and S. Blake, "Investigating the potential impact of superconducting distribution networks,"in Proc. 22nd Int. Conf. Electricity Distribution, Jun. 2013.
  - [35] A. Morandi, B. Gholizad, M. Stieneker, H. Stagge, R. Doncker, "Technical and economical evaluation of DC high-temperature superconductor solutions for the grid connection of offshore wind parks," IEEE Trans. Appl. Supercond., vol. 26, no. 6, Sep. 2016
  - [36] KEPCO, "Strategy of high-temperature superconducting platform for an urban power system," Naju, South Korea, 2017
  - [37] KEPCO, "Strategy roadmap to the commercialization enhancement of the high-temperature superconducting cables," Naju, South Korea, 2015
  - [38] M. Sjoström, D. Politano, "Technical and economical impacts on a power system by introducing an HTS FCL," IEEE Trans. Appl. Supercond. Vol. 2, No. 1, Mar. 2001
  - [39] J. Yoon, S. Lee, B. Yang, "Optimal design specification of 22.9 kV HTS-FCL applied in real korean power system," IEEE Trans. Appl. Supercond. Vol. 21, No. 3, Jun. 2011
  - [40] J. Choi, H. Park, R. Baldick, "Transmission investment and expansion planning for systems with high-temperature superconducting cables," IEEE Trans. Appl. Supercond. Vol. 29, No. 8, Dec. 2019
  - [41] Y. Yang, M. Darwish, M. Moghadam, "Power cable cost benefit analysis: a critical review," 53<sup>rd</sup> International universities power engineering conference, 2018
  - [42] Korean Ministry of Strategy and Finance, "General guidelines for conducting preliminary feasibility studies," Order No. 9999, Mar. 2017
  - [43] KIET, "Economic analysis of transmission-voltage HTS cable's application

- to a real power system,” a report of Korean Institute for Industrial Economics and Trade (KIET), May, 2019
- [44] K. Malmedal, P. K. Sen, “A better understanding of load and loss factors,” 2008 IEEE Industry Applications Society Annual Meeting, 2008
- [45] D. Kottonau, M. Noe, S. Grohmann, “Opportunities for high-voltage AC superconducting cables as part of new long-distance transmission lines,” IEEE Trans. Appl. Supercond., vol. 27, no. 4, Jun. 2017
- [46] X. Xiao, Y. Liu, J. Jin, C. Li, F. Xu, “HTS applied to power system: benefits and potential analysis for energy conservation and emission reduction,” IEEE Trans. Appl. Supercond., vol. 26, no. 7, Oct. 2016

## PAPER LISTS

- [1] C. LEE, J. Choi, H. Yang, M. Park, and M. Iwakuma, "Economic evaluation of 23 kV Tri-axial HTS cable application to power system," *IEEE Trans. Appl. Supercon.*, vol.29, no.5, Aug. 2019
  
- [2] C. LEE, H. Son, Y. Won, Y. Kim, C. Ryu, M. Park, and M. Iwakuma, "Progress of the first commercial project of high-temperature superconducting cable by KEPCO in Korea," *Supercond. Sci. and Technol.*, vol. 33, no 4, Feb. 2020
  
- [3] C. LEE, H. Yang, M. Park, and M. Iwakuma,, "Feasibility assessment of the new configuration of electric power grid using 23kV HTS cable system for urban power supply," *under review for publication in Journal of Physics Conference Series, Submitted to IEEE ASC in Glasgow, UK*, 2019
  
- [4] S. Lee, M. Park, I. Yu, Y. Won, Y. Kwak, and C. LEE, "Recent status and progress on HTS cables for AC and DC power transmission in Korea," *IEEE Trans. Appl. Supercon.*, vol.28, no.4, June 2018
  
- [5] C. Lee, H. Yang, M. Park, "Recent progress and the research activities on the HTS power cable projects in Korea," *IEEE Supercon. News Forum* vol.13, no.46, Feb. 2019